RSC Advances

REVIEW

View Article Online
View Journal | View Issue



Cite this: *RSC Adv.*, 2017, **7**, 9194

# Recent studies of the synthesis, functionalization, optoelectronic properties and applications of dibenzophospholes

Paulina Hibner-Kulicka,[ab] John Arthur Joule,[c] Joanna Skalik[a] and Piotr Bałczewski*[ad]

Received 4th November 2016
Accepted 23rd January 2017

DOI: 10.1039/c6ra26333j

rsc.li/rsc-advances

The first dibenzophospholes were described in the 1950s, but only recently have they gained greater importance, due to their use in organic electronics and the possibility of designing new π-conjugated, optoelectronic materials that incorporate these heterocycles. Our comprehensive review covering a period of 15 years (2001–2016), includes methods of synthesis of these compounds, methods for their functionalization, a description of their optoelectronic properties and their first use in optoelectronic devices. The review represents the current state of knowledge in this field and shows the great potential of simple and functionalized dibenzophospholes. The work described in this review suggests that dibenzophospholes should also be investigated more intensively as single materials, as well as in structural combinations with other π-extended conjugated aromatic and heteroaromatic systems containing phosphorus, nitrogen, silicon or sulfur atoms.



## 1. Introduction

Interest in π-conjugated compounds has increased greatly following the investigations of Heeger, MacDiarmid and Shirakawa,[1] that led to the award of the Chemistry Nobel Prize in 2000. There followed a period of dynamic development in the field of synthesis and studies on the properties of oligomeric and polymeric systems applicable to flexible, lightweight and low-cost electronic devices. A great deal of attention has been paid not only to structural modifications, but also to

[a]*Department of Heteroorganic Chemistry, Centre of Molecular and Macromolecular Studies, Polish Academy of Sciences, Sienkiewicza 112, 90-363 Łódź, Poland. E-mail: pbalczew@cbmm.lodz.pl; Fax: +48 42 684 71 26; Tel: +48 42 684 71 26*

[b]*Department of Molecular Physics, Technical University of Łódź, Żeromskiego 116, 90-924 Łódź, Poland. Fax: +48 42 631 32 18; Tel: +48 42 631 32 05*

[c]*The School of Chemistry, The University of Manchester, Manchester M13 9PL, UK*

[d]*Jan Długosz University in Częstochowa, Institute of Chemistry, Environmental Protection and Biotechnology, The Faculty of Mathematics and Natural Sciences, Armii Krajowej 13/15, 42-201 Częstochowa, Poland. Tel: +48 34 378 41 00*

*Paulina Hibner-Kulicka received her BSc in chemistry from the Jan Długosz University in Częstochowa, Poland. Within an Erasmus program with the University of Caen-Normandy (ENSICAEN), France, she was involved in the synthesis of ladder-type heteroacenes as materials for light-emission and charge transport. She graduated (MSc) from the University of Łódź, in the area of chemistry and nanotechnology of new materials in collaboration with the Centre of Molecular and Macromolecular Studies, Polish Academy of Science, Łódź (Prof. P. Bałczewski). Currently, she is a PhD student working on photovoltaic and OLED device fabrication at Łódź University of Technology, Poland.*

*John Joule grew up and went to school in Llandudno, Wales, moving to the University of Manchester for BSc, MSc, and PhD degrees, the last with Dr George F. Smith. Following post-doctoral studies with Richard K. Hill (Princeton) and Carl Djerassi (Stanford) he returned to Manchester for an academic career of 41 years. His research there produced more than 230 papers on aspects of heterocyclic chemistry, especially indoles and quinoxalines and pteridines related to the molybdenum cofactor. His textbook 'Heterocyclic Chemistry' co-authored originally with George Smith and latterly with Keith Mills, his one-time PhD student, is now in its 5th Edition.*

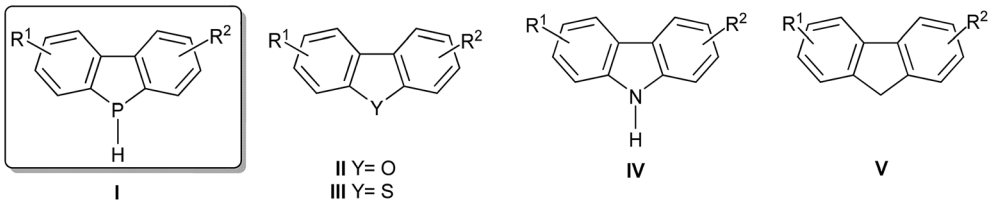


Scheme 1



supramolecular organization of such compounds to achieve optimal properties of the final materials. The use of conjugated polyaromatic, polyacetylenic, polyolefinic compounds and fused aromatic systems, as well as their structural combinations, not only guarantees satisfactory properties and excellent stability of these compounds, but also the possibility for their easy chemical functionalization using modern synthetic tools. A disadvantage of the systems containing aromatic building blocks has often been a too high degree of aromaticity, which inhibits an easy electron delocalization along the conjugated rings when in an oxidized state.[2–4]

Therefore, this type of molecular system requires a beneficial incorporation of heteroaromatic rings, for example five-membered pyrrole, thiophene or furan, possessing lower aromatic stabilization energies ($ASE_{calc}$: 20.57, 18.57, 14.77 kcal $mol^{-1}$, respectively) than a benzene ring. The aromatic character of the phosphole ring ($ASE_{calc}$ = 3.2 kcal $mol^{-1}$) is relatively low due to the pyramidal geometry of the phosphorus atom. Overlap between the lone pair and the diene unit is thus limited, resulting in a lower aromatic character compared with other five-membered heterocycles with nitrogen, sulfur or oxygen. The low aromatic character allows hyperconjugation of the endocyclic 4-π-electron system with the exocyclic P–R bond. Closely related dibenzophospholes **I** (Scheme 1) and their derivatives, being further examples of such fused heterocyclic systems, have been used successfully, alone or as building blocks, for preparation of more complex π-conjugated systems useful as electronic and optoelectronic materials. However, they are still an underestimated group of compounds in this field.

Dibenzophospholes **I** together with dibenzofurans **II**, dibenzothiophenes **III** and carbazoles **IV** belong formally to a family of heteroanalogs of fluorene **V**, or to be more precise, the fluorene anion (Scheme 1).

Important reviews by Réau,[5] Baumgartner[6,7] and Hissler[8,9] serve as brief introductions to phospholes and other organophosphorus derivatives in the molecular electronics context. Hissler's reviews focus mainly on nonfused phospholes and diheteroaromatic derivatives of phospholes fused to thiophene, pyrrole, furan, pyridine moieties and other P-derivatives with a particular emphasis on incorporation into electronic devices while the (micro)reviews by Réau and Baumgartner focus on development of phosphole-containing oligo- and polythiophene materials. A 2015 review by Gouygou[10] discussed phosphole-based ligands, including dibenzophospholes, which have potential in metal and organocatalysed reactions.[10]

In our comprehensive review, we summarise the literature on the newest methods of synthesis and functionalisation of the dibenzophospholes as well as their applications as optoelectronic materials (Fig. 1). This work continues the comprehensive coverage in a previous review devoted to synthesis of dibenzophospholes by Aitken in 2001[11] and thus it deals with work from the years 2001–2016.

*Joanna Skalik graduated from the Jan Długosz University in Częstochowa, Faculty of Mathematics and Natural Sciences (2008). She received her PhD with distinction at the Center of Molecular and Macromolecular Studies, Polish Academy of Sciences (CMMS, PAS) (2015). Since 2008, she has been a member of the scientific staff in the group of Prof. Piotr Bałczewski at the Department of Heteroorganic Chemistry, CMMS, PAS. She is a co-author of several patents, original and review articles, and chapters in books (Organophosphorus Chemistry, RSC, vol. 40–42, 44, 46). She is actively involved in the realization of Polish national and European research projects.*

*Piotr Bałczewski studied chemistry at the Technical University of Łodź. MSc/PhD theses (P/S/Si and cyclopentanoid chemistry) were with Prof. M. Mikołajczyk at the Centre of Molecular and Macromolecular Studies (CM & MS), Polish Academy of Sciences (PAS), Łódź. Doctoral studies at the Warsaw PAS, Institute of Organic Chemistry, then a post-doctoral period at Manchester University (UK) in alkaloid chemistry (Prof. J. A. Joule) led to habilitation and appointment as full professor at CM & MS PAS, Łódź. He currently leads materials research groups at CM & MS PAS, Łodź and the J. Długosz University in Częstochowa, and is currently Vice-President of the Polish Chemical Society.*

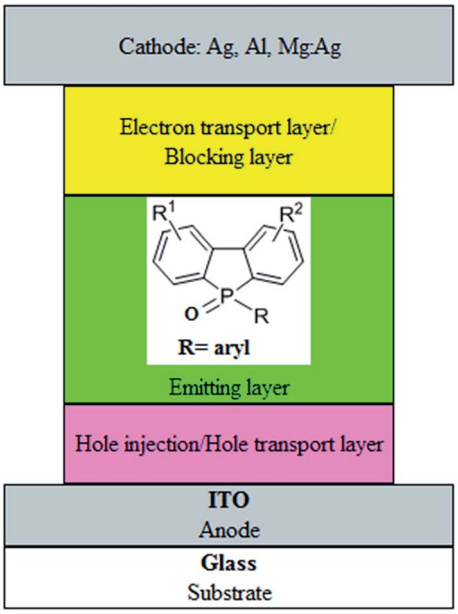


Fig. 1 The application dibenzophospholes in construction of various OLED devices.

Although the first dibenzophospholes were described in the 1950s, in recent times, these interesting compounds have gained importance due to the possibility of using them in new π-conjugated materials. The presence of the two flanking benzene rings in a dibenzophosphole gives the system several advantages over monocyclic phospholes in the context of incorporation into molecular electronics roles. The synthesis and synthetic manipulation of the tricyclic system allows adjustment of overall electronic structure by the introduction and manipulation of benzene-ring substituents. In particular, the linking of dibenzophosphole units to other electronically active components or its incorporation into polymer chains is facilitated by the benzene-ring units.

An important advantage of dibenzophospholes is their high resistance to thermal decomposition. For example, the temperature of thermal decomposition for dibenzophosphole is 365 °C, while for the phospholes and dithienophospholes thermal decomposition temperatures are between 200 and 300 °C.[12]

Dibenzophospholes and analogous tricyclic, dithienophospholes, are each well delocalized over the entire molecule and possess a smaller HOMO–LUMO gap than any of the component rings. Consequently the dibenzophospholes represent an independent class of compounds and should not be considered as classic, monocyclic phospholes. The dithienophosphole system, developed by Baumgartner *et al.*,[13–18] also possesses some advantages with respect to wavelength, intensity, especially tunability, as well as optical and thermal stability.

In this context, dibenzophospholes can be regarded as complementary optoelectronic materials and it is interesting to make a comparison of some selected properties of non-fused phospholes, fused dibenzophospholes and dithienophospholes, such as ranges of light absorption and light emission maxima, and luminescence quantum efficiencies. Thus for phospholes, the data are 350–450 nm, 450–620 nm, up to 0.143, for dibenzophospholes the significantly different values are 290–365 nm, 360–490 nm, up to 0.98, and for dithienophospholes the values are 330–420 nm, 415–630 nm, up to 0.90.[17,18]

The first described dibenzophosphole (IUPAC, CAS: 5*H*-benzo[*b*]phosphindole]) was 5-phenyl substituted derivative **1**,[19] obtained by Wittig in 1953, in low yield from a thermal decomposition of pentaphenylphosphorane $Ph_5P$. Other early methods, most of which were also elaborated by Wittig and coworkers, involved reactions of $Ph_5P$, $Ph_3P$, and $Ph_4P^+X^-$ (X = Cl, Br), $Ph_3P(O)$, with both weak (Py) and strong bases (PhMet, $Et_2NMet$; Met = Li, Na)[20–23] as well as the reaction of $Ph_3P$ with benzyne (Scheme 2).[24]

The phosphorus atom in dibenzophospholes offers the possibility of expanding its valency and forming new bonds to O, S, Se, B, N, P, Cl, C and metals in derivatives **2**, **3** and **6–8**. Dibenzophospholes possessing ionic structures, like the cation **4** and the anion **9** are also known. The phosphorane structure **5** containing two dibenzophosphole units was reported for the first time by Hellwinkel in 1960.[25]

## 2. Synthesis of dibenzophospholes

### 2.1. From $PH_3$ and derivatives

In the years 2001–2015, new methods of synthesis of dibenzophospholes have been elaborated starting from $PH_3$ and its derivatives. Stelzer, Sheldrick *et al.* obtained 5-phenyl-2,2′-bis(-sulfonato)-5*H*-dibenzophosphole dipotassium salt **11** by reaction of primary phenylphosphine with 5,5′-bis(sulfonato)-2,2′-difluoro-1,1′-biphenyl dipotassium salt **10** in superbasic medium DMSO/KOH in 60% yield (Scheme 3).[26]

This research group also obtained the P-unsubstituted dibenzophosphole **14** by reaction of 5,5′-bis(sulfonato)-2,2′-difluoro-1,1′-biphenyl disodium salt **12** with $NaPH_2$ in liquid ammonia. In this reaction, the trisodium salt **13** was formed first, which upon acidification with aqueous HCl under aerobic conditions gave the dibenzophosphole disalt **14** accompanied by its dimer **15** (Scheme 4).[26]

Various bridged dibenzophospholes **17–21** have been obtained by a radical phosphanylation. An example of this approach is the reaction of tetrabromobiphenyls **16** (R = H, Ph) with $(Me_3Sn)_2PPh$ in benzene or trifluoromethylbenzene, in the presence of V-40 (1,1′-azobis(cyclohexane-1-carbonitrile)) as a radical initiator followed by a subsequent oxidation of the corresponding intermediate with $H_2O_2$. In this process, two *cis*/*trans* isomers **17** and **18** were formed in a ratio of 1.0 : 1.1 in 10% and 11% yields, in benzene and in the same ratio in 27% and 29% yields in trifluoromethylbenzene, respectively. Interestingly, the dibenzophosphole **19** precipitated pure, in 40% yield, by stirring the crude reaction mixture at room temperature overnight. The radical phosphanylation of the biphenyl **16** (R = aryl) led to formation of 4,4′-diaryl-substituted bis(phosphoryl)-bridged biphenyls **20** and **21** in 22% and 13% yields, respectively (Scheme 5).[27]

 

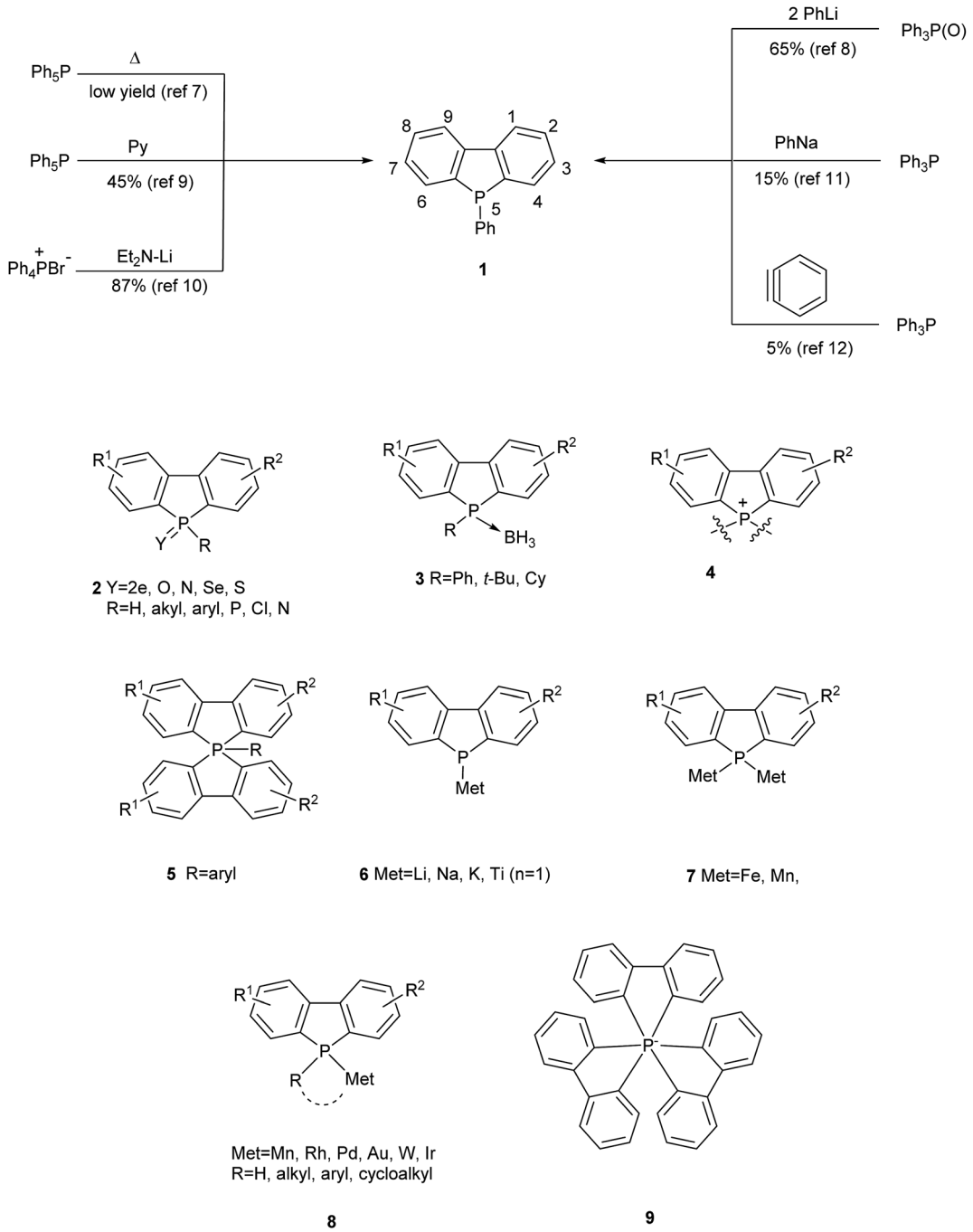


Scheme 2

Zhou and Breit *et al.* obtained 3,7-di-*tert*-butyl substituted dibenzophospholes functionalized at the phosphorus atom by pyridin-2-(1*H*)-on-6-yl, 6-pivalamidopyridin-2-yl and isoquinolin-1(2*H*)-on-3-yl moieties starting from 2,2′-dibromo-4,4′-di-*tert*-butylbiphenyl.[28]

Gaunt, Girolami and Kozimor *et al.* described the reaction of $PCl_3$ with 2,2′-dibromo-1,1′-biphenyl that unexpectedly gave a mixture of 5-chloro- and 5-bromo-5*H*-dibenzophospholes in a 3 : 2 ratio as a result of halogen exchange. Both 5-halodibenzophospholes after separation behaved similarly in the subsequent conversion into a new family of dibenzophosphole-based dithiophosphinic acids using elemental sulfur and sodium hydrosulfide hydrate.[29]

### 2.2. From $ArPCl_2$, $Ar_2PCl$ or $RPCl_2$

Due to easy access to chlorophosphines, the synthesis of dibenzophospholes involving dilithiobiaryls constitutes a convenient source of these compounds. Using this method, Delft *et al.* obtained symmetrical dibenzophospholes **1**, **23** and **24** from the corresponding 2,2′-dibromobiphenyl precursors

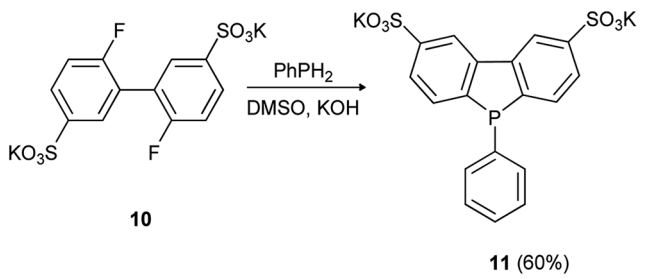


Scheme 3

bearing H, MeO or $CF_3$ groups by generation of the corresponding dianion with *n*-BuLi in $Et_2O$ at room temperature followed by quenching the reaction mixture with dichlorophenylphosphine to give 5-phenyldibenzophosphole **1**, 2,8-dimethoxy-5-phenyldibenzophosphole **23** and 2,8-bis(trifluoromethyl)-5-phenyl-dibenzophosphole **24** in 55%, 30% and 57% yields, respectively (Scheme 6).[30]

Gouygou, Leroux *et al.* obtained symmetrical and unsymmetrical dibenzophospholes **26–37** in 30–96% yields starting from 2,2′-dihalobiaryls *via* double halogen/lithium exchange with *n*-BuLi in THF at −78 °C followed by trapping the resulting dilithium derivatives with dichlorophenylphosphine (Scheme 7).[31]

The phosphoniafluorene **39** has been obtained according to the above procedure by dilithiation of the 5,5′-disubstituted 2,2′-dibromo-1,1′-biphenyl **38** followed by condensation of the resulting dilithio derivative with dichlorophenylphosphine $PhPCl_2$ and then quaternization of the dibenzophosphole phosphorus atom with MeI in THF. After exchange of the iodide

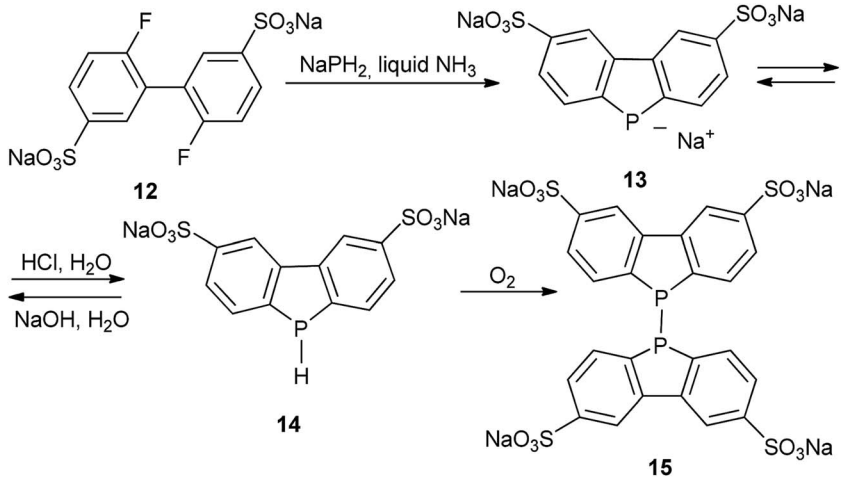


Scheme 4

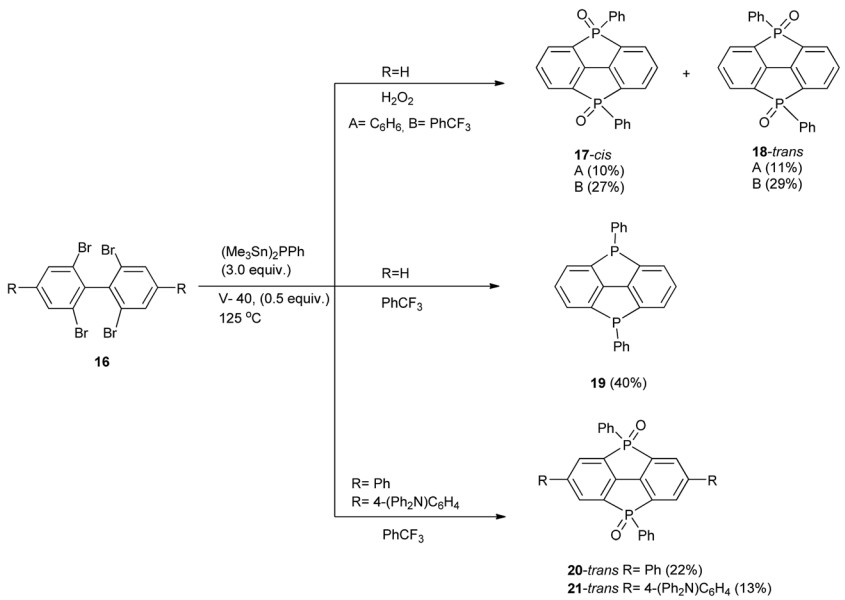


Scheme 5

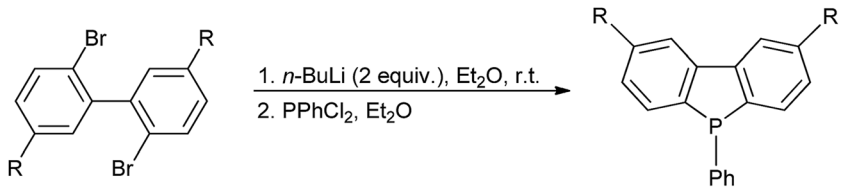


**22**

**1** R= H (55%)
**23** R= OMe (30%)
**24** R= $CF_3$ (57%)

Scheme 6

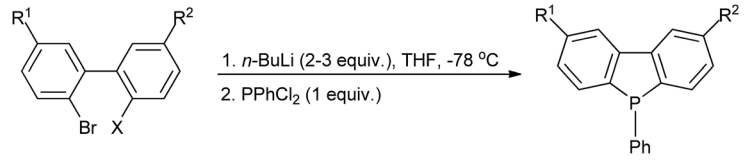


**25** X= Br, I

**26- 37**

**26** $R^1$= H, $R^2$= H, X= Br (82%)
**27** $R^1$= H, $R^2$= F, X= Br (53%)
**28** $R^1$= H, $R^2$= Me, X= Br (40%)
**29** $R^1$= H, $R^2$= OMe, X= Br (49%)
**30** $R^1$= H, $R^2$= Cl, X= Br (56%)
**31** $R^1$= H, $R^2$= Br, X= Br (37%)

**32** $R^1$= H, $R^2$= Ph, X= Br (63%)
**33** $R^1$= H, $R^2$= $N(CH_3)_2$, X= Br (39%)
**34** $R^1$= H, $R^2$= $OCF_3$, X= Br (61%)
**35** $R^2$= $OCH_2O$, X= Br (96%)
**36** $R^2$= $OCF_2O$, X= I (30%)
**37** $R^2$= $OCF_2CF_2O$, X= I (45%)

Scheme 7

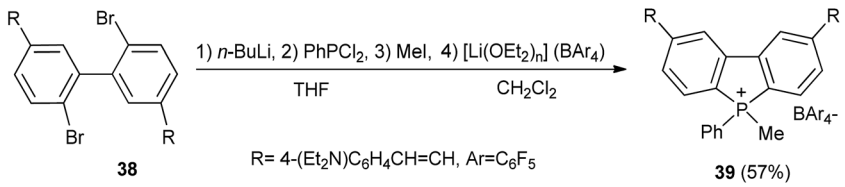


**38**

**39** (57%)

Scheme 8

ion to the $BAr_4$ anion, compound **39** was obtained as a red solid in 57% yield (Scheme 8).[32]

This method was also used for the preparation of 2-hydroxy-substituted dibenzophosphole oxides **41–44**. After bromine/lithium exchange on the dibromobiphenyl derivative **40**, the dilithiated intermediate was treated with either $PhPCl_2$ or (L-menthyl)$PCl_2$. Then, the dibenzophospholes were oxidized *in situ* with $H_2O_2$ and the *tert*-butyldimethylsilyl (TBS) group was removed by reaction with tetra-*n*-butylammonium fluoride (TBAF) to give oxides **41** and **42** in 75% yields. The hydroxy groups

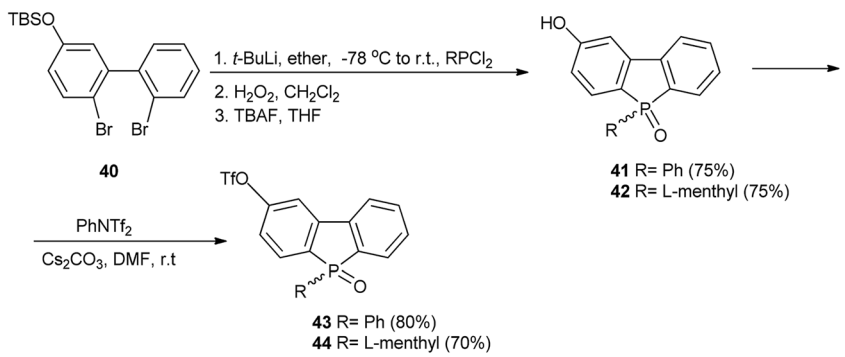


**40**

**41** R= Ph (75%)
**42** R= L-menthyl (75%)

**43** R= Ph (80%)
**44** R= L-menthyl (70%)

Scheme 9

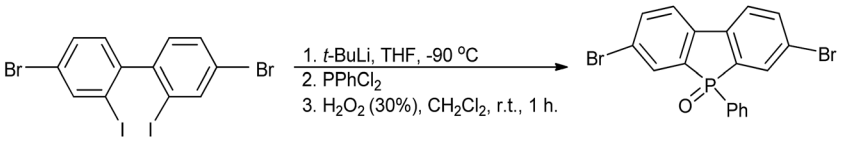


Scheme 10

in the latter were converted into the corresponding triflates **43** and **44** by treatment with $PhNTf_2$. For R = L-menthyl, the dibenzophosphole oxide **42** was obtained as a mixture of two epimers with opposite configuration at the stereogenic phosphorus center. The mixture was converted into triflates **44** and the two diastereomers were separated by HPLC (Scheme 9).[33]

*t*-Butyllithium in THF, at −90 °C was also used for iodine/lithium exchange in **45** followed by reaction with $PhPCl_2$ and oxidation with $H_2O_2$ to give 3,7-dibromo-5-phenyl dibenzophosphole oxide **46** in 47% yield (Scheme 10).[27]

Another method, described by Ionkin and Marshall in 2003, involved the reaction of the dichloroarylphosphine **47** with potassium in hexanes to give the 5-chlorodibenzophosphole derivative **48** in 64% yield (Scheme 11).[34]

In 2006, Wehmschulte *et al.* described the intramolecular Friedel–Crafts type reaction of the dichlorophosphines **49** or **50** initiated by $AlCl_3$ in [$d_6$]-benzene at room temperature. In this reaction dibenzophospholes **55** and **56** were formed in 29% and 43% yields, respectively, *via* intermediates **51**/**52** and **53**/**54**, as yellow-orange oils, which were decomposed to the final products by addition of pyridine (Py) (Scheme 12).[35]

The same research group synthesised 5-chloro disubstituted dibenzophospholes **58–60** *via* thermolysis of the aryldichlorophosphine **57** at 200–230 °C with HCl evolution (Scheme 13).[35]

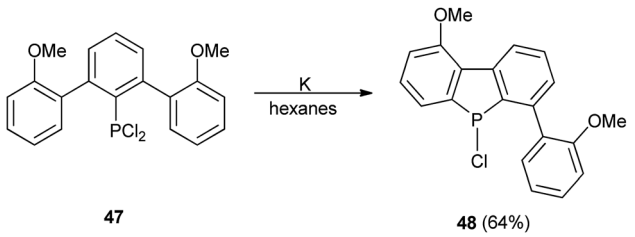


**47** **48** (64%)

Scheme 11

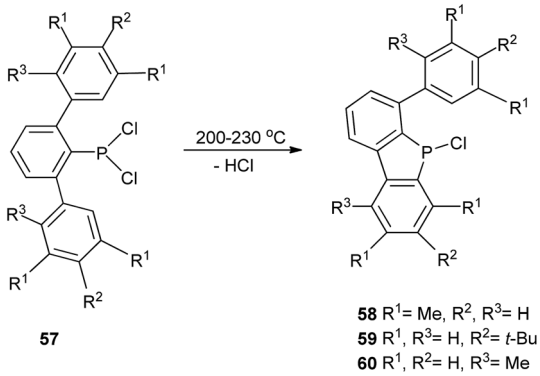


**57**

**58** $R^1$= Me, $R^2$, $R^3$= H
**59** $R^1$, $R^3$= H, $R^2$= *t*-Bu
**60** $R^1$, $R^2$= H, $R^3$= Me

Scheme 13

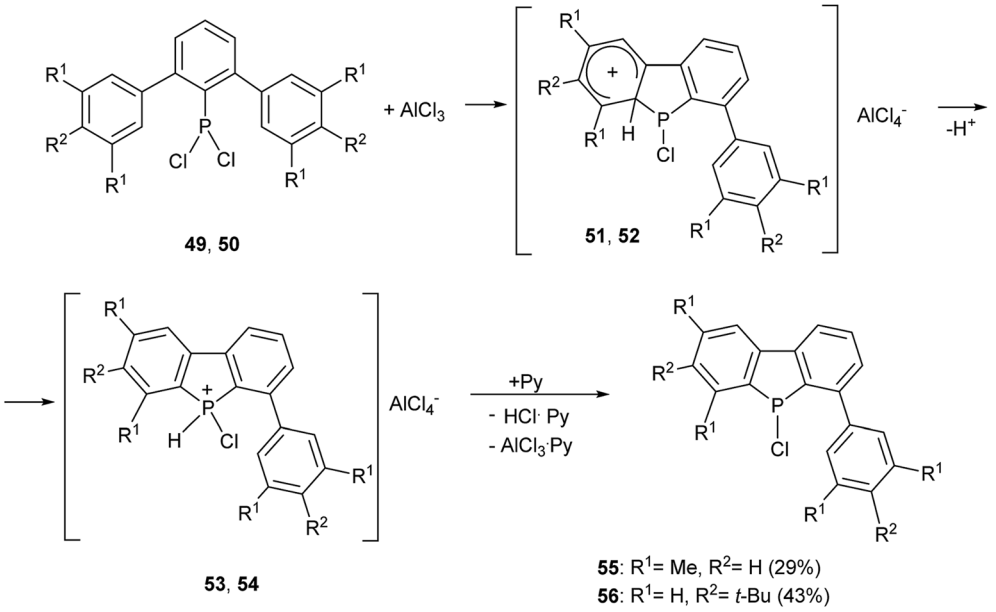


**49**, **50** **51**, **52** **53**, **54**

**55**: $R^1$= Me, $R^2$= H (29%)
**56**: $R^1$= H, $R^2$= *t*-Bu (43%)

Scheme 12

### 2.3. From $RAr_2P$ or $Ar_3P$

5-Phenyldibenzophosphole **1** has also been obtained in a two-step reaction involving addition of 1-lithio-2-diphenylphosphinylbenzene **61** to benzyne **62** followed by cyclisation of the resulting lithio adduct **63.** The starting materials **61** and **62** were obtained from 2-bromophenyl-diphenyl phosphine and 1,2-dibromobenzene, respectively (Scheme 14).[36]

The next method, published by Tobisu, Chatani *et al.* in 2013, involves intramolecular cyclisation of biphenyl derivatives **64** containing $PPh_2$ and PMePh groups in the presence of catalytic amounts of $Pd(OAc)_2$ (5 mol%) in toluene through the cleavage of the C–H bond and exclusive cleavage of the P–Ph bond rather than the P–Me one. The dibenzophospholes formed first in these reactions were easily oxidized with hydrogen peroxide at room temperature which led to dibenzophosphole oxides **66** and **67** in 92%, 64% yields, respectively or reacted with borane dimethylsulfide to give the dibenzophosphole borane **68** in 61% yield (Scheme 15).[37]

The same reaction, carried out with 1 equivalent of $Pd(OAc)_2$ (in air), gave **66** in 50% yield, suggesting that the dimeric metallacycle **70** (X-ray analysis) was a plausible intermediate for the catalytic cycle. Dibenzophospholes bearing a range of functional groups (Br, F, $CO_2Me$, Ac, CN) and an array of fused rings (naphthalene, anthracene, furan, pyrrole) could also be synthesised using this method (Scheme 16).[37]

The route was also successfully applied to the synthesis of a diverse array of dibenzophospholes **71–88.** The high functional group tolerance allowed access to a range of electronically different dibenzophospholes bearing alkyl **71**, **80**, **83**/**84**, ether **72**, alkoxyl **82**, amine **73** and **81**, acyl **74**, ester **75**, nitrile **76**, fluoride **77**, chloride **78**, and bromide **79** groups. The C–P bond formation also took place with substrates bearing *ortho* substituents to afford 1-substituted dibenzophospholes **80** and

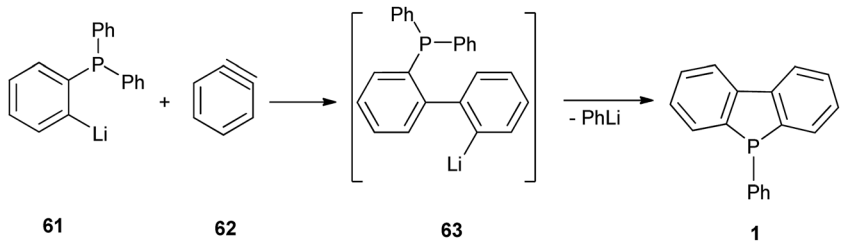


Scheme 14

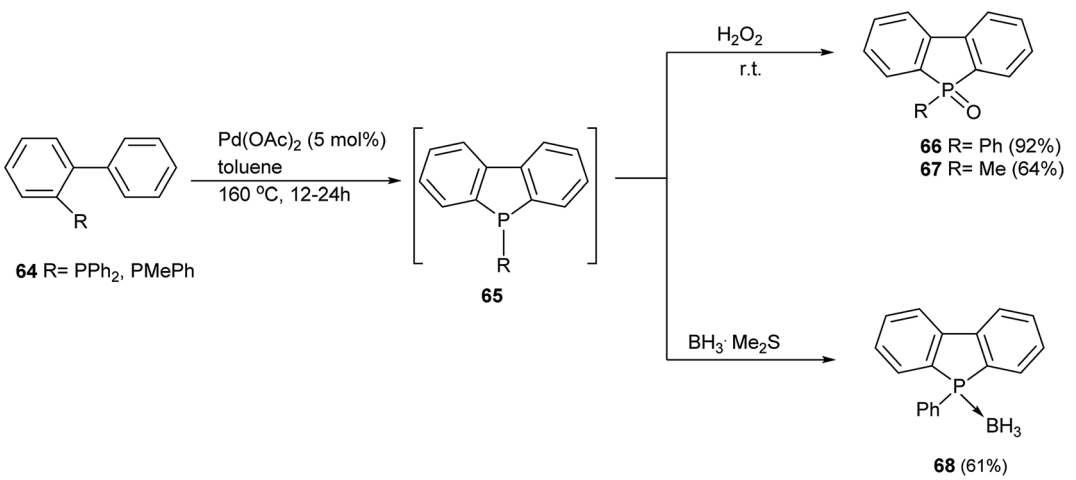


Scheme 15

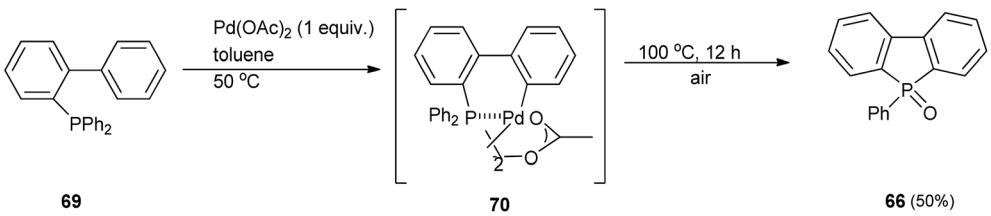


Scheme 16

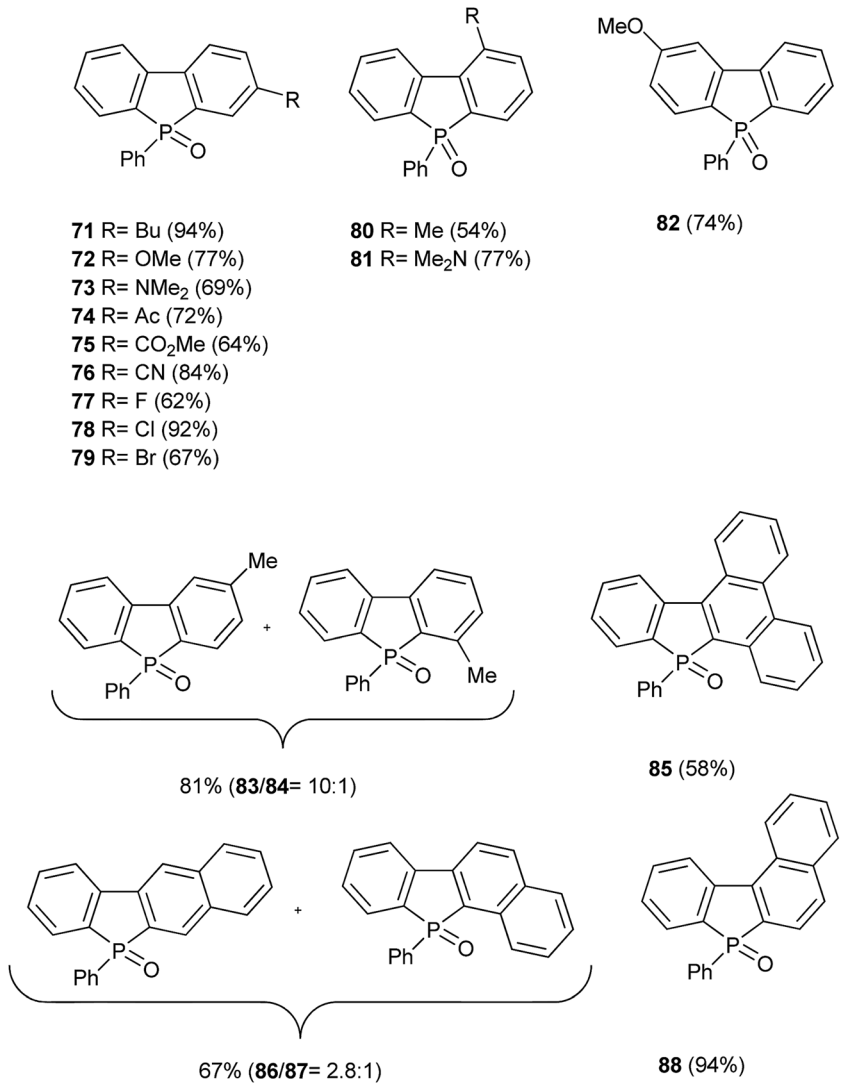


Scheme 17

**81**. Substrates with *meta* substituents underwent a regioselective cyclisation at the less hindered site to form **83** as a major product. This synthesis enabled various π systems including naphthalene and phenanthrene moieties, to be incorporated into the dibenzophosphole core of the compounds **85–88** (Scheme 17).[37]

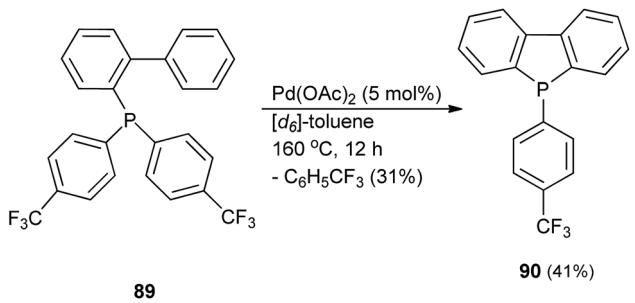


Scheme 18

In a special case, this method could also be applied to the synthesis of 5-P-aryl substituted dibenzophosphole **90** bearing an electron-withdrawing *p*-trifluoromethyl on the aryl group, by cyclisation of bis(trifluoromethylphenyl)-*o*-(1,1′-biphenyl)phosphine **89** in the presence of $Pd(OAc)_2$, in [$d_6$]-toluene, the final dibenzophosphole **90** being obtained in 41% yield (Scheme 18).[37]

In the phosphine **91**, carrying one $CF_3C_6H_4$ group and one phenyl, a mixture of dibenzophosphole oxides **66** and **92** was obtained upon oxidation with $H_2O_2$, indicating a preference of the P–$CF_3C_6H_4$ bond cleavage over the unactivated P–$C_6H_5$ unit (Scheme 19).[37]

Another modification of this approach involved the synthesis of the starting phosphine *via* the Suzuki–Miyaura cross-coupling of *o*-bromophenyldiphenylphosphine with 2,4-dimethoxyphenylboronic acid, followed by cyclisation *in situ*, without isolation, to give the final dibenzophosphole oxide.[37]

Satoh and Miura *et al.* described the transformation of phenylphosphinothioic amides into fused dibenzophosphole

 

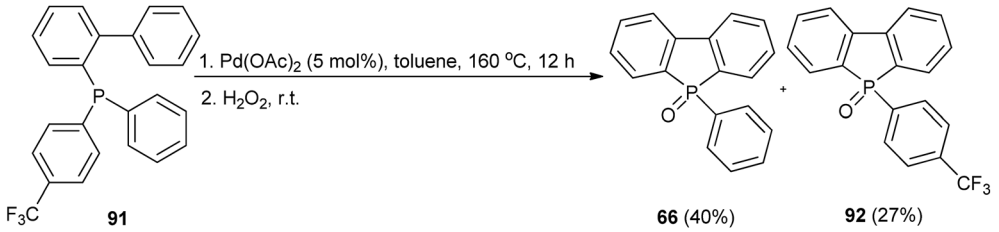


Scheme 19

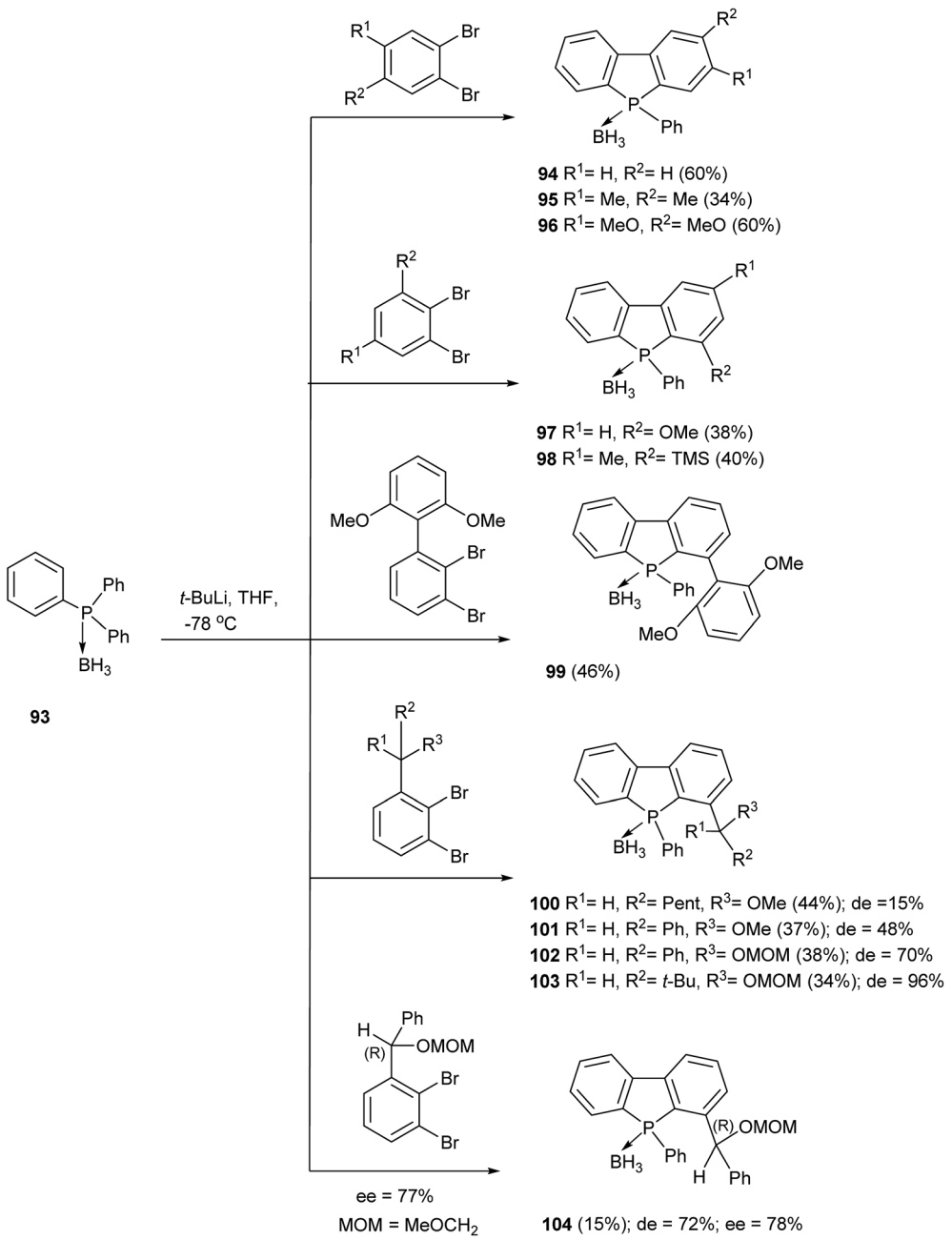


Scheme 20

derivatives through rhodium-catalyzed coupling with heterobicyclic alkenes and intramolecular phospha-Friedel–Crafts reactions in a one-pot manner.[38]

### 2.4. From $Ar_3P$–$BH_3$

Jugé, Leroux, Colobert *et al.* reported the first chemo-, regio-, and diastereoselective syntheses of P-chirogenic dibenzophosphole boranes **94–104** based on a transition metal-free, aryne cross-coupling methodology. Most of the reactions started from the tertiary phosphine-borane **93** and a variety of *o*-dibromobenzenes to simultaneously create an aryl–aryl bond and the five-membered ring of the dibenzophosphole moiety in 15–60% yields (Scheme 20).[36]

The use of P-modified boranes **105** in which $R^3$ or $R^4$ = Ph has been replaced by *tert*-butyl (*t*-Bu), cyclohexyl (Cy) or *ortho*-anisyl (*o*-An) (2-$MeOC_6H_4$) groups did not improve yields of these reactions (27–44%). Interestingly, in the case of **105** ($R^3$ = Ph, $R^4$ = *o*-An), preferential P-*o*-An cleavage occurred to give **109** ($R^3$ = Ph) in 44% yield (Scheme 21).[36]

### 2.5. From $Ar_2P(O)H$ or $Ar(R)P(O)H$

Aryl or alkyl biphenyl hydrophosphine oxides have been applied successfully to the synthesis of 5-aryl and 5-alkyl substituted dibenzophosphole oxides. Thus, starting from secondary hydrophosphine oxides **110**, Kuninobu *et al.* obtained 5-aryl substituted dibenzophospholes **111–117** *via* phosphine–hydrogen and carbon–hydrogen bond cleavages in the presence of a catalytic amount of palladium(II) acetate (Scheme 22). This process was also carried out with [2-(2-naphthyl)phenyl]phenylphosphine oxide as a substrate to give the corresponding dibenzophosphole in 92% yield.[39]

The same methodology was applied to the synthesis of a mixture of 5-i-Pr substituted dibenzophospholes **120** and **121**. These compounds were obtained in a ratio of 70 : 30, respectively, starting from a mixture of nondeuterated and deuterated phosphine oxides **118** and **119** in the ratio 1 : 1. Based on these results, it could be assumed that the C–H bond activation of one of the aromatic rings was the rate-determining step (Scheme 23).[39]

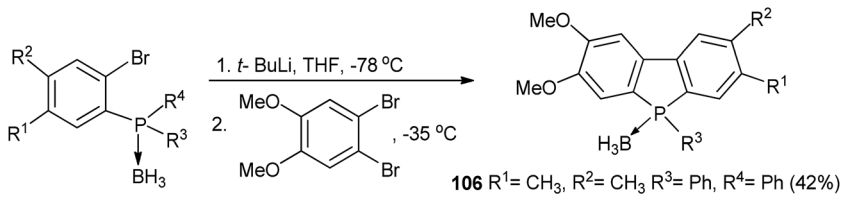


**105**

**106** $R^1$= $CH_3$, $R^2$= $CH_3$ $R^3$= Ph, $R^4$= Ph (42%)
**107** $R^1$= H, $R^2$= H, $R^3$= *t*-Bu, $R^4$= Ph (27%)
**108** $R^1$= H, $R^2$= H, $R^3$= Cy, $R^4$= Ph (33%)
**109** $R^1$= H, $R^2$= H, $R^3$= Ph, $R^4$= *o*-An (44%)

Scheme 21

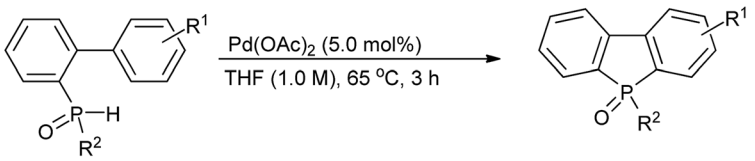


**110**

**111** $R^1$= H, $R^2$= Ph (94%)
**112** $R^1$= 4-MeO, $R^2$= Ph (93%)
**113** $R^1$= 4-$CF_3$, $R^2$= Ph (86%)
**114** $R^1$= 4-Cl, $R^2$= Ph (90%)
**115 a**,**b** $R^1$= 3-Me, $R^2$= Ph (90%)

**115a** :**115 b**= 88:12 (90%)

**116** $R^1$= 2-MeO, $R^2$= Ph (93%)
**117** $R^1$= 4-Ph, $R^2$= Ph (61%)

Scheme 22

 

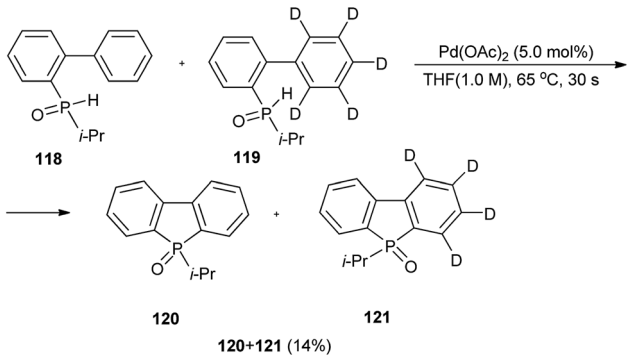


Scheme 23

Terphenyl bis(hydrophosphine oxide) **122** was also applied in the same manner by Kuninobu *et al.* for the synthesis of a polycyclic, conjugated bis(dibenzophosphole oxide) **123** in 87% yield (Scheme 24).[39]

Dibenzophospholes were also obtained by the intramolecular radical cyclisation of 2-biphenylaryl and biphenylalkylphosphine oxides **124–126** in the presence of various initiators: 2,2′-azobis-isobutyronitrile (AIBN), benzoyl peroxide (BPO) or $Et_3B/O_2$ under different reaction conditions. In the case of the phosphine oxide **124** (R = Ph), the use of typical initiators, such as AIBN and BPO in refluxing benzene, gave the corresponding products **127** in 48% and 41%, according to procedures A and B, respectively. Performing the reaction under milder conditions by using triethylborane and oxygen as a radical initiator gave **127** in higher yields of 73% and 87%, respectively (procedures C and D). These reaction conditions were applicable to other substrates **125** and **126** bearing *p*-anisyl and *tert*-butyl groups on the phosphorus atom, respectively to give the corresponding products **128** and **129** in good 96% and 85% yields, respectively (Scheme 25).[40]

This radical methodology has also been applied to the synthesis of bis(dibenzophosphole oxides) having spatially extended systems of π-conjugated bonds, by using a double, intramolecular radical cyclisation of the phosphine oxide **130** in the presence of $Et_3B/O_2$, in MeOH. The products of this reaction were two diastereoisomeric bis(dibenzophosphole oxides): **131**-*anti* and **132**-*syn* obtained in 16% and 28% yields, respectively (Scheme 26).[40]

### 2.6. From $Ar_3P(O)$ or $ArR_2P(O)$

In this subsection, the syntheses of dibenzophospholes that are described start from phosphine oxides containing at least one aryl group. In 2014, Cui, Jiang *et al.* developed a new method for the synthesis of dibenzophosphole oxides **134–142**

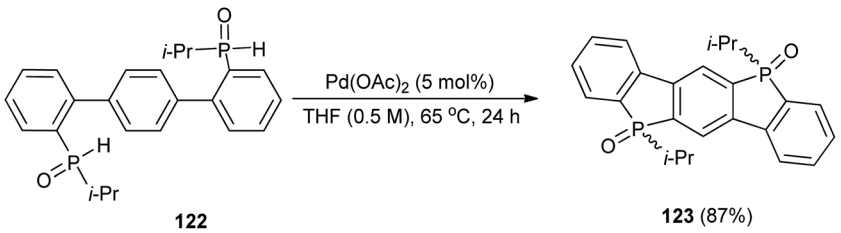


Scheme 24

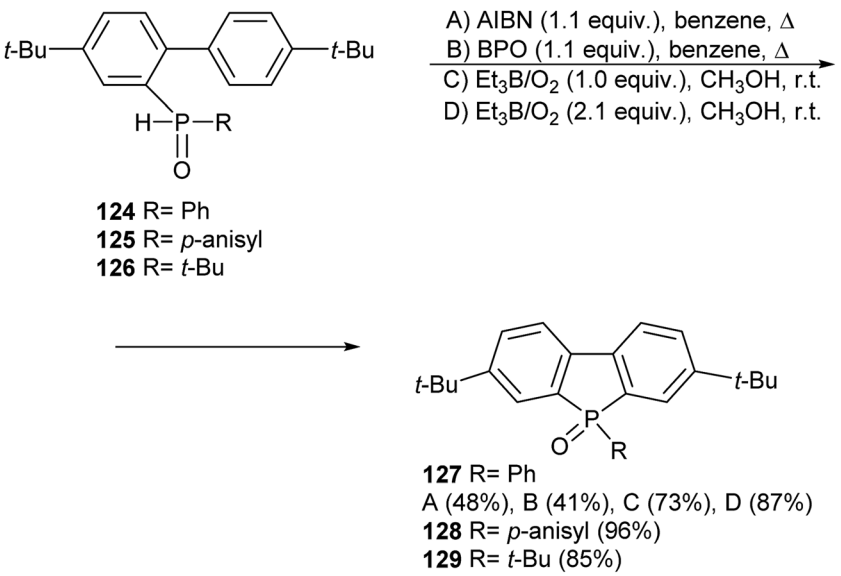


Scheme 25

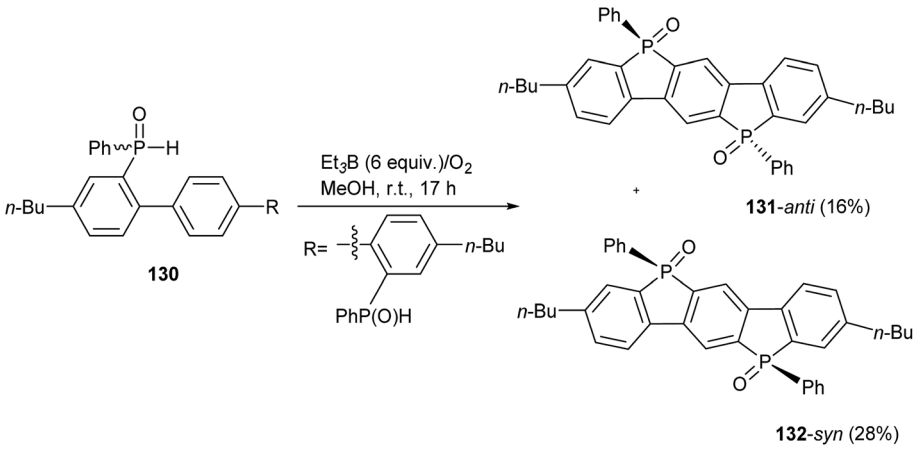


Scheme 26

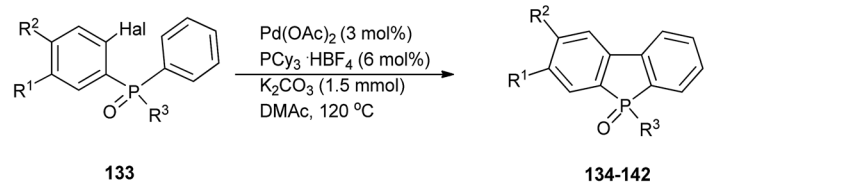


**134** $R^1$= H, $R^2$= H, $R^3$= Ph, Hal= Br (98%)
**135** $R^1$= H, $R^2$= H, $R^3$= Ph, Hal= Cl (97%)
**136** $R^1$= H, $R^2$= Me, $R^3$= Ph, Hal= Br (85%)
**137** $R^1$= MeO, $R^2$= H, $R^3$= Ph, Hal= Br (96%)
**138** $R^1$= H, $R^2$= Cl, $R^3$= Ph, Hal= Br (94%)
**139** $R^1$= H, $R^2$= F, $R^3$= Ph, Hal= Br (97%)
**140** $R^1$= H, $R^2$= $EtO_2C$, $R^3$= Ph, Hal= Br (90%)
**141** $R^1$= H, $R^2$= NC, $R^3$= Ph, Hal= Br (83%)
**142** $R^1$= H, $R^2$= H, $R^3$= *i*-Pr, Hal= Br (94%)

Scheme 27

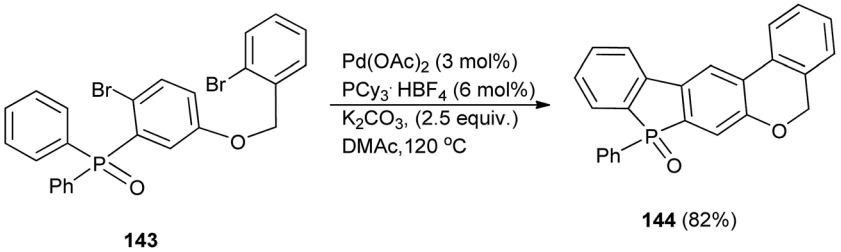


Scheme 28

from the readily available *ortho*-halodiarylphosphine oxides **133** by use of $Pd(OAc)_2$ as a catalyst complexed with $PCy_3$ leading to intramolecular palladium-catalysed arylation (Scheme 27).[41]

An intramolecular double arylation catalysed by $Pd(OAc)_2$ was applied to the synthesis of polycyclic dibenzophosphole oxide **144** starting from the dibromo derivative **143** in 82% yield (Scheme 28).[41]

Another intramolecular version of the double arylation was realised by the same research group starting from diaryl-2,5-dibromophosphine oxide **145** and arylboronic acids or heteroarenes. Here, the phosphine complexed $Pd(OAc)_2$ as a catalyst brought about the intramolecular arylation and, in the same pot, afforded further functionalised dibenzophosphole oxides **146–152** in 75–87% yields by a Suzuki–Miyaura cross-coupling (**146–148**) or direct cross-coupling with a heteroarene (**149–152**) (Scheme 29).[41]

Ishikawa and Manabe obtained the dibenzophosphole **154** in 35% yield by an intramolecular heteroaromatic electrophilic substitution reaction of the phosphine oxide **153** in the presence of triflic anhydride $Tf_2O$ in pyridine. In this reaction, the oxygen atom of the phosphoryl group first reacted with triflic anhydride $Tf_2O$ to generate an electrophilic intermediate and this was followed by electrophilic aromatic ring closure enhanced by the electron-releasing hydroxyl group; final OH/OTf conversion afforded **154** in 35% yield (Scheme 30).[42]

 

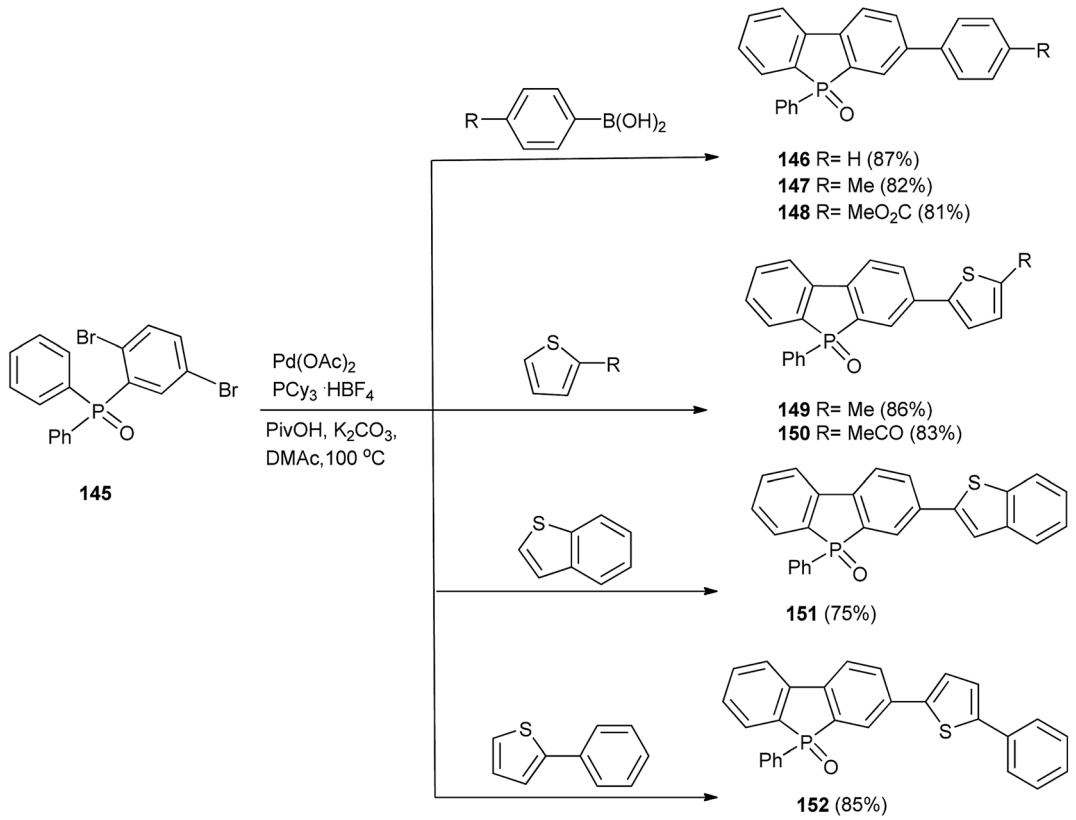


Scheme 29

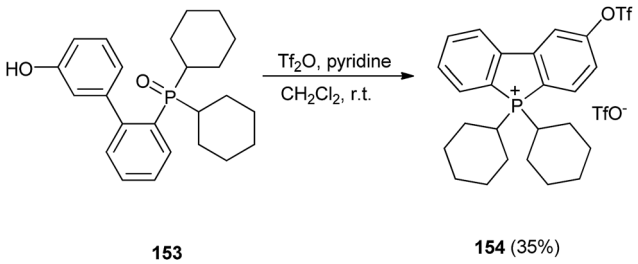


Scheme 30

Stankevič *et al.* synthesised a new group of bulky 5-*tert*-butyldibenzophosphole 5-oxides from acyclic diaryl-*tert*-butylphosphine oxides and organolithiums.[43]

Other syntheses of dibenzophospholes starting from phosphine oxides of type $ArR_2P(O)$ and $R_3P(O)$ are described in the subsection 2.7.

### 2.7. From $R_2P(O)CH_3$ or $R_2P(O)OCH_3$

Tanaka *et al.* synthesized enantioenriched benzopyrano- or naphthopyrano-fused helical dibenzophosphole oxides **156**, **157**, **160**, **161**, **165** by the rhodium-catalyzed, enantioselective, double [2+2+2] cycloaddition of methyl dialkynylphophinates **155** ($R^2$ = OMe) with phenol or naphthol-linked tetraynes in 16–40% yields. In a similar way, dialkynyl methyl and phenyl phosphine oxides **155** ($R^2$ = Me, Ph) were employed to afford **158**, **159**, **162**, **163**, **164** and **165** in 30–59% yields (Scheme 31).[44]

Synthesis of dibenzophospholes from aryl substituted phosphine oxides $Ar_3P(O)$ and $ArR_2P(O)$ has been described in the previous subsection 2.6.

### 2.8. From $(RO)_3P(O)$

Only one synthesis of dibenzophospholes has been reported starting from organic phosphates. The spirobiphosphoniafluorene **167** was obtained by the reaction of the dilithio derivative, obtained from the 2,2′-dibromo-1,1′-biphenyl **38**, with triphenyl phosphate followed by I/$BAr_4$ counterion exchange, in 32% yield (Scheme 32).[32]

### 2.9. From $Ar_3P{=}N{-}R$

Synthesis of dibenzophospholes utilizing organophosphorus reagents containing a P=Y bond, where Y is a heteroatom (Y = N, P) other than oxygen, sulfur or selenium are also rare transformations. Nief *et al.* obtained dibenzophospholes by transmetalation of the intramolecularly stabilized lithium derivative **171** to give the potassium salt **172**, followed by intramolecular nucleophilic attack of the latter on the phenyl ring to form the intermediate **173**. Further aromatization by deprotonation with PhK produced the potassium salt of the 5-amino-dibenzophosphole **174** (R = *n*-Bu) as a white, insoluble solid. The starting lithium derivative **171** was obtained *via* NH and CH deprotonation of the phosphonium bromide **170** followed by *ortho*-lithiation of one of the phenyl rings with *n*-butyllithium in toluene/hexane. The phosphonium bromides

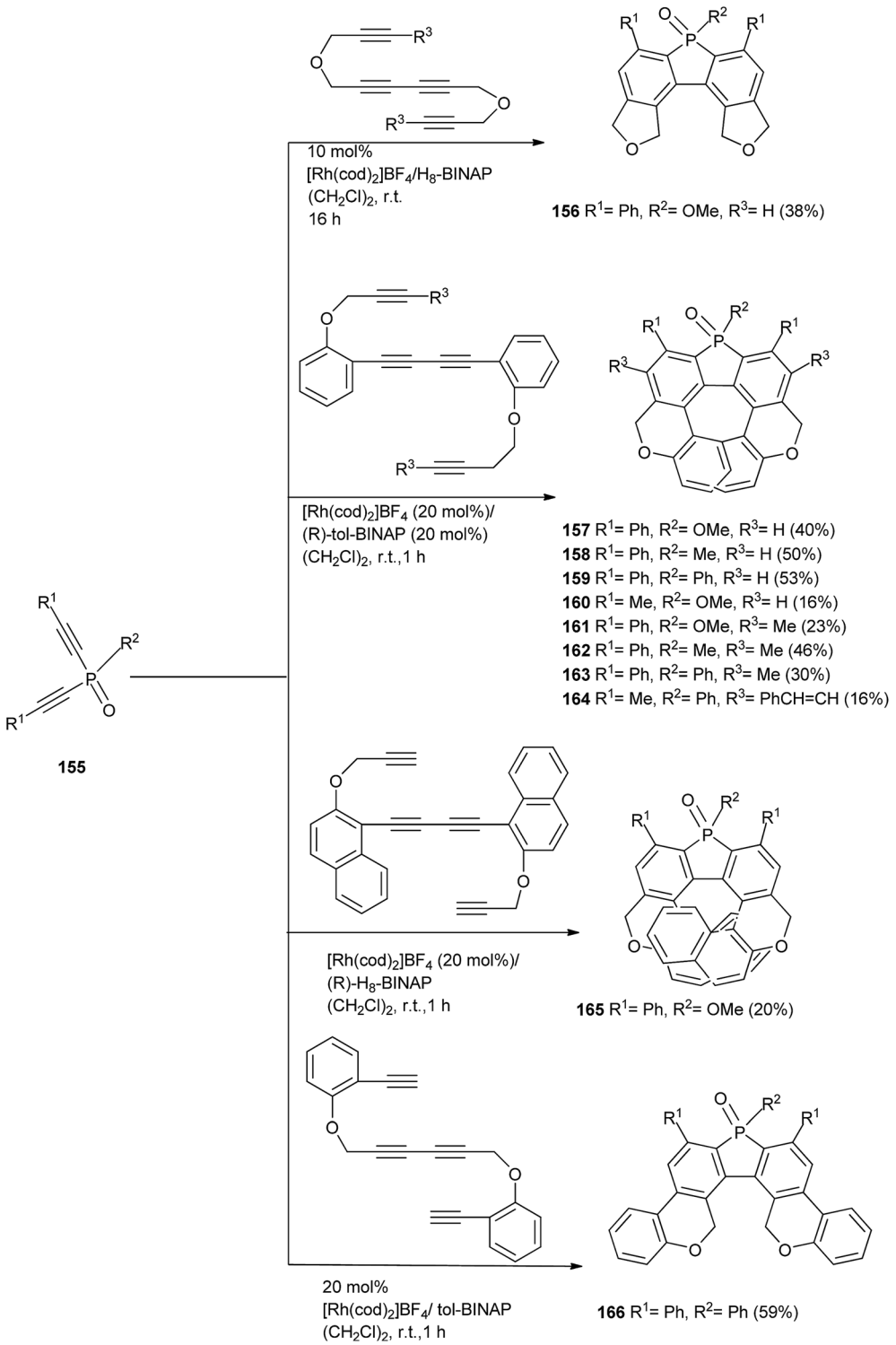


Scheme 31

**170** were synthesized from triphenylphosphine **168** and primary alkyl amines (R = *t*-Bu, i-Pr, *n*-Bu) (Scheme 33).[45]

### 2.10. From ArP=PMe$_3$

Simpson, Protasiewicz *et al.* obtained a sterically hindered dibenzophosphole **176** by photolysis of the phosphorane derivative **175** in 90% yield (Scheme 34).[46]

### 2.11. From phospholes and benzophospholes

An interesting synthesis of dibenzophospholes and their heteroaromatic analogs, in which one benzene moiety was replaced by thiophene, furan, pyrrole or indole, was presented by Mathey *et al.* using a classical 7-phosphanonorbornadiene route developed by this group. First, 3,4-dimethyl-1-cyanophosphole **177** was converted into the phospha-

 

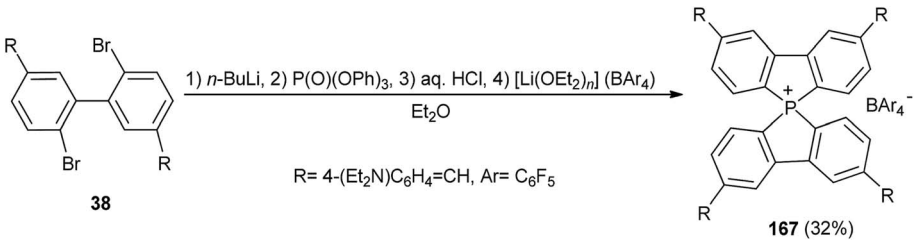


Scheme 32

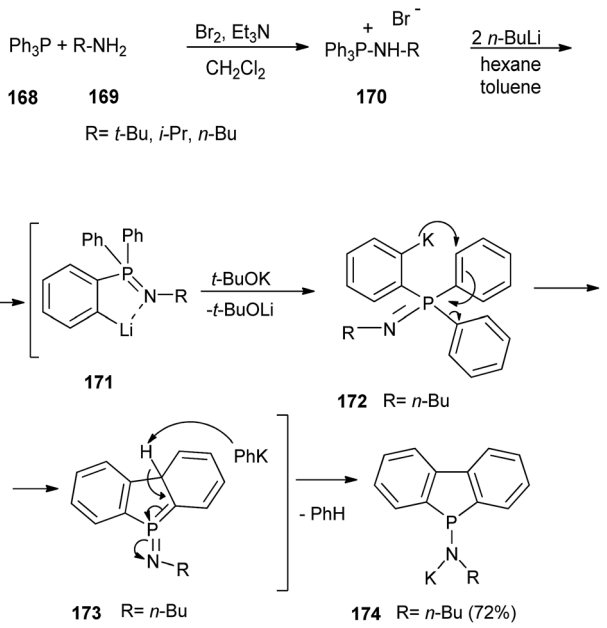


Scheme 33

norbornadiene **178** in a three-step sequence involving a replacement of the CN groups by the corresponding $Ar^1$–$Ar^2$–Li derivative followed by metalation with $W(CO)_5$-(MeCN) and cycloaddition of the resulting phosphole with acetylenedicarboxylate. Next, thermolysis of **178** gave tungsten complexes of the dibenzophospholes **180–184** in 60–72% yields, as a result of insertion of the electrophilic phosphinidene intermediate **179** into a C–H bond using carbene-like chemistry (Scheme 35).[47]

Nyulászi, Hissler, Réau *et al.* obtained the air-stable dibenzophosphole sulfide **186** and the dibenzophosphole oxide **187** under aerobic irradiation (320–400 nm) of dilute toluene solutions of 1-phenyl-2,3,4,5-tetra(3-thienyl)thiooxophosphole **185** (Y = S) and 1-phenyl-2,3,4,5-tetra(3-thienyl)-oxophosphole **185** (Y = O) containing a catalytic amount of iodine, in 10% and 26% yields, respectively (Scheme 36).[48]

The photocyclisation of **188**, using the Katz-modified approach, gave a mixture of the monocyclised derivative **189** and the fully cyclised target dibenzophosphapentaphene **190**, in 50% and 20% yields, respectively after separation. Then, treatment of **190** with methyl triflate afforded the phospholium salt **191** in 60% yield. The final phosphapentaphene **192** was obtained by desulfurisation of the latter with $P(NMe_2)_3$, in 50% yield (Scheme 37).[49]

Another method, reported by Matano *et al.* is the cycloaddition of alkynes to biaryls containing a benzophosphole unit, catalysed by palladium(II) acetate, in the presence of pivalic acid (PivOH) and $Bu_4NBr$. The examples of this method are with compounds **193** (Y = S, NMe) and 4-octyne, in which the authors obtained polycyclic aromatic compounds **195** and **196** containing dibenzophosphole oxide and dibenzothiophene or carbazole units in 14% and 53% yields, respectively (Scheme 38).[44]

# 3. Functionalisation of dibenzophospholes

Dibenzophospholes can be functionalised at the phosphorus atom and on the two peripheral benzene rings. The functionalisation can be achieved during synthesis of the dibenzophosphole rings or as a result of post-ring-synthesis modifications.

### 3.1. Functionalisation at phosphorus atom

One of the most important features of the phosphole ring is a low degree of aromaticity and easy availability of a free electron pair on the phosphorus atom, which enables chemical

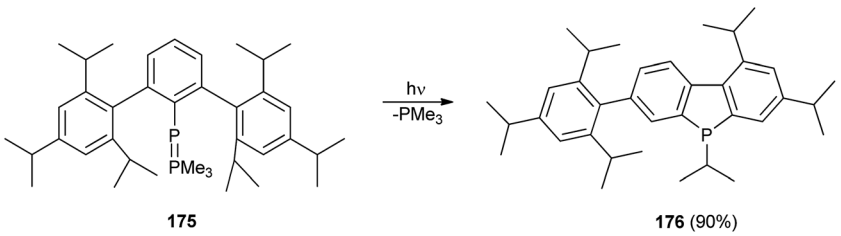


Scheme 34

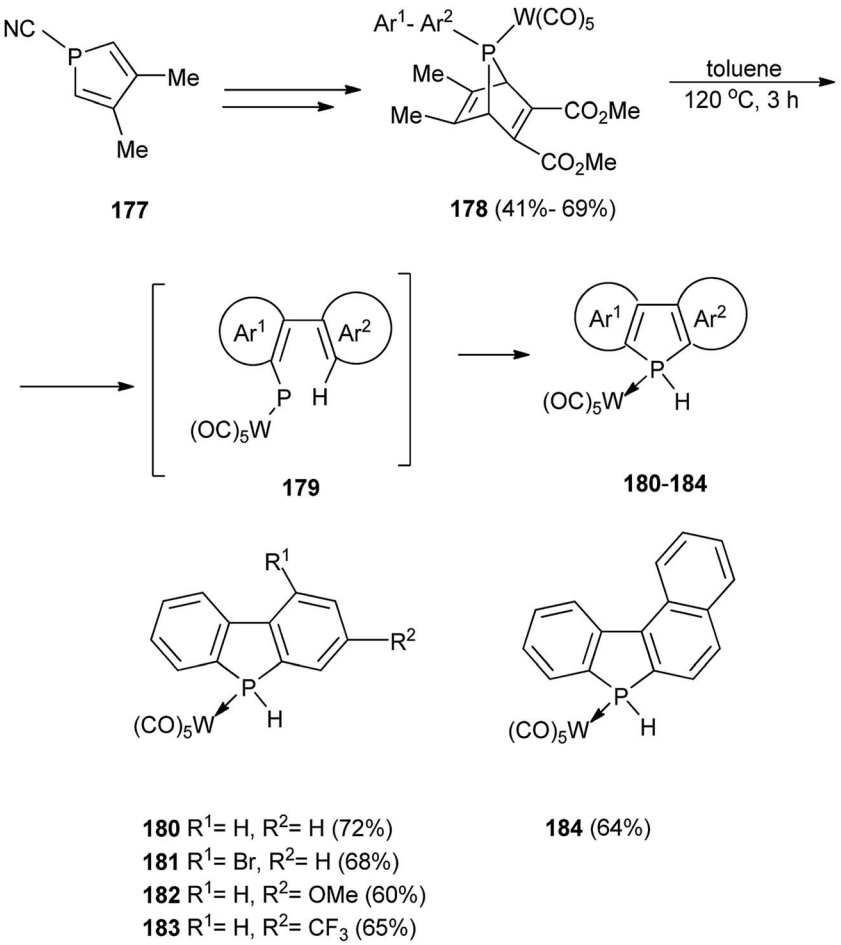


Scheme 35

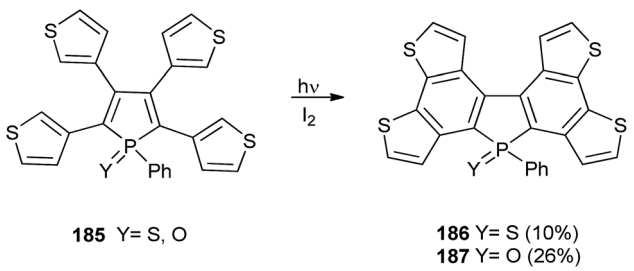


Scheme 36

modifications of phospholes by oxidation, sulfurization (addition of elemental sulfur), metalation or quaternization. This is due to the fact that tricoordinate phosphorus atom assumes a pyramidal geometry and the lone electron pair at the phosphorus atom has a high degree of s orbital character. These two properties limit the effective interaction between the lone electron pair and the conjugated π-electron system of the phosphole ring.

**3.1.1. Oxidation.** Oxidation of trivalent phosphorus in dibenzophospholes to the corresponding oxides includes direct methods with oxidizing reagents and indirect ones *via* phosphonium salts or iminophosphoranes.

Stelzer, Sheldrick *et al.* obtained 5-phenyl-2-2′-bis(sulfonato)-5*H*-dibenzophosphole-5-oxide dipotassium salt **197** directly in 92% yield by treating an aqueous solution of the salt **11** with hydrogen peroxide (Scheme 39).[26]

The dibenzophosphole tripotassium salt **199** was obtained by reaction of 5,5′-bis(sulfonato)-2,2′-difluoro-1,1′-biphenyl dipotassium salt **10** with $PH_3$ using DMSO/KO*t*Bu as a basic medium. In this reaction, the tripotassium salt **198** was formed first and next reacted with hydrogen peroxide to give **199** in 41% yield (Scheme 40).[26]

Other examples of the direct oxidation are reactions of substituted 5-phenyldibenzophospholes **200** with hydrogen peroxide in diethyl ether which gave the corresponding oxides **1**, **23** and **24** in 85%, 83% and 86% yields, respectively (Scheme 41).[51]

The same reagent was employed in the synthesis of fully perfluorinated dibenzophosphole oxide **202** starting from the dibenzophosphole **201** in dichloromethane. Symmetrical diphenyl-, dithienyl- and diphenylethynyl-substituted hexafluorodibenzophosphole oxides **203–205**, could also be obtained in 25%, 60% and 50% yields, respectively (Scheme 42).[52]

The conversion of P-phenyl into P-alkyl using 5-phenyldibenzophosphole **1** followed by P-oxidation to give the

 

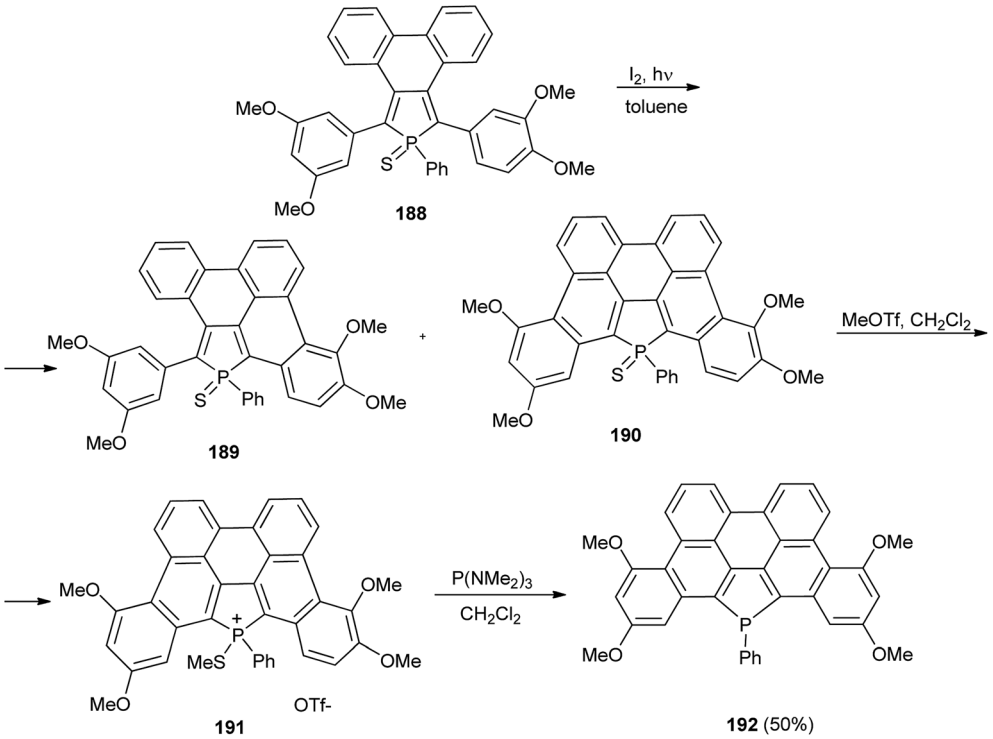


Scheme 37

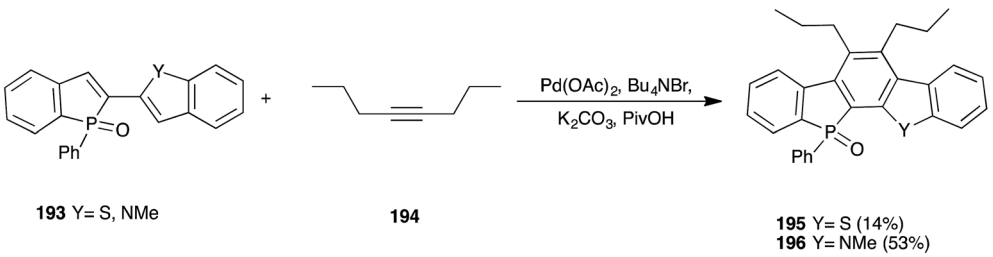


Scheme 38

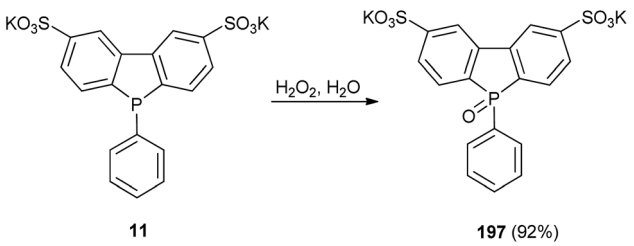


Scheme 39

corresponding oxides has been realized by Durán *et al.* Thus, the reaction of **1** with lithium in tetrahydrofuran delivered a P-lithium derivative, which was first reacted with methyl iodide or ethyl bromide and then was oxidised with hydrogen peroxide. The final oxides **206** and **207** were obtained in 96% yields (Scheme 43).[53]

In contrast, treatment of **1** with lithium and direct oxidation of the resulting P-lithium salt with peracetic acid ($H_2O_2$/AcOH) at 45 °C led to the corresponding phosphinic acid **208** in 63% yield (Scheme 44).[54]

Hissler, Réau *et al.* oxidized the phosphorus atom in the dibenzophosphapentaphene **192**, containing a fused dibenzophosphole moiety, with sodium metaperiodate ($NaIO_4$) in dichloromethane giving the corresponding oxide **209** in 70% yield (Scheme 45).[49]

Chi, Chou and Chang *et al.* modified 5*H*-dibenzophosphole **211**, which was synthesised *in situ* from 5-phenyl dibenzophosphole, by the cross-coupling reaction of the P–H bond with aryl bromide **210** in the presence of CuI as a catalyst, was followed by oxidation of the resulting intermediate with $H_2O_2$ to give 5-[4-(carbazo-9-yl)phenyl]dibenzophosphole 5-oxide **212** in 34% yield (Scheme 46).[55]

**3.1.2. Reduction of P═O and P═N bonds.** Diphenylsilane was used by Delft *et al.* in reduction of the P═O bond in dibenzophosphole oxides **213** in [$d_8$]-1,4-dioxane, at 100 °C to give 5-phenyldibenzophosphole **1**, 2,8-dimethoxy-5-phenyldiben-

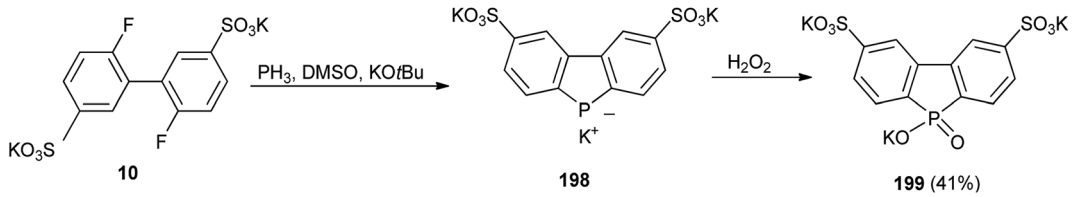


10 198 **199** (41%)

Scheme 40

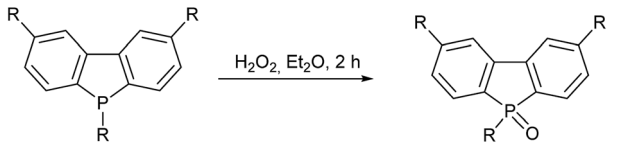


**200**

**1** R= H (85%)
**23** R= OMe (83%)
**24** R= CF3 (86%)

Scheme 41

zophosphole **23** and 5-phenyl-2,8-bis(trifluoromethyl)-dibenzophosphole **24** in 19–55% yields (Scheme 47).[51]

Delft *et al.* also reduced dibenzophosphole iminophosphoranes **214**, by means of diphenylsilane in [$d_8$]-1,4-dioxane at 101 °C producing the corresponding dibenzophospholes **1** or **23**. For the compound **23** (R = MeO), the reduction of the P=N bond was faster, than for the unsubstituted compound **1** (R = H) (Scheme 48).[56]

The same research group used diphenylsilane $Ph_2SiH_2$ for reduction of the water-sensitive P=N bond in the dibenzophosphole iminophosphorane **215** which was obtained in the Staudinger reaction of **1** with benzyl azide. Much faster reduction was observed with $PhSiH_3$. Other alkyl, cycloalkyl, allyl and aryl azides were also employed in the Staudinger reaction with a catalytic amount (10% mol) of the dibenzophosphole **1**. This methodology was utilised practically in the synthesis of primary

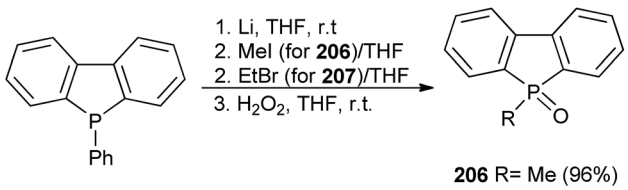


**1**

**206** R= Me (96%)
**207** R = Et (96%)

Scheme 43

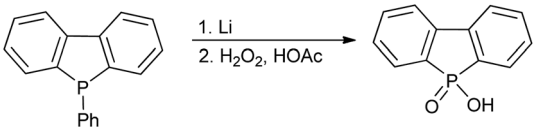


**1** **208** (63%)

Scheme 44

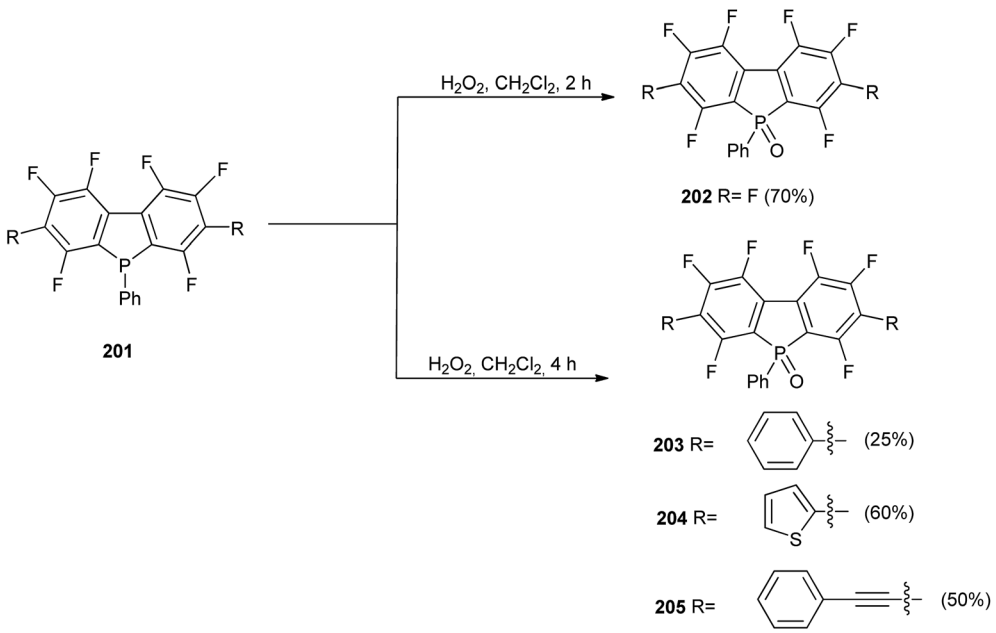


**201** **202** R= F (70%)

Scheme 42

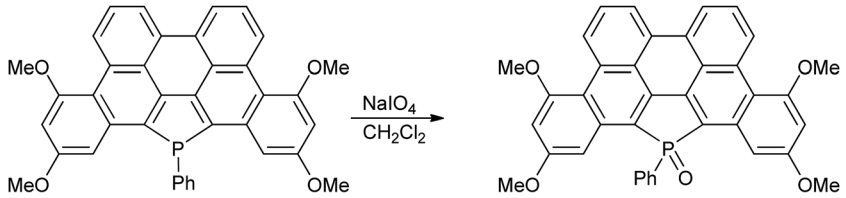


**192** **209** (70%)

Scheme 45

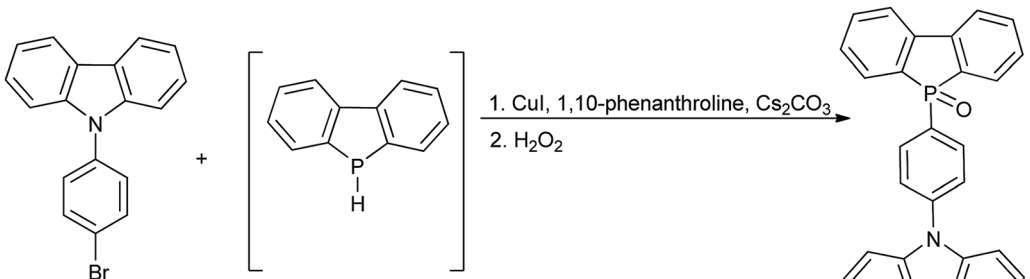


**210** **211** **212** (34%)

Scheme 46

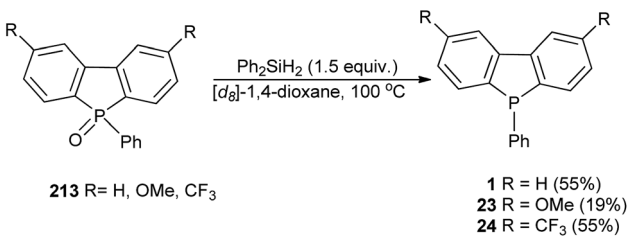


**213** R= H, OMe, $CF_3$

**1** R = H (55%)
**23** R = OMe (19%)
**24** R = $CF_3$ (55%)

Scheme 47

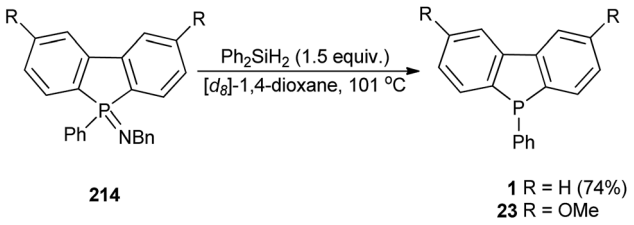


**214**

**1** R = H (74%)
**23** R = OMe

Scheme 48

amines *via* intermediate iminophosphoranes **215** which could be easily hydrolysed with $H_2O$ to the dibenzophosphole oxide **66** (Scheme 49).[57]

López-Calahorra *et al.* used trichlorosilane in toluene to reduce dibenzophosphole oxides **216** to dibenzophospholes **217–219**. The dibenzophosphole **217** was isolated as a colorless oil in 93% yield while **218** and **219** were directly converted into the corresponding cyclopalladates due to a rapid oxidation in air (Scheme 50).[58]

Further examples of reduction of dibenzophosphole oxides are described in subsection 3.1.5 (Schemes 57 and 59).

**3.1.3. Sulfurization.** In 2012, Hissler, Réau *et al.* obtained the dibenzophosphapentaphene sulfide **190** by the reaction of $\sigma^3,\lambda^3$-dibenzophosphapentaphene **192** containing in its fused structure a dibenzophosphole unit, with $S_8$ in triethylamine, in 20% yield (Scheme 51).[49]

The dibenzophosphole sulfides **220**-*anti* and **221**-*syn* were prepared by conversion of the corresponding oxides **131**-*anti* and **132**-*syn* with Lawesson's reagent in toluene. X-ray studies confirmed two, almost flat P-terphenyl units of the ladder-type. These compounds were obtained in 67% and 54% yields, respectively (Scheme 52).[40]

Voituriez and Marinetti *et al.* obtained the phosphine sulfide **223** from the corresponding oxide **222** ($R_p$) by using Lawesson's reagent, in 79% yield. Photolysis of compound **223** afforded the helicene **224**, with M helical configuration, as the major product in 50% yield (Scheme 53).[33]

A ferrocene-containing dibenzophosphole sulfide **226** was obtained in the reaction of 5-cyanophosphole **225** with *t*-butyllithium followed by treatment of the resulting 5-P lithium derivative with a ferrocene (FER) derivative and addition of elemental sulfur. The final product was further converted into the corresponding aldehyde which was then reduced to a primary alcohol (Scheme 54).[59]

**3.1.4. Selenylation.** A series of substituted dibenzophosphole selenides **228–232** was obtained by addition of elemental selenium to the corresponding dibenzophosphole derivatives **227**. Since the reaction was carried out in deuterated

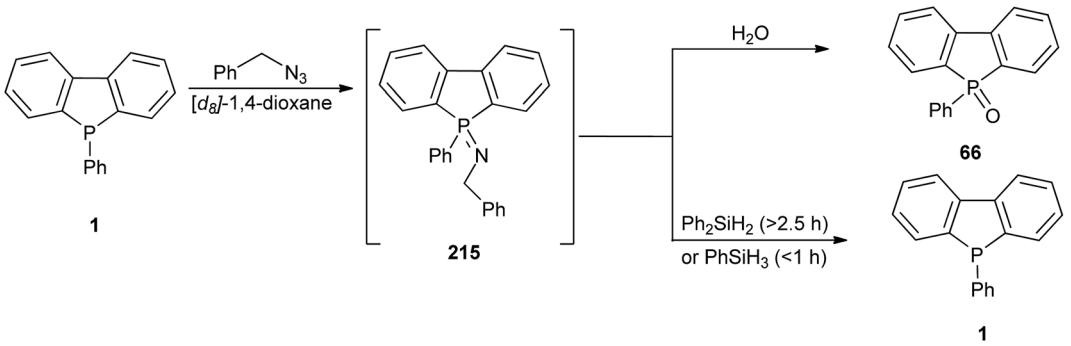


**1** **215** **66** **1**

Scheme 49

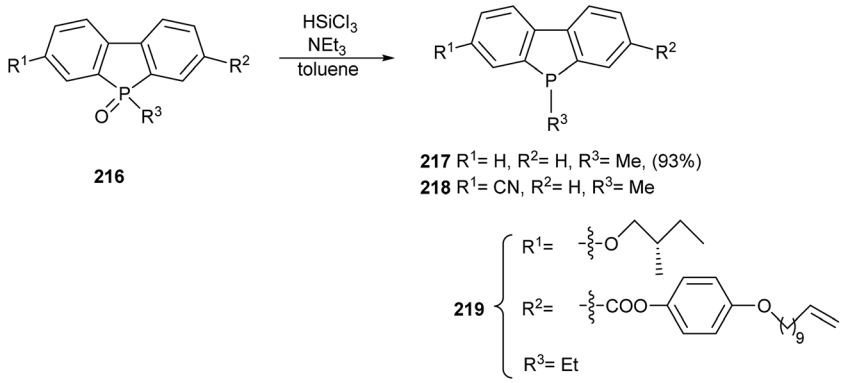


**216**

**217** $R^1$= H, $R^2$= H, $R^3$= Me, (93%)
**218** $R^1$= CN, $R^2$= H, $R^3$= Me

**219** $R^1$=  $R^2$=  $R^3$= Et

Scheme 50

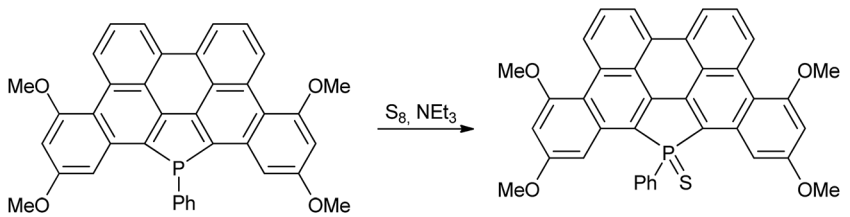


**192** **190** (20%)

Scheme 51

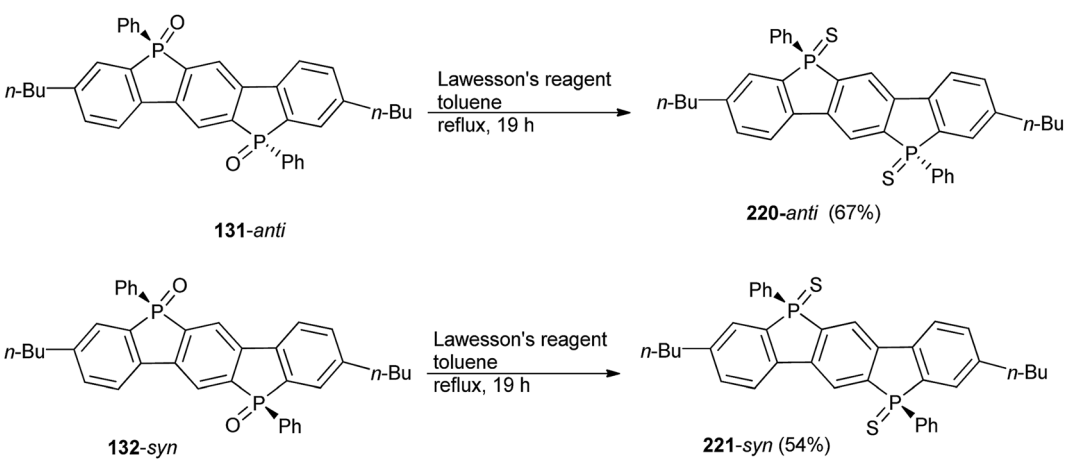


**131**-*anti* **220**-*anti* (67%)

**132**-*syn* **221**-*syn* (54%)

Scheme 52

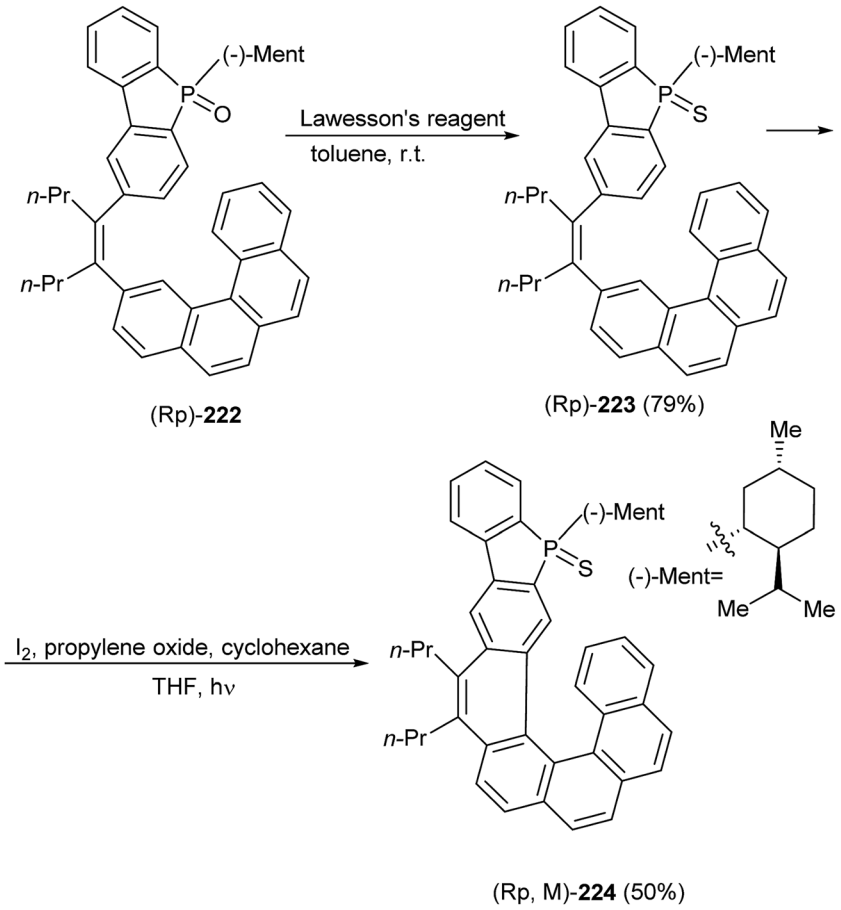


Scheme 53

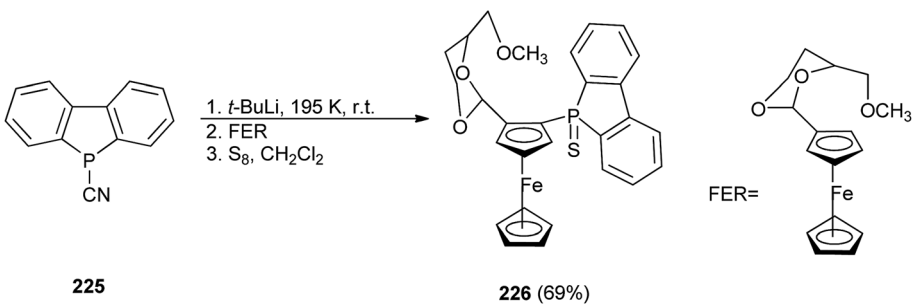


Scheme 54

chloroform, at room temperature, in an NMR tube, the yields of this reaction were not determined (Scheme 55).[31]

**3.1.5. Metalation.** The dibenzophosphole binding with metals *via* the phosphorus atom requires either a direct availability of a dibenzophosphole $P^{III}$ atom or reduction of $P^{IV}$ to $P^{III}$ atom prior to the binding so that the P-electron pair is available to interact with a metal. Thus, the reduction of the P-phenyl substituted helicene dibenzophosphole oxide ($R_p$,M) **233** with $HSiCl_3/Et_3N$ followed by reaction with a mixture of $NaAuCl_4 \cdot 2H_2O$ and 2,2′-thiodiethanol as a reducing agent, afforded the gold chloride complex ($R_p$,M) **234** in 46% yield (Scheme 56).[33]

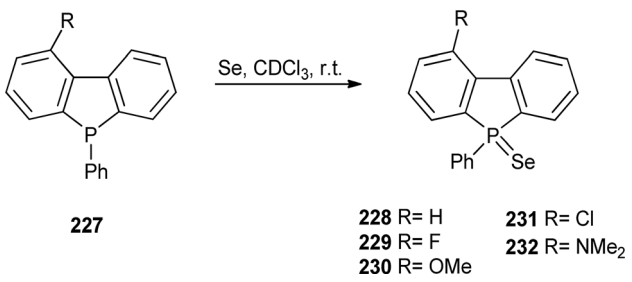


Scheme 55

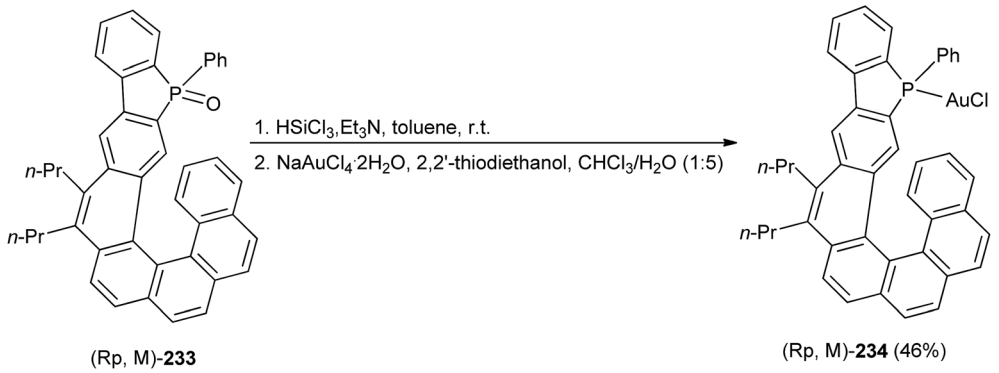


(Rp, M)-**233** (Rp, M)-**234** (46%)

Scheme 56

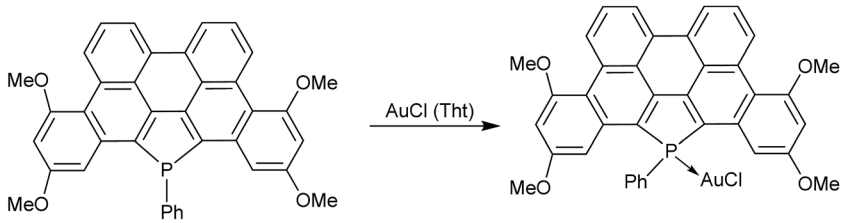


**192** **235** (75%)

Scheme 57

Another gold chloride complex **235** was obtained in the reaction of the dibenzophosphapentaphene **192** with chloro(tetrahydrothiophene) (Tht) gold(I) in 75% yield (Scheme 57).[49]

The P-menthyl substituted [6]helicene ($R_p$,P) **236** was reduced under analogous conditions and reacted with [{Ir(cod)IrCl}$_2$] (cod = 1,5-cyclooctadiene) to give the helicene **237** in 37% yield (Scheme 58).[33]

The dibenzophosphole Fe-complex **239** was obtained in the reaction of 6-substituted dibenzophosphole **238** with $Fe_2(CO)_9$ after crystallisation from benzene, in 76% yield. Analogously, the Ru-complex **240** was obtained in 68% yield after crystallization from chloroform (Scheme 59).[35]

In 2002, Decken *et al.* obtained Fe-complexes **242** and **243** from dibenzophospholyl-Li **241** and $CpFe(CO)_2X$ (X = Br, I) in THF, at room temperature, in 93% and 87% yields, respectively. Heating **242** or **243** in refluxing xylenes resulted in the formation of trace amounts of **244** as well as large amounts of intractable green solids, however, in the reaction of bis(1,1′-dibenzophospholyl) **245** and $Cp_2Fe_2(CO)_4$ in refluxing xylenes a mixture of *cis*- and *trans*-isomers **244** was obtained in a 1 : 15 ratio, in 75% yield (Scheme 60).[60]

The same research group obtained ($\mu_2$-dibenzophospholyl)-($\mu_2$-bromo)-dimanganese-octacarbonyl **246** from dibenzophospholyl-Li and $Mn(CO)_5Br$ in THF in 69% yield (Scheme 61).[61]

The bis($\mu_2$-dibenzophospholyl)-dimanganese-octacarbonyl **247** was obtained by heating of bis(1,1′-dibenzophospholyl) **245** and $Mn_2(CO)_{10}$ in refluxing xylenes in 78% yield. The same compound was formed by refluxing ($\mu_2$-dibenzophospholyl)-($\mu_2$-bromo)-dimanganese-octacarbonyl **246** in the same solvent (Scheme 62).[61]

A mixture of (1-phenyldibenzophosphole)-dimanganese-nonacarbonyl **248** and di(1-phenyldibenzophosphole)-

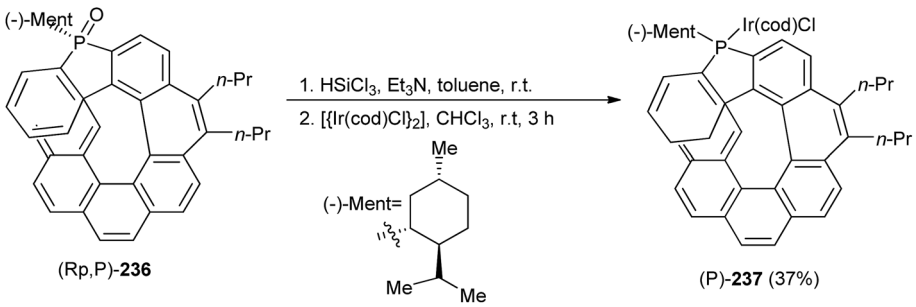


(Rp,P)-**236** (P)-**237** (37%)

Scheme 58

 

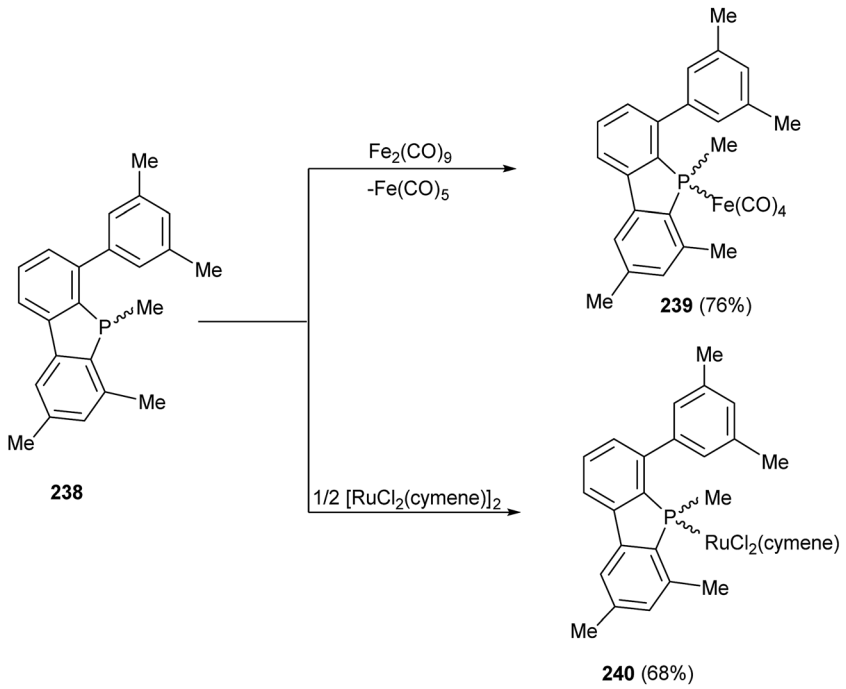


Scheme 59

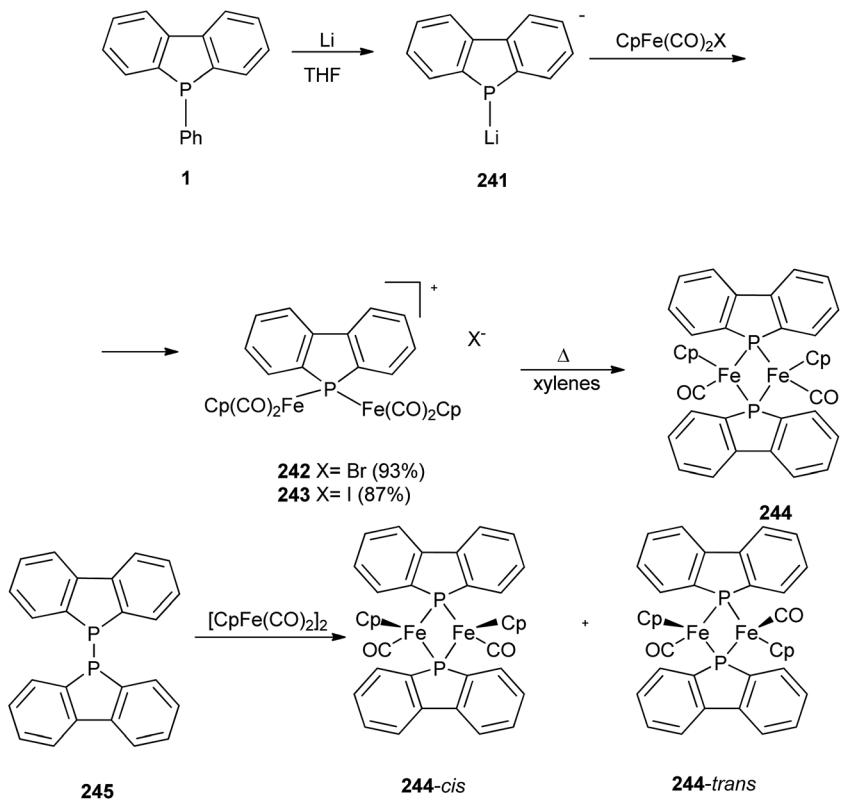


Scheme 60

dimanganese-octacarbonyl **249** was obtained by reaction of 5-phenyldibenzophosphole **1** with dimanganese decacarbonyl in xylenes, in 17% and 13% yields, respectively. ($\eta^1$-Dibenzophospholyl)tris(dimethylamido)titanium **250** was formed by a reductive cleavage of the P–Ph bond in the 5-phenyldibenzophosphole **1** using potassium followed by

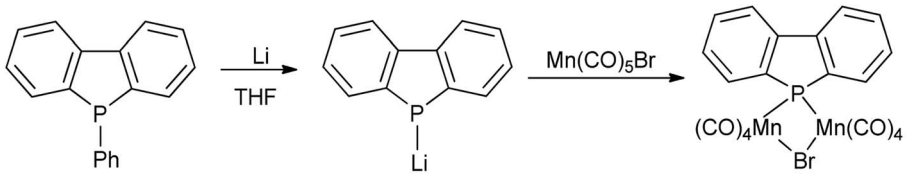


1 241 **246** (69%)

Scheme 61

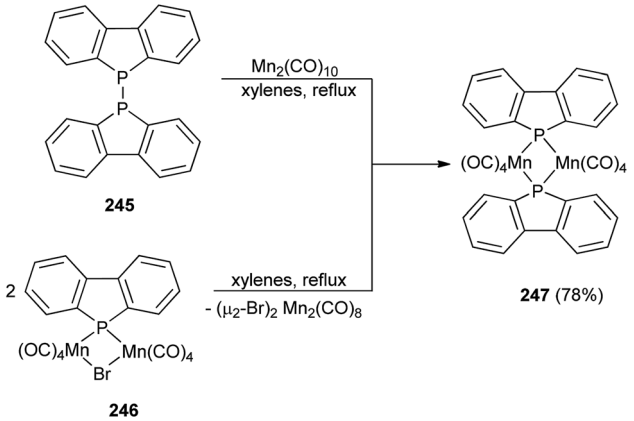


**245** **247** (78%) **246**

Scheme 62

a subsequent acidification with acetic acid and reaction with tetrakis(dimethylamido)titanium ($Ti(NMe_2)_4$) in 41% yield (Scheme 63).[53,61]

Jugé and Gouygou *et al.* obtained the dibenzophosphole Rh-complex **252** by reaction of chloro-(1,5-cyclooctadiene)rhodium(I) with the dibenzophosphole **251** in dichloromethane, in the presence of silver tetrafluoroborate, in 86% yield (Scheme 64).[62]

The dibenzophosphole Pd-complex **254** was formed in the reaction of the dibenzophosphole **253**, obtained from **211** and chlorodibenzotropilydene (toluene, reflux), with dichloro-(1,5-cyclooctadiene)palladium(II) ($Pd(cod)Cl_2$) in dichloromethane, at room temperature, in 95% yield (Scheme 65).[63]

López-Calahorra *et al.* synthesized the Pd-complexes **255–257** from dibenzophospholes **217–219** and an optically active dimeric cyclopalladium compound. The reaction of the dimer with the dibenzophosphole **217** gave the complex **255**. In the cases of **256** and **257**, a mixture of diastereomers was separated by column chromatography followed by decoordination of the dibenzophospholes by the reaction of the pure diastereomers with 1,2-bis(diphenylphosphino)ethane and oxidation of the enantiomerically pure dibenzophospholes to their oxides using $H_2O_2$ (Scheme 66).[58]

**3.1.6. P-Alkylation.** The dibenzophosphole sodium salt **13** obtained from 2,2′-difluoro-5,5′-disulfonato-1,1′-biphenyl **12** by treatment with $NaPH_2$ in liquid ammonia, was utilised as a reactive intermediate in reactions with electrophiles, such as benzyl chlorides and tosylates. Thus, coupling of the sodium salt **13** with 2,2′-bis(chloromethyl)-1,1′-biphenyl in DMF afforded the bidentate ligand **258** containing sulfonated dibenzophospholes moieties in 94% yield. Bis-[2,2′-bis(sulfonato)-5*H*-dibenzophospholyl]-2,3-*O*-isopropylidene-D-threitoltetrasodium salt **259** was obtained by reaction of the sodium salt **13** with 1,4-di-*O*-*p*-toluenesulfonyl-2,3-*O*-isopropylidene-D-threitol in 1,4-dioxane or THF in 20% yield (Scheme 67).[26]

The reaction of the lithium derivative **261** with (chloromethyl)phosphine borane **260**, in the presence of 5%

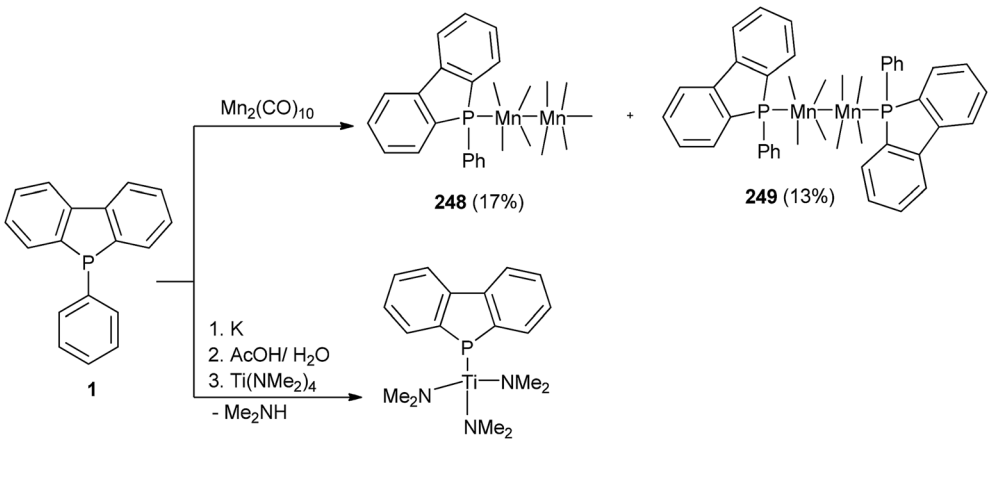


**248** (17%) **249** (13%)

1 **250**

Scheme 63

 

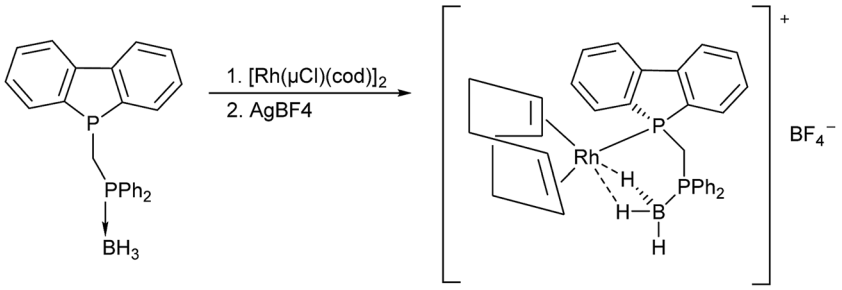


**251** **252** (86%)

Scheme 64

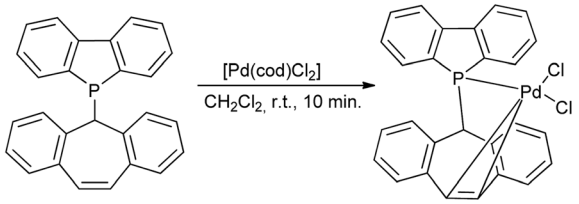


**253** **254** (95%)

Scheme 65

$Pd(OAc)_2$/dppf gave 5-diphenylphosphinylmethylene dibenzophosphole borane **251** in 52% isolated yield. Direct alkylation of **261** without the presence of the Pd catalyst gave **251** in <10% yield (Scheme 68).[62]

**3.1.7. P-Arylation.** P-Arylation of unsubstituted dibenzophospholes was realised by a two-step reaction starting with P–H deprotonation of the tungsten complex **180** followed by reaction with BrCN and then with PhLi afforded the tungsten P-arylated dibenzophosphole **262** in 26% yield. The final step involved removal of the $W(CO)_5$ tungsten moiety by heating with 1,1′-(1,2-ethanediyl)bis(1,1-diphenyl)phosphine in refluxing xylene to give 5-phenyldibenzophosphole **1** in 25% yield (Scheme 69).[47]

**3.1.8. P-Quaternisation.** The phosphorus atom in the dibenzophosphapentaphene **192** could be quaternised *via* the corresponding dibenzophosphapentaphene sulfide by reaction with methyl triflate to give **191**, or directly with MeOTf to give **263** in 45% yield (Scheme 70).[49]

### 3.2. Functionalisation of benzene units

The second method of functionalization of dibenzophospholes is introduction of substituents onto one or two benzene rings including functional group interconversions. An example of such a process is shown in Scheme 71. Electrophilic bromination of 5-ethyl-5*H*-dibenzophosphole 5-oxide **264** with bromine in acetic acid at 45 °C gave the 5-ethyl-3-bromo-5*H*-dibenzophosphole 5-oxide **265** in 53% yield followed by electrophilic nitration of the second benzene ring and reduction of the $NO_2$ to $NH_2$ group with iron under acidic conditions. Further diazotization with sodium nitrite in a cooled mixture of sulfuric acid and water led to the corresponding diazonium salt which was decomposed by addition of copper(I) oxide in the presence of copper(II) nitrate. Subsequent reaction of the phenolic OH group so formed with (*S*)-2-methyl tosylate in the presence of potassium carbonate gave the chiral product **267** in 95% yield. Conversion of the bromine atom to a carboxylic group was

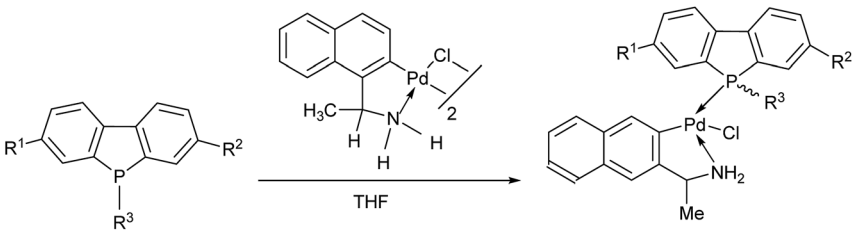


**217-219**

**255** $R^1$= H, $R^2$= H, $R^3$= Me (83%)
**256** $R^1$= CN, $R^2$= H, $R^3$= Me (85%)

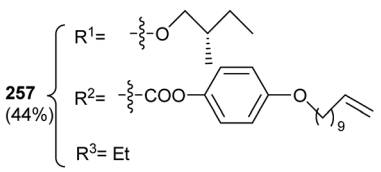


Scheme 66

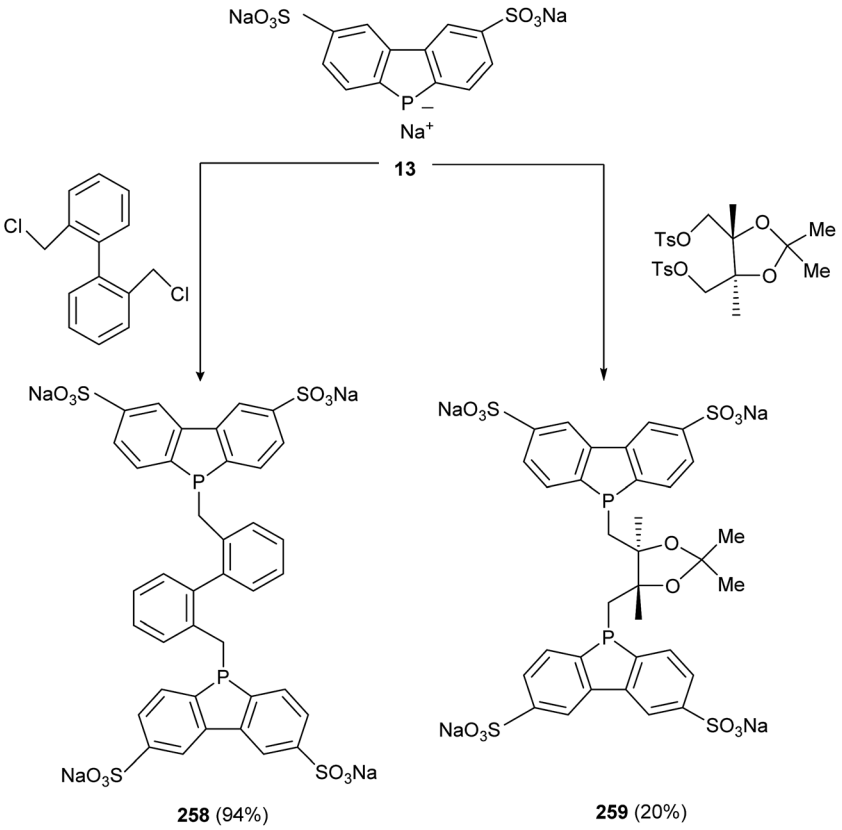


Scheme 67

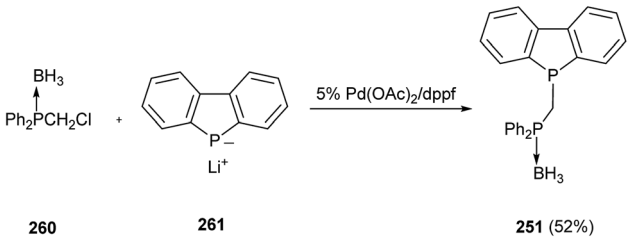


Scheme 68

realised by a cross-coupling reaction with potassium cyanide in the presence of palladium(II) acetate followed by alkaline hydrolysis with $Ca(OH)_2$ to give the acid **268** in 80% yield. Finally, the latter was esterified with 4-(undec-10-enoxy)phenol to give **269** also in 80% yield (Scheme 71).[64]

Dibenzophosphole ring elongation was realised *via* the cross-coupling reaction of the 3-bromo dibenzophosphole **270** with (2-benzylaminophenyl)pinacolatoboron to give the biaryl derivative **271**, followed by cyclisation of the latter to afford a fused polyaromatic compound **272** in 71% yield (Scheme 72).[37]

3,7-Bis(4-diphenylamino)phenyl substituted dibenzophosphole **273** was obtained *via* the double Suzuki–Miyaura cross-coupling reaction of **46** with 4-(diphenylamino)phenylboronic acid in the presence of $Pd(PPh_3)_4$ in 80% yield (Scheme 73).[27]

Voituriez and Marinetti *et al.* functionalised dibenzophosphole oxides by incorporating them into larger [6]- and [8]-helicenes. The triflates of the dibenzophosphole oxides **43**, ($S_p$) **274** and ($R_p$) **275** were submitted to Suzuki cross-coupling reactions with a benzophenanthrene-substituted olefinic boronate. The coupling reactions were performed in the presence of $[PdCl_2(SPhos)_2]$ (SPhos = 2-dicyclohexyl-phosphino-2′,6′-dimethoxybiphenyl) as the catalyst under standard conditions. The corresponding olefinic derivatives **276**, ($S_p$) **277** and ($R_p$) **278** were obtained in high yields (78–87%). The photochemical cyclisation of compound **276** (R = Ph) in cyclohexane/THF led to

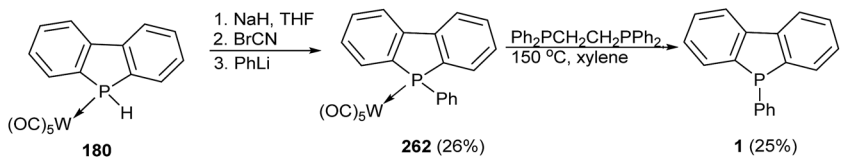


Scheme 69

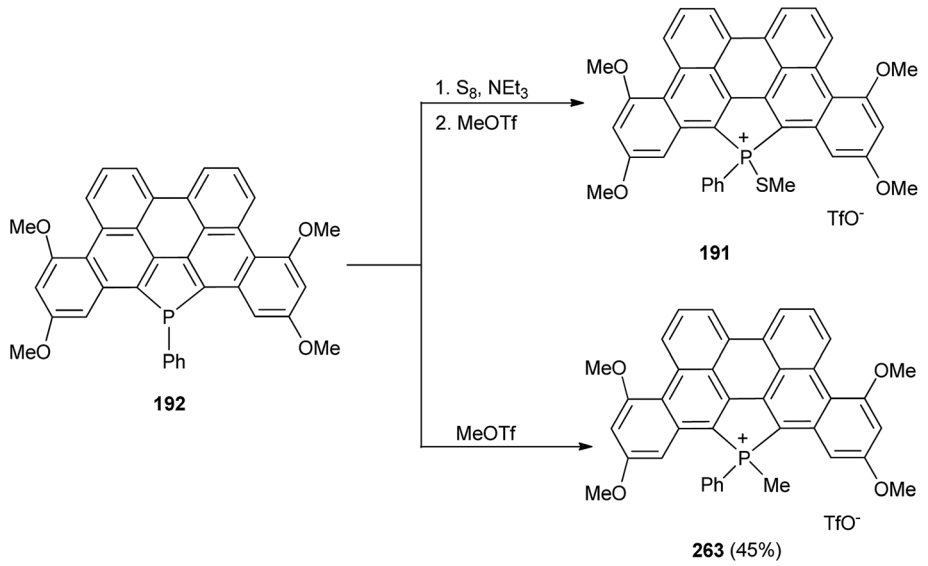


Scheme 70

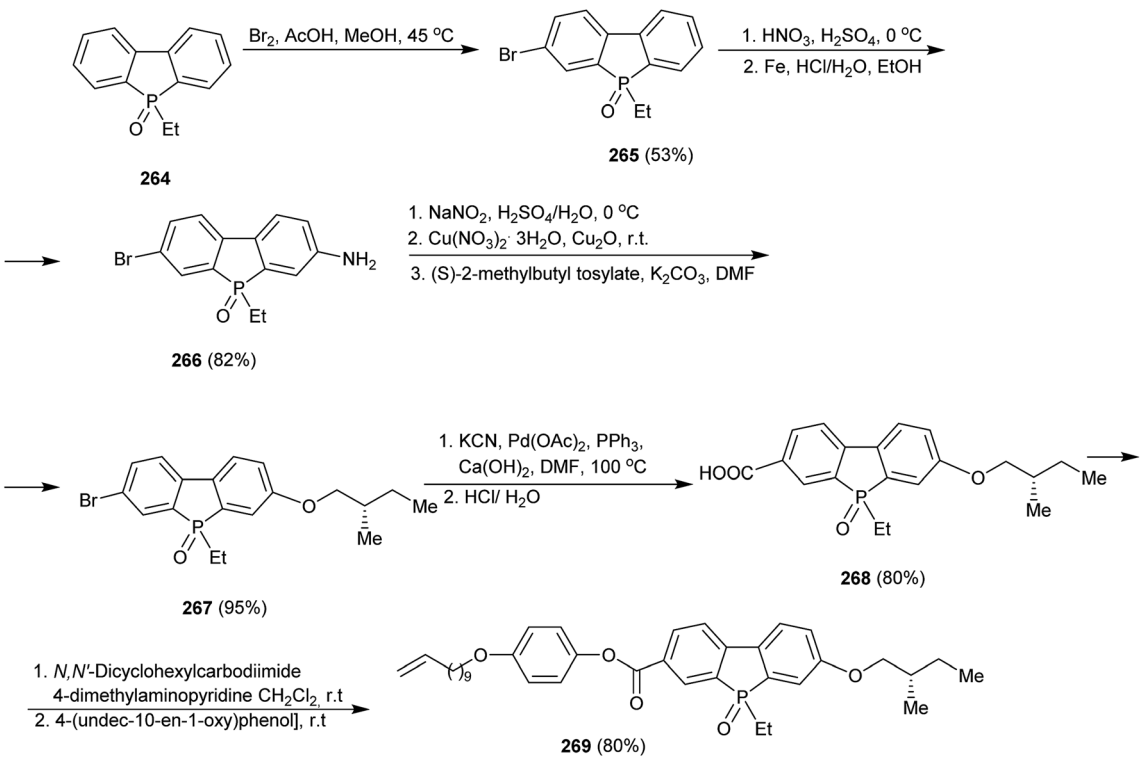


Scheme 71

the formation of a mixture of [6]- and [8]-helicenes **279** and **282**, in a 7 : 3 ratio, in 31% and 20% yields after purification, respectively. The cyclisation of **277** afforded a mixture of isomeric **280** from which ($S_p$,P) **280** was isolated in 40% yield. The oxidative photocyclisation of **278** led to a mixture of ($R_p$,M) **281** and ($R_p$,P) **283**, in a 50 : 42 ratio. Each isomer was isolated in 30% yield (Scheme 74).[33]

## 4. Optoelectronic properties of dibenzophosphole derivatives

Dibenzophospholes and their derivatives belong to a group of polycyclic fused heteroaromatic compounds with spatially developed systems of π-type bonds, which play an important role in modern, lightweight and low-cost electronic elements

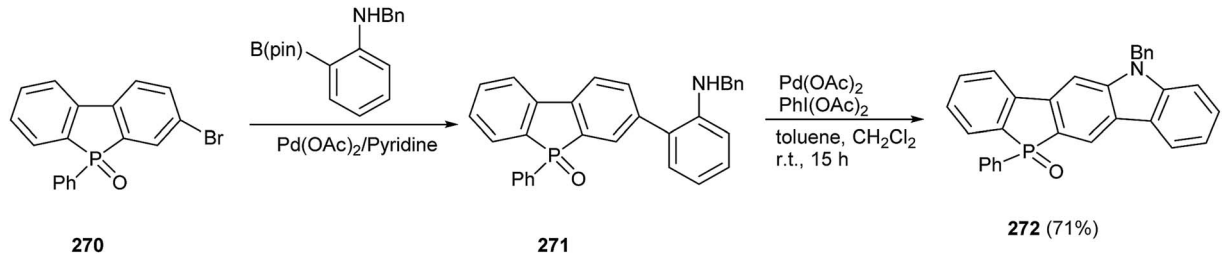


Scheme 72

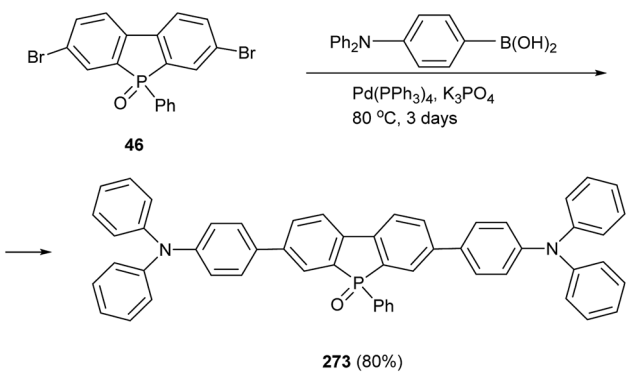


Scheme 73

such as photovoltaic cells (PV), organic light emitting diodes (OLEDs) and field effect transistors (FETs). The functionalisation of one or both benzene rings and/or derivatization of the $P^{III}$ atom (as $P^{+}$ or P═X, where X = N, O, P, S, Se) necessarily results in modification of physicochemical properties of the dibenzophospholes such as: solubility, HOMO/LUMO energy levels, ionization potentials, energy gap, wavelength as well as intensity of absorption and emission. By careful selection of such modifications, new optoelectronic materials with improved properties can be produced.

### 4.1. Non-fused dibenzophospholes

**4.1.1. Simple dibenzophospholes.** Several promising compounds for optoelectronics have been reported and include dibenzophospholes **1**, **66**, **228**, **284–291** containing various substituents on the phosphorus atom. These have potential applications in sundry optoelectronic elements including photovoltaic cells, organic light-emitting diodes (OLEDs), bio- and chemical sensors and nonlinear optical devices NLOs (Scheme 75).[12,65]

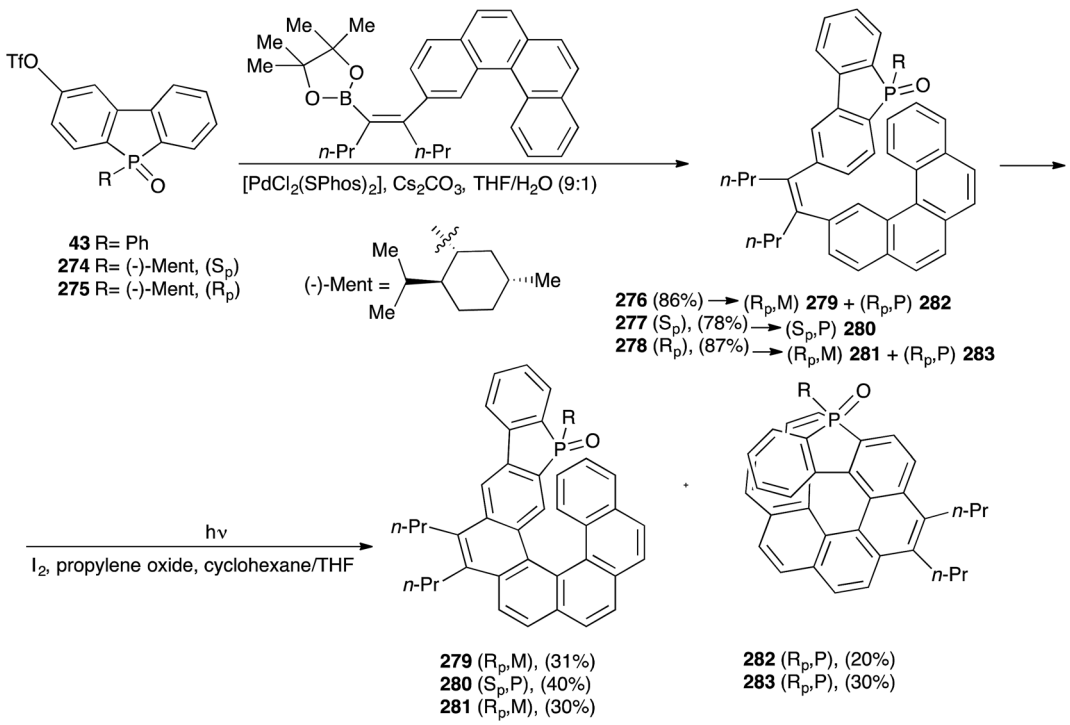


Scheme 74

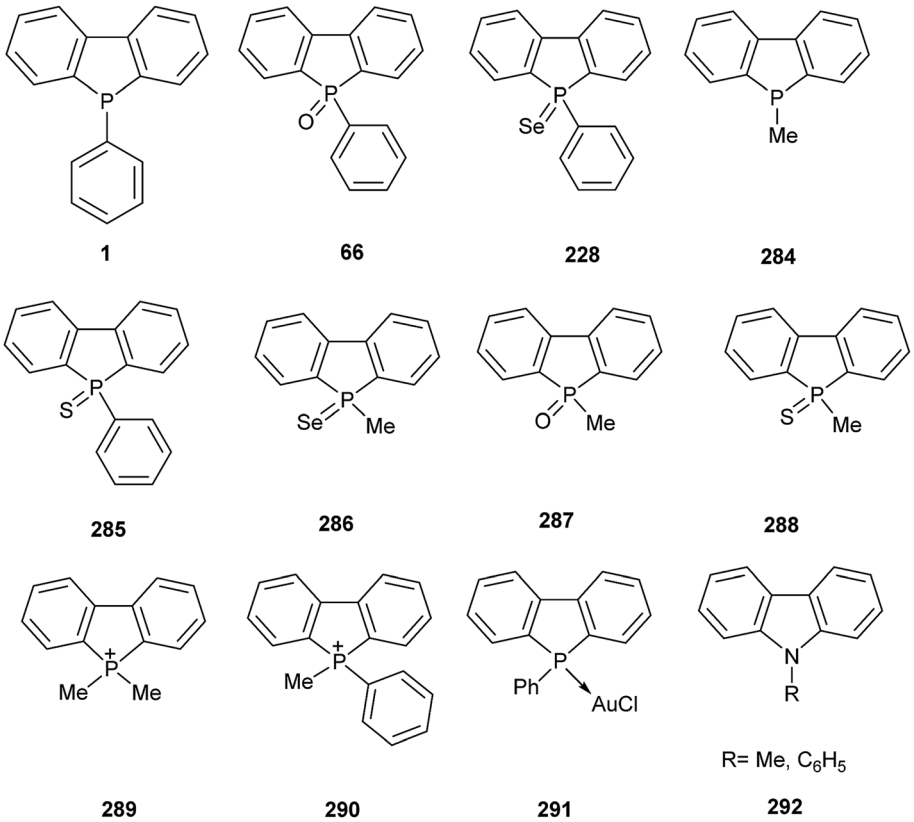


Scheme 75

Chen and Huang *et al.* presented a theoretical study on the optical and electronic properties of dibenzophospholes **1**, **66**, **228**, **284–290**, involving calculations of the highest occupied molecular orbitals (HOMO), the lowest unoccupied molecular orbitals (LUMO), triplet energies ($^3E_g$), energy gaps ($E_g$) as well as other calculations leading to: ionization potentials (IPs), electron affinities (EAs), including calculations of the reorganization energies ($\lambda$) and singlet exciton generation fractions ($\chi_s$), together with radiative lifetimes and emission spectra. Optoelectronic properties of these compounds were compared with carbazoles **292**, which are currently one of the most commonly used chemical units in optoelectronic devices. The dibenzophospholes **1**, **66**, **228**, **284–290** had lower levels of the HOMO and LUMO than the carbazoles **292**. However, the compounds **1** and **284** had a wider range of energy gaps, relative to carbazole analogues due to the nonplanar molecular structures and stronger electron-donating ability of the phosphorus atom. Chemical modifications of the $P^{III}$ atom through oxidation, sulfurization and selenylation led to a gradual increase of the HOMO levels in the following order: −6.26 eV (**287**) < −5.83 eV (**288**) < −5.43 eV (**286**), −6.23 eV (**66**) < −5.86 eV (**285**) < −5.51 eV (**228**), while the LUMO decreased to around −1.55 eV, which was far below the LUMO levels of **1** and **284**. This correlation showed that introduction of electron-withdrawing substituents (O, S, Se atoms) enhanced the injection and electron-transport abilities of the dibenzophospholes **66**, **228**, **285–286** and **288**. For the ionized compounds **289** and **290** ($P^+$Me and $P^+$Ph), the positively charged phosphorus atom reduced the hole injection, but enhanced the electron-accepting ability of these compounds. The energy gap decreased in the following order: 4.95 (**284**) > 4.94 (**1**) > 4.80 (**287**) > 4.75 (**66**) > 4.52 (**290**) > 4.51 (**289**) > 4.33 (**285**) > 4.28 (**288**) > 3.97 (**228**) > 3.88 eV (**286**). The triplet energies ($^3E_g$) of the dibenzophospholes **1**, **66**, **228**, **284–288** showed their potential applications as host materials, as well as revealed that dibenzophospholes **1** and **284** could be promising building blocks for the host materials. For the dibenzophospholes **1**, **66**, **284** and **287**, the calculated singlet and triplet exciton-formation cross section $\sigma_s$/$\sigma_t$ and corresponding singlet exciton generation fractions ($\chi_s$) suggested their potential as highly efficient fluorescent-light-emitting materials. The chemical modification of the $P^{III}$ atom with S and Se atoms, in the dibenzophospholes **228**, **285**, **286** and **288** caused a slight decrease of the $\chi_s$ values in the range of 15–20%. The calculated values of the ionization potentials (IPs) and electronic affinities (EAs) showed that dibenzophospholes could be used simultaneously as electron-transport and hole-transport materials according to different substitutions on the P atom. The abilities to create holes and to accept electrons were improved by the introduction of strong electron-withdrawing substituents or replacement of P-methyl for P-phenyl. For the dibenzophospholes **66** and **287**, smaller hole transport reorganization energies ($\lambda_{hole}$) were calculated than their electron transport reorganization energies ($\lambda_{electron}$), which means faster hole transport than electron transport in these compounds. The

opposite correlation occurred in the dibenzophospholes **228** and **286** for which values of $\lambda_{hole}$ were bigger than their values of $\lambda_{electron}$ and indicated a slower hole transfer, than the electron transfer. The time-dependent density functional theory (TD-DFT) calculations showed electron transitions for dibenzophospholes **1**, **66**, **284–285**, **287–288** as well as their effect on the emission spectra in both vacuum and solvent (THF) as shown in Fig. 2.[65]

Based on the theoretical emission spectra, the dibenzophospholes **1**, **66**, **284–285**, **287–288** may constitute deep blue light emitting materials in the range of $\lambda_{em} = 327–419$ nm. The Stokes shifts of **1** and **284** were calculated to about 45 nm, and the shifts of their derivatives **66**, **285**, **287** and **288** were all around 65 nm relative to carbazoles **292**, the Stokes shifts of which were within 10 nm. The calculated emission spectra of dibenzophospholes **66**, **285**, **287** and **288** in vacuum, were red shifted and thio-modified dibenzophospholes **285** and **288** showed a small intramolecular charge-transfer emission at $\lambda =$ 415 nm. The solvent effects led to larger Stokes shifts of dibenzophospholes **284**, **287** and **288** in comparison to the carbazole analogues **292**. For the compounds **284** and **287**, THF stabilized their excited states, causing small red shifts (4–10 nm) of the emission spectra in comparison with those in vacuum. The opposite correlation was observed in the dibenzophosphole **288**, where the solvent effects stabilized the ground state and induced the blue shift of the emission spectra.

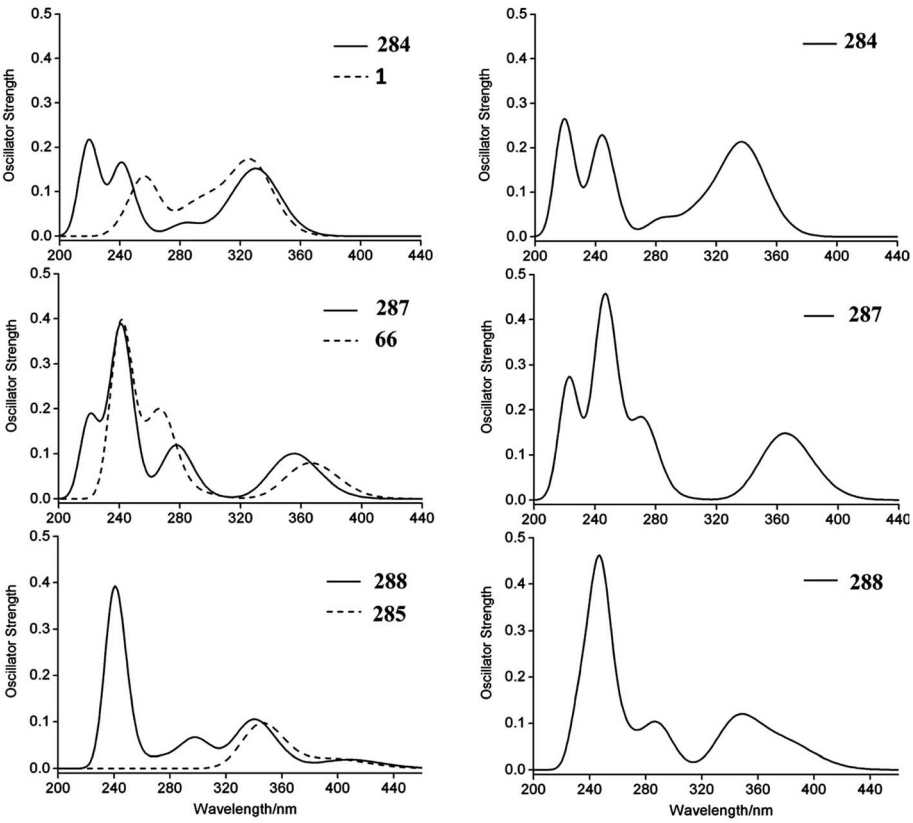


Fig. 2 The simulated emission spectra of dibenzophospholes **1**, **66**, **284–285**, **287–288**, in vacuum (left) and in solution (THF, right)[65] (reprinted with permission from the American Chemical Society).

Table 1 Wavelengths of maximum absorption ($\lambda_{abs}$), half-wave potential ($E_{p1/2}$), wavelengths of maximum emission ($\lambda_{em}$), quantum yields of photoluminescence ($\phi_{PL}$), decomposition temperature ($T_d$) and molar absorption coefficient ($\varepsilon$) of the compounds **66**, **285** and **291**, in $CH_2Cl_2$

| | UV-Vis absorption | | Photoluminescence (PL) | | Electrochemical properties | Thermal properties |
|---|---|---|---|---|---|---|
| Compound | $\lambda_{abs}$ [nm] | log $\varepsilon$ | $\lambda_{em}$ [nm] | $\phi_{PL}$ | $E_{p1/2}$ [eV] | $T_d$[a] [°C] |
| **66** | 332 | 2.9 | 366 | 0.042 | −1.93 | 213 |
| **285** | 330 | 2.9 | 366 | 0.002 | −1.92 | 220 |
| **291** | 330 | 3.0 | 366 | 0.134 | −1.80 | 220 |

[a] TGA, 10% weight loss.

 

The radiative lifetimes were calculated by using Einstein transition probabilities for the compounds **1**, **66**, **284–285**, **287** and **288**. The dibenzophospholes **285** and **288** showed longer lifetimes than commonly used carbazoles **292**, whereas the dibenzophospholes **1**, **66**, **284** and **287** had similar radiative lifetimes in comparison to the commonly used carbazoles **292**.

In addition to this theoretical study, further investigations with thermogravimetric analysis (TGA) showed that the derivatives **66**, **285** and **291** possess good thermal stabilities. This is important for the fabrication of OLEDs, because low-molecular weight species are often deposited as thin films by vacuum evaporation. The derivatives **66**, **285** and **291** emitted in the UV region and were photoluminescent. The Stokes shifts of these compounds were relatively small (about 32–36 nm), which suggested a minimal rearrangement of molecules during photoexcitation. The quantum yields were dependent on the nature of the groups attached to the phosphorus atom. Selected photophysical, electrochemical and thermal data for these compounds are presented in Table 1.[12]

In 2011 the group of Anzenbacher Jr *et al.*[66] investigated solid-state interactions, fluorescence and phosphorescence properties of dibenzophospholes **66**, **228** and **285** as single crystals and the mixed crystals of **228** and **285** acquired in $CH_2Cl_2$/MeOH glass at 77 K. Moreover, an X-ray diffraction analysis was carried out, which indicated that the mixed crystal of **228** and **285** showed a larger number of intermolecular interactions such as π–π and Se–H, than each of them in the single crystals. The fluorescence maxima of the dibenzophospholes **66**, **228**, **285** in a glass corresponded to the wavelength at $\lambda = 363$–364 nm. However, in the compounds **228** and **285** the fluorescence was strongly suppressed due to the higher spin–orbit coupling of selenium **228** and sulfur **285**. Additionally, these compounds exhibited comparable emission spectra with broad phosphorescence at $\lambda = 450$–660 nm. The phosphorescence lifetimes ($\tau_{ph}$) of the dibenzophospholes **66**, **228** and **285** were $\tau_{ph} = 312$ ms, 0.54 ms and 21 ms, respectively. The emission and phosphorescence spectra of the single crystal of **66** were red-shifted compared to the spectrum reported in the glass, due to the intermolecular interactions in the solid state, however, the lifetime of **66** was shorter when compared to the glass. Similar red-shifts were observed for single crystals of **228** and **285**, in the fluorescence and phosphorescence spectra. Furthermore, the mixed crystals of **228** and **285** exhibited only phosphorescence and presented carrier transport and emission properties. This advantage may be applied in the light-emitting single crystal organic field-effect transistors (SC-OFETs).[66]

Chi, Chou and Chang *et al.* obtained 5-[4-(carbazo-9-yl) phenyl]dibenzophosphole-5-oxide **212**, which was used in the construction of the three-layer OLEDs as a bipolar host material.

This compound consisted of carbazole and dibenzophosphole moieties, which served as electron donor and acceptor, respectively. The carbazole derivatives are known as hole-transporting materials, with high triplet energy gap, which makes them efficient host materials for the phosphorescent dopants. Moreover, the phosphine oxide moiety facilitates the

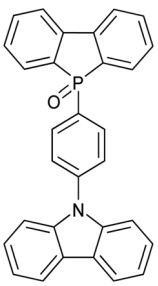


**212**

Scheme 76

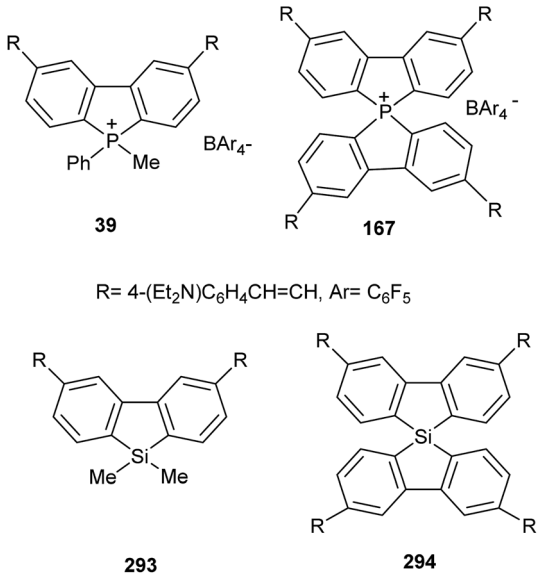


Scheme 77

Table 2 Selected properties of the compound **212**[a]

| Photophysical properties | | | Electrochemical properties | | | | | Thermal properties |
|---|---|---|---|---|---|---|---|---|
| $\lambda_{abs}$ [nm] | $\lambda_{Ph}$ [nm] | $\lambda_{PL}$ [nm] | $E^{ox}_{1/2}$ [V] | $E^{red}_{1/2}$ [V] | HOMO [eV] | LUMO [eV] | $E_s$ [eV] | $T_d$ [°C] |
| 292 | 425 | 458 | 0.98 | −2.33 | −5.78 | −2.33 | 3.55 | 365 |

[a] The oxidation and reduction experiments were conducted in $CH_2Cl_2$ and THF solution, $E_{1/2}$ (V) refers to $[(E_{pa} + E_{pc})/2]$, where $E_{pa}$ and $E_{pc}$ were the anodic and cathodic peak potentials referenced to the $Fc^+$/Fc couple, $E_s = |HOMO - LUMO|$ from the redox data.

electron injection and transport without lowering of the triplet energy gap (Scheme 76).[55]

The selected electrochemical, thermal and photophysical characterisation of the dibenzophosphole **212** is presented in Table 2.

Additionally, thermogravimetric analysis (TGA) of the dibenzophosphole **212**, which decomposed at 365 °C, showed that this compound is capable of forming stable films upon thermal evaporation.

Other potential optoelectronic materials are dibenzophospholes **39** and **167**. These compounds exhibited strong acceptor properties and showed enhanced two-photon absorptions at $\lambda =$ 932 nm, therefore these compounds should be useful as long-wavelength emissive materials (Scheme 77).[32]

Table 3 Selected optical properties of the dibenzophospholes **39** and **167** and their silicon analogues, in $CH_2Cl_2$ (ref. 32)[a]

| | UV-Vis absorption | | Fluorescence | | Two photon absorption (TPA) |
|---|---|---|---|---|---|
| Compound | $\lambda_{max}$ [nm] | $\varepsilon/10^5$ $M^{-1}$ [$cm^{-1}$] | $\lambda_{em}$ [nm] | $\phi_F$ | $\lambda_{max}{}^2$ [nm] |
| **39** | 464 | 0.57 | 647 | 0.52 | 932 |
| **167** | 496 | 1.03 | 715 | 0.04 | 932 |
| **293** | 376 | 0.76 | 464 | 0.16 | 752 |
| **294** | 395 | 2.37 | 492 | 0.28 | 775 |

[a] $\sigma^{(2)}$ divided by the molar mass (MW).

The absorption and emission maxima of the dibenzophospholes **39** and **167** showed bathochromic shifts compared with their silicon analogues **293** and **294**, due to the strong acceptor properties of the phosphonium cores. The effect of solvents on optical properties in toluene, acetone and dichloromethane was also investigated for these compounds. The longest absorption wavelengths of the dibenzophospholes **39** and **167** were at $\lambda = 460$ and 495 nm, respectively in toluene and were almost the same as those in $CH_2Cl_2$. However, in acetone, the dibenzophospholes **39** and **167** exhibited blue-shifted absorption maxima at $\lambda = 430$ and 467 nm, respectively. The dibenzophosphole **39** exhibited higher fluorescence quantum yield, than its spirocyclic analog **167**, which emitted much weaker fluorescence. The opposite trend was observed for the silicon compounds, in which spirocyclic framework of **293** improved the quantum yield. Another important difference was reported for fluorescence properties of dibenzophospholes and their silicon analogues. The emission bands of silicon derivatives **293** and **294** exhibited maxima at $\lambda = 464$ and 492 nm, while dibenzophospholes **39** and **167** were bathochromically shifted to $\lambda = 647$ and 715 nm, respectively, in $CH_2Cl_2$. The two-photon absorption (TPA) showed maxima for the silicon

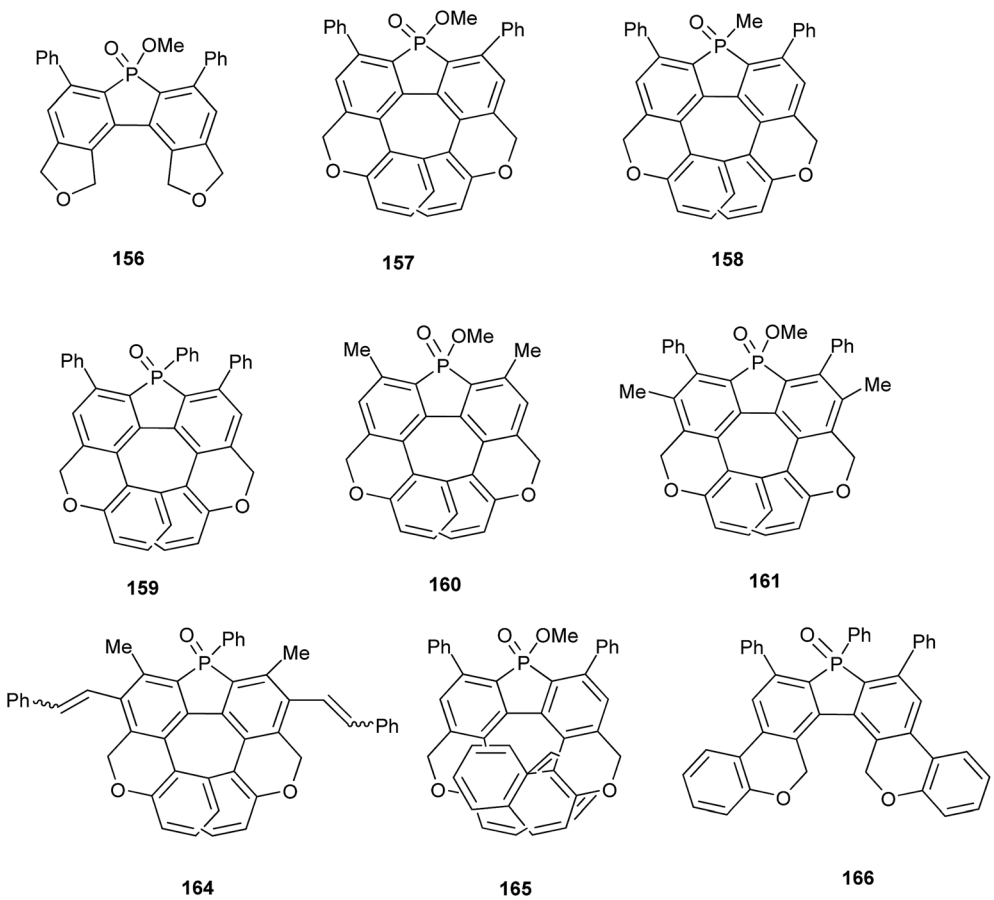


Scheme 78

 

analogues **293** and **294** at $\lambda$ = 752 and 775 nm, respectively. However, for the dibenzophospholes **39** and **167**, the TPA maxima were in accordance with the bathochromic shifts and were red-shifted. Photophysical characterisation of the investigated compounds is summarized in Table 3.

**4.1.2. Helicene type dibenzophospholes.** Structurally unique benzopyrano- and naphthopyrano-fused helical dibenzophospholes **156–161** and **164–166** are also interesting candidates for organic semiconducting materials (Scheme 78).[44]

Optical data for the dibenzophospholes **157–161** and **164–166** compared with the dibenzophosphole **156**, which does not contain the 2-alkoxyphenyl group, showed large red-shifts of absorption and emission maxima. The substituents on the phosphorus atom showed a small impact on the absorption and emission maxima in dibenzophospholes **157–159**, which oscillated around at $\lambda$ = 288 nm and 475 nm, for the absorption and emission maxima, respectively. The same effect was observed for substitutions at the 2- and 7-positions in dibenzophospholes **161** and **164**. Compound **160** exhibited absorption maximum at a similar wavelength as **164**, but the emission was less shifted. The farthest red-shifts for the absorption and emission maxima were observed for the dibenzophosphole **165** (Table 4 and Fig. 3).[44]

Table 4 Photophysical properties of the fused helical dibenzophospholes **156–161** and **164–166** in $CHCl_3$ ($10^{-5}$ M)

| | UV absorption | Emission[a] |
|---|---|---|
| Compound | $\lambda_{max}$ [nm] | $\lambda_{max}$ [nm] |
| **156** | 259, 341 | 375 |
| **157**-(−) | 288, 341 | 477 |
| **158**-(−) | 288, 344 | 471 |
| **159**-(−) | 289, 337 | 474 |
| **160**-(−) | 281, 338 | 469 |
| **161**-(−) | 285, 343 | 464 |
| **164**-(+) | 281, 348[b] | 482[b] |
| **165**-(+) | 308, 386 | 490 |
| **166** | 275 | 406 |

[a] Excited at 280 nm. [b] Measured for a *E*/*Z* mixture.

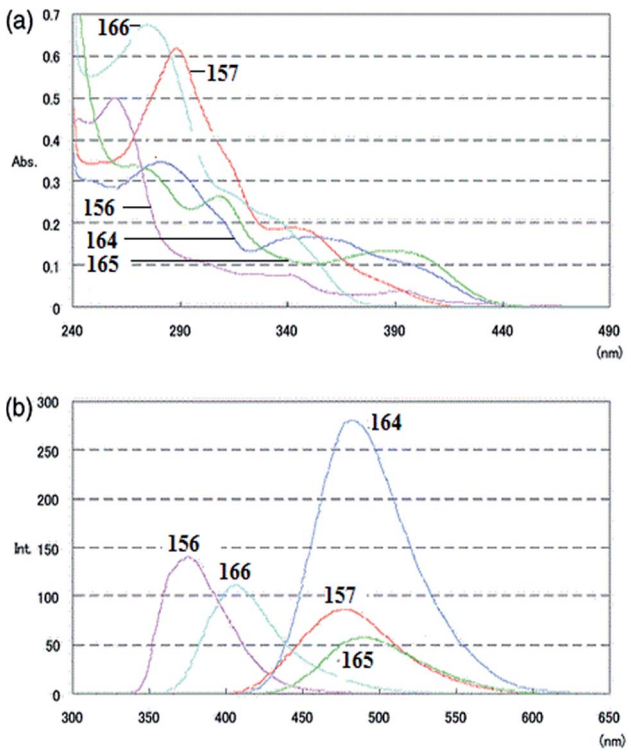


Fig. 3 UV-Vis absorption and emission spectra of compounds **156–157** and **164–166**, in $CHCl_3$ ($10^{-5}$M)[44] (reprinted with permission from the American Chemical Society).

**4.1.3. Perfluorinated dibenzophospholes.** Interesting examples of benzene ring functionalisation are perfluorinated derivatives **202–205**. The fluorine atoms in the aromatic systems stabilised LUMO energy levels and improved electron transport and cofacial packing. The dibenzophospholes **202–205** have a potential application as n-type electronic components with useful electron transport properties what makes them interesting candidates for devices based on electro- and photoluminescence (Scheme 79).[52]

The absorption and emission spectra of the derivatives **203–205** were slightly red-shifted in comparison to the dibenzophosphole **202**. The photoluminescence spectra of all

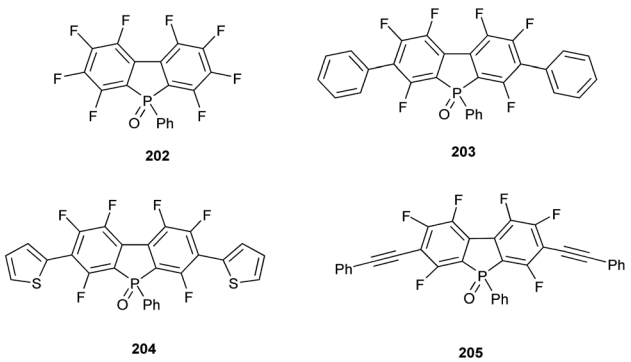


Scheme 79

Table 5 Wavelengths of absorption ($\lambda_{abs}$), emission maxima of photoluminescence ($\lambda_{em}$), quantum yields ($\phi_{PL}$) of the compounds **202–205**, in solution and solid state

| | UV-Vis absorption | | Photoluminescence | | |
|---|---|---|---|---|---|
| Compound | $\lambda_{abs}$ [nm] | log $\varepsilon$ | $\lambda_{em}$ [nm] solution | $\phi_{PL}$ solution | $\lambda_{em}$ [nm] solid |
| **202** | 325 | 3.6 | 365 | 0.18[a] | 378 |
| **203** | 338 | 3.8 | 395 | 0.60[a] | 428 |
| **204** | 385 | — | 424 | 0.54[b] | — |
| | 369 | | 443 | | |
| **205** | 380 | 3.7 | 414 | 0.98[b] | 472 |
| | | | 432 | | |

[a] Referenced to 1,4-bis-(5-phenyl-2-oxazolyl)benzene (POPOP) in THF ($\phi_F$ = 0.97). [b] Referenced to 9,10-diphenylanthracene in THF ($\phi_F$ = 0.9).

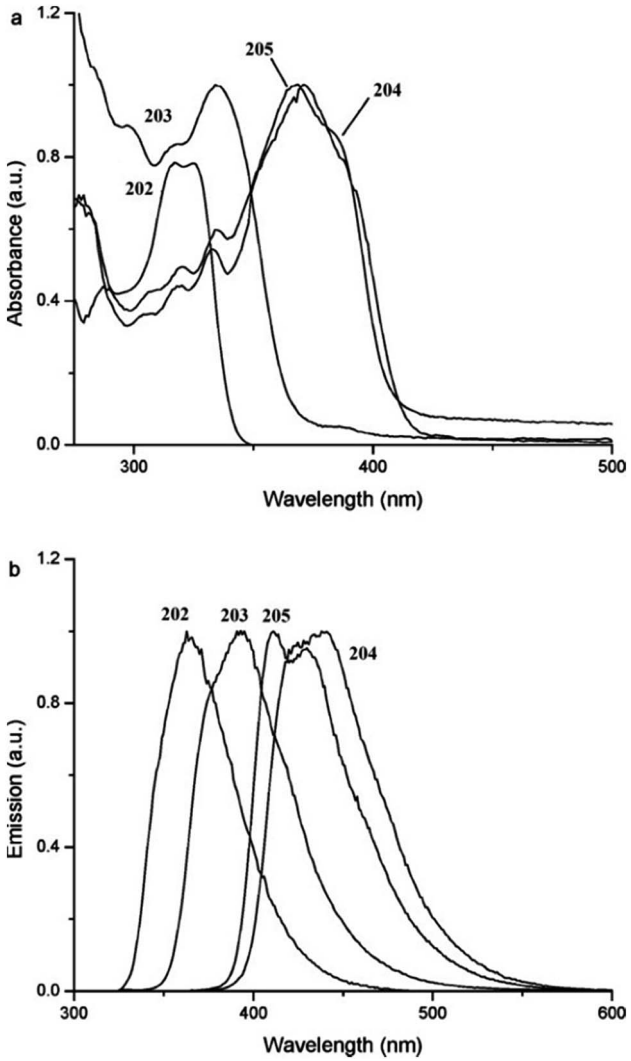


Fig. 4 UV-Vis absorption (a) and emission (b) spectra of the compounds **202–205** in THF[52] (reprinted with permission from the American Chemical Society).

investigated compounds **202–205** showed maxima between $\lambda_{em}$ = 365 to 432 nm. These values were in the ultraviolet to violet range and corresponded to blue light emission, for the solution and solid states. The quantum yields of dilute solutions varied significantly with the nature of the 3,7-substituents. The highest value was observed for the derivative **205**. The optical properties of these compounds are presented in Table 5 and Fig. 4.[52]

Tilley *et al.* investigated electrochemical properties of dibenzophospholes **202–205**. Selected results are summarized in Table 6.

The 3,7-thienyl and alkynyl disubstituted derivatives **204** and **205** exhibited a decrease of LUMO values by 0.1–0.3 eV compared to the dibenzophosphole **202**, due to their slightly longer conjugation length. Additionally, the thienyl dibenzophosphole **204** exhibited higher HOMO energy level, than the alkynyl derivative **205**. The derivative **203** had the widest range of the energy gap. The low values of LUMO levels in

Table 6 Values of HOMO, LUMO energy levels and energy gap ($E_g$) of the compounds **202–205** in acetonitrile (0.1 M $n$-$Bn_4N^+PF_6^-$ in $CH_3CN$)

| Compound | HOMO[a] [eV] | LUMO[a] [eV] | $E_g$ [eV] solution |
|---|---|---|---|
| **202** | — | −3.0[b] | — |
| **203** | −6.7 | −3.0[b] | 3.7 |
| **204** | −6.2 | −3.1[b] | 3.1 |
| **205** | −6.5 | −3.3[b,c] | 3.2 |

[a] Referenced to $Fe/Fe^+$. [b] Reversible reduction. [c] Three drops of toluene was added to improve solubility in $CH_3CN$.

dibenzophospholes **202–205**, suggested that these compounds could be useful as n-type conducting materials.[52]

### 4.2. Fused dibenzophospholes

**4.2.1. Linearly fused dibenzophospholes.** Several dibenzophospholes have been reported that are attractive prospects for optoelectronic uses, including **129**, **131**-*anti*, **133**-*syn*, **220**-*anti*, **221**-*syn*. These compounds attract increasing attention due to relatively small HOMO–LUMO energy gaps and the possibility to tune their properties through diverse functionalisations at the phosphorus atom (Scheme 80).[40]

The dibenzophosphole oxide **129** showed absorption maximum at $\lambda_{abs}$ = 340 nm and emission at $\lambda_{em}$ = 382 nm, for the $CH_2Cl_2$ solution. The absorption and emission maxima of the dibenzophospholes **131**-*anti* and **133**-*syn* were red-shifted compared to the derivative **129** related to π-expansion through the σ*–π* conjugation of the π-framework to the σ* orbital of the exocyclic P–C bonds. The dibenzophosphole oxides **131**-*anti* and **133**-*syn* exhibited high fluorescence quantum yields of 0.89 and 0.79, in solution. In the solid state, the quantum yields of both compounds were somewhat lower. In this state, the quantum yield of **133**-*syn* ($\phi_F$ = 0.63) was larger than that of **131**-*anti* ($\phi_F$ = 0.46), indicating that interactions in the solid state were different for both diastereomers due to conformational difference.

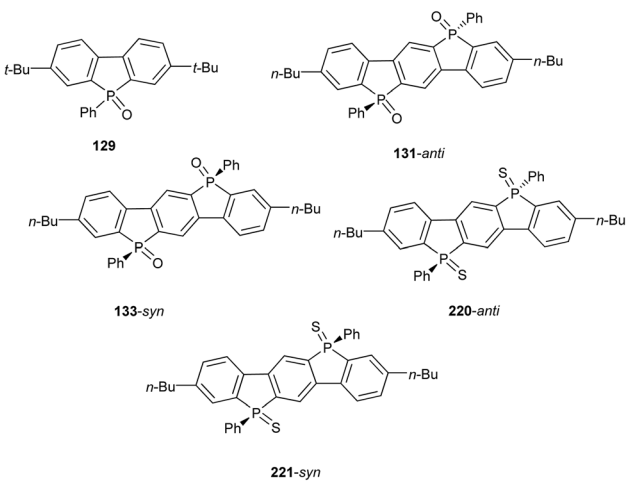


Scheme 80

Table 7 The values of absorption and fluorescence maxima of the compounds **129**, **131**-*anti*, **133**-*syn*, **220**-*anti* and **221**-*syn*, in $CH_2Cl_2$

| | UV-Vis absorption | | Fluorescence | | | |
|---|---|---|---|---|---|---|
| Compound | $\lambda_{abs}$ [nm] | log $\varepsilon$ | $\lambda_{em}$ [nm] solution | $\phi_F$[a] solution | $\lambda_{em}$ [nm] solid | $\phi_F$[a] solid |
| **129** | 340 | 3.19 | 382 | 0.67 | — | — |
| **131**-*anti* | 391 | 3.68 | 426, 438 | 0.89 | 454 | 0.46 |
| **133**-*syn* | 391 | 3.61 | 426, 438 | 0.79 | 476 | 0.63 |
| **220**-*anti* | 385 | 3.73 | 430 | 0.004 | 437, 471, 501 | 0.12 |
| **221**-*syn* | 386 | 3.72 | 431 | 0.004 | 476, 500 | 0.04 |

[a] Absolute quantum yield determined by an integrating sphere system.

The dibenzophosphole sulfides **220**-*anti* and **221**-*syn* revealed different photophysical properties compared with the dibenzophosphole oxides **131**-*anti* and **133**-*syn*. The absorption maxima of the sulfides had almost the same values of $\lambda_{abs}$ = 385 nm (log $\varepsilon$ = 3.73) and $\lambda_{abs}$ = 386 nm (log $\varepsilon$ = 3.72) for **220**-*anti* and **221**-*syn*, respectively. These electronic properties led to blue-shifted absorption maxima of the dibenzophospholes sulfides in comparison with those of the dibenzophosphole oxides. The fluorescence quantum yields of the sulfides **220**-*anti* and **221**-*syn*, in solution dramatically dropped down to 0.004 in comparison to oxides **131**-*anti* and **133**-*syn*, but in the solid state increased to 0.12 and 0.04 for **220**-*anti* and **221**-*syn*, respectively. The selected photophysical properties of the investigated compounds are summarized in Table 7.[40]

The linearly fused dibenzophospholes **195** and **196** are also promising for optoelectronics devices, in which optical properties were highly dependent on the combination of benzo[*b*](thiophene or pyrrole) subunits (Scheme 81).[50]

The UV-Vis absorption and emission spectra of the dibenzophospholes **195** and **196** were significantly blue shifted relative to the corresponding non-fused biaryl substrates **193** (see subsection 2.11). The Stokes shifts of the rigid fused structures of **195** (3829 $cm^{-1}$) and **196** (4810 $cm^{-1}$) were smaller than those of the biaryl substrates **193** (R = S) (4250 $cm^{-1}$) and **193** (R = NMe) (7000 $cm^{-1}$).

Table 8 The optical characterisation of the compounds **195** and **196** and their precursors **193** (R = S, NMe), in $CH_2Cl_2$ (ref. 50)

| | UV-Vis absorption | | Fluorescence | |
|---|---|---|---|---|
| Compound | $\lambda_{abs}$ [nm] | log $\varepsilon$ | $\lambda_{em}$ [nm] | $\phi_F$[a] |
| **193** (R = S) | 377 | 4.31 | 450 | 0.17 |
| **193** (R = NMe) | 393 | 4.07 | 542 | 0.44 |
| **195** | 344 | 3.96 | 396 | 0.13 |
| **196** | 355 | 4.08 | 431 | 0.24 |

[a] Excited at $\lambda_{abs}$ 400 nm for the $\phi_F$ measurements.

Density functional theory (DFT) calculations at the B3LYP/6-31G* level showed widening of the HOMO–LUMO gap upon acetylene fusion. The energy gaps were changed from 3.53/3.34 eV for **193** (R = S, NMe) to 4.10/3.85 eV, for **195** and **196**, respectively.

The fluorescence decay curves of the compounds **195** and **196** in $CH_2Cl_2$ were fitted as a single exponential with lifetimes of 2.2 and 7.9 ns. More photophysical properties of **195** and **196** including quantum yields are displayed in Table 8.[50]

**4.2.2. Thiophene modified fused dibenzophospholes.** The compounds **186** and **187** obtained from **185** (Y = S, O) possess

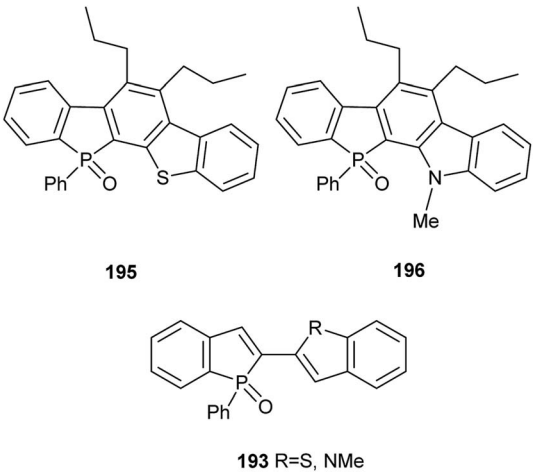


**195** **196**

**193** R=S, NMe

Scheme 81

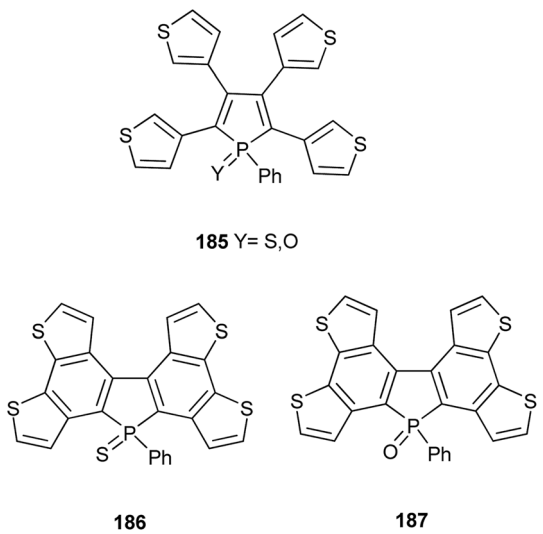


**185** Y= S,O

**186** **187**

Scheme 82

a considerable dibenzophospholes character based on optical properties in the solid state (Scheme 82).[48]

The dibenzophospholes **186** and **187** compared to the respective nonfused precursors **185** (Y = S, O) showed blue-shift absorption maxima, higher oxidation and lower reduction potential values, which indicated the less efficient electron π-delocalization over the $sp^2$-C atoms of **186** and **187** and typical for the dibenzophospholes, increased localization of the π-electrons within aromatic subunits. Although, the dibenzophospholes **186** and **187** were emissive materials with $\lambda_{max}$ = 475 and 477 nm, respectively, their quantum yields oscillated at around 1%. Photophysical properties of these compounds are presented in Table 9.[48]

Table 9 The optical data of the dibenzophospholes **186** and **187** and their precursors **185** (Y = S, O) in $CH_2Cl_2$

| | UV-Vis absorption | | Fluorescence |
|---|---|---|---|
| Compound | $\lambda_{max}$ [nm] | log ε | $\lambda_{em}$ [nm] |
| **185** (Y = S) | 413 | 3.48 | 484 |
| **185** (Y = O) | 411 | 3.83 | — |
| **186** | 391 | 3.56 | 475 |
| **187** | 389 | 3.63 | 477 |

**4.2.3. Benzene modified fused dibenzophospholes.** Fused benzene modified dibenzophospholes **190–192**, **209**, **235** and **263**, which have the same fused aromatic C skeleton but different P moieties, have been successfully utilized as organic materials for optoelectronics (Scheme 83).[49]

The optical and electrochemical properties of these dibenzophospholes were investigated to evaluate the impact of the P modifications on their electronic properties. The absorption spectra of the all investigated fused dibenzophospholes **190–192**, **209**, **235** and **263** varied over a wide range covering the entire visible spectrum. In the absorption spectrum of the dibenzophosphole **192**, an intense characteristic band at $\lambda_{max}$ = 472 nm was observed. The absorption maxima of the $\sigma^4$-P derivatives **190**, **209** and **235** were shifted towards higher wavelengths. A larger bathochromic shift was observed for P-alkyl and P-S phospholium salts **263** and **191**. Addition of a phenyl group to phosphorus in the dibenzophosphole **192** resulted in a shift of its maximum absorption towards higher wavelengths. All of these dibenzophospholes were fluorescent in solution, with gradual red shifts of the $\lambda_{em}$ in the compounds **190–192** and **263**. The Stokes shifts for rigid structures in the compounds **192**, **190**, and **263** were relatively small (737, 1072, 1355 $cm^{-1}$, respectively). Furthermore, the emission bands indicated a small rearrangement of these molecules upon photoexcitation and for this reason their quantum yields were

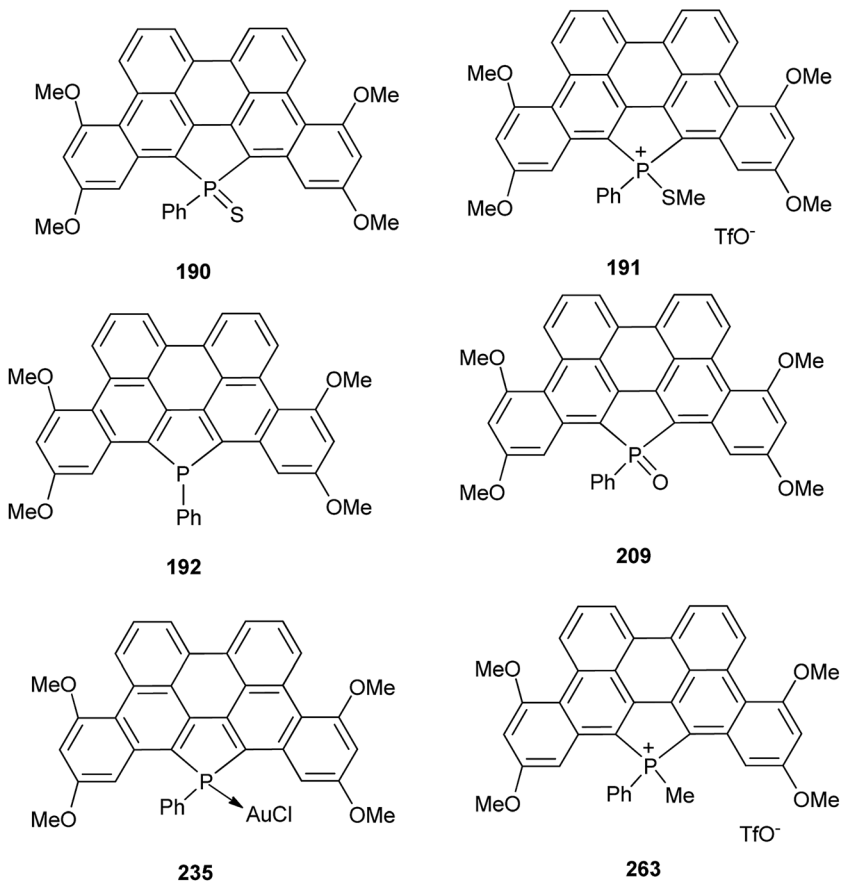


Scheme 83

 

Table 10 Wavelengths of absorption maxima ($\lambda_{abs}$), logarithm of the molar absorption coefficient (log $\varepsilon$), wavelength of emission maxima ($\lambda_{em}$), fluorescence quantum yields ($\phi_F$), oxidation potentials ($E_1^{ox}$), reduction potentials ($E_1^{red}$)

| | UV-Vis absorption | | Fluorescence | | Redox potentials | |
|---|---|---|---|---|---|---|
| Compound | $\lambda_{abs}$[a] [nm] | log $\varepsilon$[a] | $\lambda_{em}$[a] [nm] | $\phi_F$ [a,b] | $E_1^{ox}$[b] | $E_1^{red}$[c] |
| **190** | 514 | 4.04 | 544 | 0.21 | 0.71 | −1.70 |
| **191** | 569 | 3.95 | 669 | 0.03 | 1.01 | −1.04[d] |
| **192** | 472 | 4.34 | 489 | 0.80 | 0.44 | −2.10[d] |
| **209** | 524 | 4.11 | 549 | 0.52 | 0.77 | −1.71[d] |
| **235** | 508 | 4.14 | 537 | 0.08 | 0.75 | −1.67[d] |
| **263** | 554 | 4.00 | 599 | 0.19 | 0.97 | −1.31[d] |

[a] In dichloromethane ($10^{-5}$ M). [b] Measured relative to fluorescein (NaOH, 0.1 M, $\phi_F$ = 0.9). [c] In dichloromethane and $Bu_4N^+PF_6^-$ (0.2 M). [d] Reversible process.

relatively high (>0.20), as opposed to the derivative **191**, which presented a larger Stokes shift (2875 $cm^{-1}$) accompanied by a decrease in the fluorescence quantum yield to 0.03.

Cyclic voltammetry measurements of these compounds showed that the chemical functionalisation of the P center in the dibenzophospholes **190–192** and **263** led to a gradual increase in the oxidation and reduction potentials as well as indicated that the phospholium salts **191** and **263** had high electron affinities. Moreover, the dibenzophospholes **190**, **209**, **235** and **263** presented reversible reduction waves, which suggested stability in their reduced state, under the measurement conditions. It is noteworthy that the evolution of the redox potentials within the compounds **190–192** and **263** were consistent with the decrease in the optical gap. Accurate photophysical and electrochemical data of these compounds are presented in Table 10 and Fig. 5.[49]

Time-dependent density functional theory (TD-DFT) calculations were performed to gain more insight into the electronic properties of the dibenzophospholes **190–192**, **209**, **235** and **263**. These results showed that the long-wavelength UV-Vis absorption of these dibenzophospholes resulted from HOMO–LUMO transitions. The frontier molecular orbitals were comparable in **190–192**, **209** and **263**. These π molecular orbitals were delocalized on the $sp^2$-carbon skeletons with a contribution of the respective orbitals of the phosphole ring.

The HOMO with a nodal plane on the $P^{III}$ was influenced by the inductive effects of the substituents on the phosphorus atom. Additionally, both experimental and theoretical data showed that the local chemical modifications around P had a great significance on the gap fine-tuning.[49]

**4.2.4. Bridged dibenzophospholes.** Notable organic compounds for optoelectronic devices are bridged dibenzophospholes **17–18**, **20** and **21**, which were obtained by Yamaguchi and Studer *et al.* These compounds exhibited electron-accepting character and could find many applications as building blocks in molecular electronics (Scheme 84).[27]

The UV-Vis absorption spectra of the dibenzophospholes **17**-*cis* and **18**-*trans* showed an absorption band with the maxima

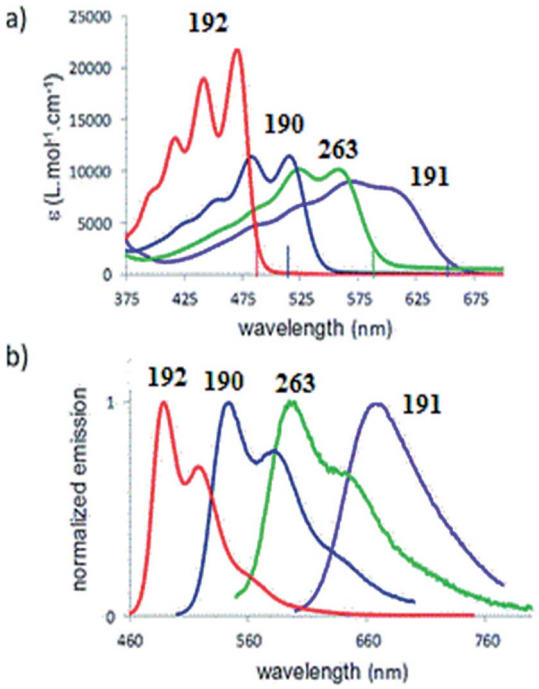


Fig. 5 UV-Vis absorption spectra (a), normalised emission spectra (b) of the compounds **190–192** and **263** in dichloromethane ($10^{-5}$ M)[49] (reprinted with permission from the American Chemical Society).

wavelength at $\lambda_{abs}$ = 347 nm and logarithms of the molar absorption coefficient 2.52 and 2.56 for **17**-*cis* and **18**-*trans*, respectively. Additionally, both isomers presented essentially identical spectra irrespective of the stereochemistry. The fluorescence spectra of **17**-*cis* and **18**-*trans* showed a violet fluorescence with the maximum wavelength at $\lambda_{em}$ = 387 nm in both cases, whereas the quantum yield was low ($\phi_F$ = 0.03).

Notably, the absorption and fluorescence spectra of **17**-*cis* and **18**-*trans* were in the longer wavelength range, than those of the dibenzophosphole oxide **66**. These results were attributable to the small HOMO–LUMO gap of isomers **17**-*cis* and **18**-*trans*. The compounds **20**-*trans* and **21**-*trans* showed absorption at $\lambda_{abs}$ = 375 and 399 nm, and fluorescence bands at $\lambda_{em}$ = 422 and 547 nm, respectively, which were related to the effective extension of π conjugation. Whereas the dibenzophospholes **17**-*cis* and **18**-*trans* showed only a faint fluorescence, the π-extended derivatives **20**-*trans* and **21**-*trans* presented more intense emission with $\phi_F$ values of 0.20 and 0.34, respectively. Remarkably, the $\lambda_{em}$ value of the dibenzophosphole **21**-*trans* was longer than that of compound **20**-*trans* in $CHCl_3$. To compare the electron-accepting properties of the bridged compounds **20**-*trans* and **21**-*trans*, the non-bridged dibenzophosphole **273** was also prepared and measured in various solvents. For the compounds **21**-*trans* and **273**, the fluorescence spectra presented considerable bathochromic shifts with increasing polarity of a solvent, whereas the absorption maxima showed small solvent dependence. These facts demonstrate that the compounds **21**-*trans* and **273** had more polar structures in the excited state than in the ground state. The use of the Lippert–Mataga equation to

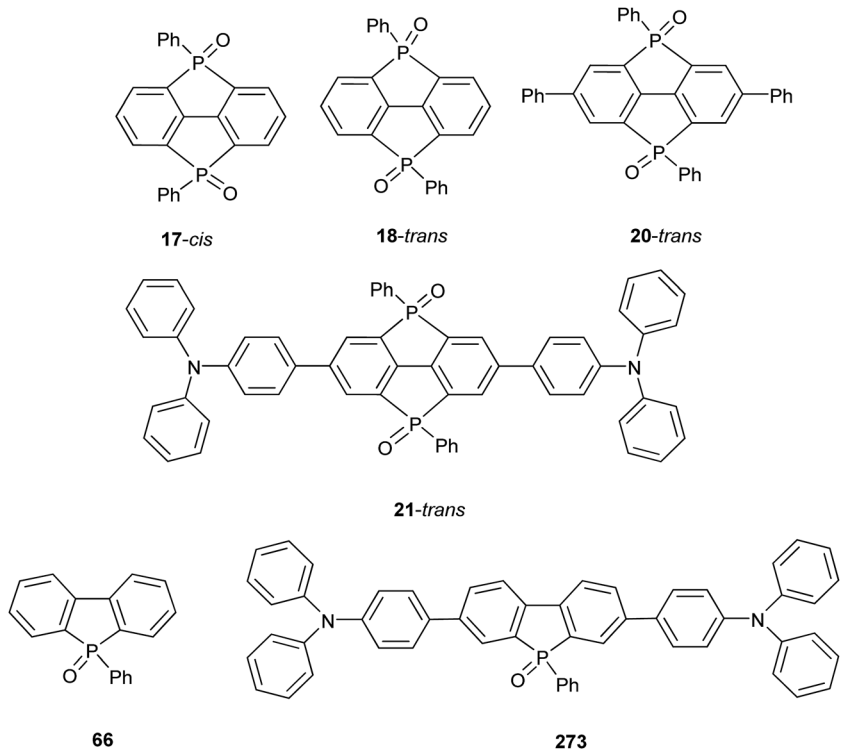


Scheme 84

compare the degree of polarity of the structures in the excited state, showed that extension of the electron-accepting character of the bridged dibenzophospholes **20** and **21**-*trans* was larger than the non-bridged dibenzophosphole analogue **273**. Noteworthy is that the dibenzophosphole **21**-*trans* retained fluorescence quantum yield in the solid state of $\phi_F = 0.30$, in contrast to the non-bridged analogue **273** which exhibited a much smaller fluorescence quantum yield than in solution ($\phi_F = 0.18$ for solid, 0.89 for solution). Individual results of the investigated compounds are summarized in Table 11.[27]

Yamaguchi and Studer *et al.* presented the cyclic voltammograms of the dibenzophospholes **21**-*trans* and **273**, showing the first reversible reduction waves with reduction potentials of −2.15 and −2.36 V, respectively. These observations indicated that the dibenzophosphole **21**-*trans* might serve as a material to enhance the electron-accepting character.

Table 11 UV-Vis absorption and fluorescence characterisation of the compounds **17**-*cis*, **18**-*trans*, **20**-*trans*, **21**-*trans*, **66**, **273**, in $CH_2Cl_2$

| | UV-Vis absorption | | Fluorescence | |
|---|---|---|---|---|
| Compound | $\lambda_{abs}$[a] [nm] | log $\varepsilon$ | $\lambda_{em}$[b] [nm] | $\phi_F$[c] |
| **17**-*cis* | 347 | 2.52 | 387 | 0.03 |
| **18**-*trans* | 347 | 2.56 | 387 | 0.03 |
| **20**-*trans* | 375 | 3.54 | 422 | 0.20 |
| **21**-*trans* | 399 | 4.57 | 547 | 0.34 (0.30) |
| **66** | 332 | 2.89 | 366 | 0.042 |
| **273** | 396 | 4.63 | 499 | 0.89 (0.18) |

[a] Only absorption maxima at the longest wavelengths were shown. [b] Emission maxima upon excitation at the absorption maximum wavelengths. [c] Absolute fluorescence quantum yields determined by a calibrated integrating sphere system within ±3% errors.

## 5. Application of dibenzophospholes for organic electronic devices

We believe that dibenzophospholes, as organic π-conjugated compounds, have enormous potential as optoelectronic materials for example in light-emitting diodes, organic field-effect transistors, nonlinear optical devices and organic solar cells.[39] However, in the years 2001–2016, only limited testing of dibenzophospholes and their derivatives as materials in these types of device took place. In the 15 years since the review by Aitken[11] in 2001, only two simple dibenzophospholes **66** and **212** were used in Organic Light-Emitting Diodes (OLEDs) in various configurations. These devices were fabricated in typical layered structures on indium-tin-oxide (ITO)-coated glass substrates (≤15 Ω) with multiple organic layers between the transparent bottom ITO anode and the top metal cathode. The organic and metal layers were deposited by thermal evaporation under high vacuum conditions with a base pressure of $<10^{-6}$ Torr. The active areas of the devices were $2 \times 2$ mm$^2$ as defined by the shadow mask for cathode deposition.

Chi, Chou and Chang *et al.* applied the dibenzophosphole **212** in the three layer OLEDs with 4 wt% of Os complex as an emitter. The dibenzophosphole **212** served as a bipolar host material with electron-donor properties due to the carbazole

 

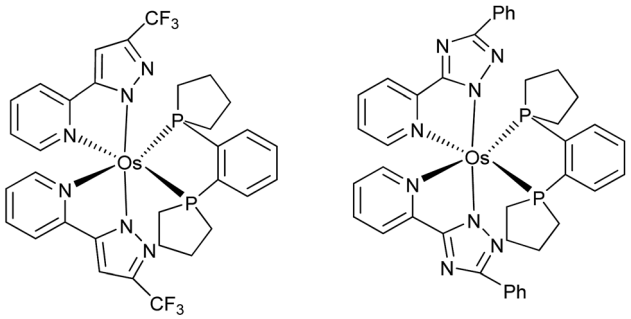


Scheme 85

moiety, as well as electron-acceptor properties by reason of the presence of phosphoryl moiety. The configurations of these devices were as follows: ITO/3DTAPBP-[2,2′-bis(3-(*N*,*N*-di-*p*-tolylamino)phenyl)biphenyl] (40 nm)/the dibenzophosphole **212** with Os complexes **A** or **B** (Scheme 85) (30 nm)/BP4mPy-[3,3′,5,5′-tetra[(3-pyridyl)-phen-3-yl]biphenyl (40 nm)]/LiF (0.8 nm)/Al (150 nm) (Fig. 6).[55]

3DTAPBP with a wide triplet gap of around 2.68 eV, was employed as the hole-transport or a host material in red-emitting OLEDs. The second material BP4mPY served as an electron transport layer. These devices exhibited a bright emission of dopants due to good transfer energy between the host and guest materials. Below are presented the Os(II) complexes used in these red-emitting OLEDs (Scheme 85).

The efficiencies of OLEDs in this configuration were as follows: *cf.* 14.3%, 34.8 cd $A^{-1}$ and 45.2 lm $W^{-1}$ for the complex **A** and 9.9%, 15.7 cd $A^{-1}$ and 20.5 lm $W^{-1}$ for the complex **B**. The luminance maxima of 52.6 and 23.7 cd $m^{-2}$ were achieved for the complexes **A** and **B**, through applying relatively low voltages of 2.5 and 2.6 V, respectively. Moreover, the internal quantum efficiency amounted to nearly 100% in both devices.

The resulting device parameters for the phosphorescent OLED containing as host dibenzophosphole **212** can be compared to the parameters of an OLED containing the standard bipolar host material CBP-4,4′-*N*,*N*′-dicarbazolebiphenyl in the following configuration: ITO/3DTAPBP (40 nm)/CBP (or dibenzophosphole **212**) doped with 4% Os complexes **A**, **B** (30 nm)/BP4mPy (40 nm)/LiF (0.8 nm)/Al (150 nm) or with other commercial materials, such as BP4mPy/3DTAPBP in the following configurations: ITO/3DTAPBP (40 nm)/3DTAPBP doped with 4% Os complexes **A**, **B** (10 nm)/BP4mPy doped with 4% of Os complexes **A**, **B** (20 nm)/BP4mPy (40 nm)/LiF (0.8 nm)/Al (150 nm).

The parameters obtained for the standard host material (CBP, BP4mPy/3DTAPBP) doped with Os complexes **A** and **B** were lower than those obtained for the host dibenzophosphole **212** doped with the Os complex **A** (14.3%, 34.8 cd $A^{-1}$ and 45.2

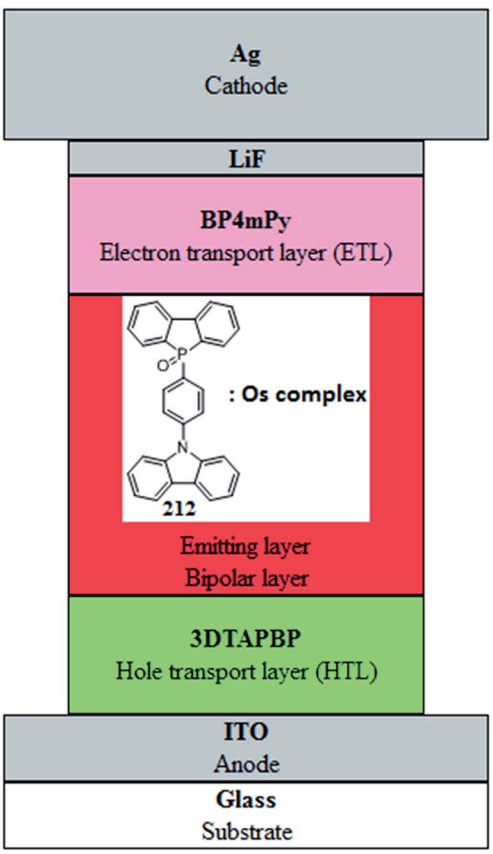


Fig. 6 Three-layer OLED.

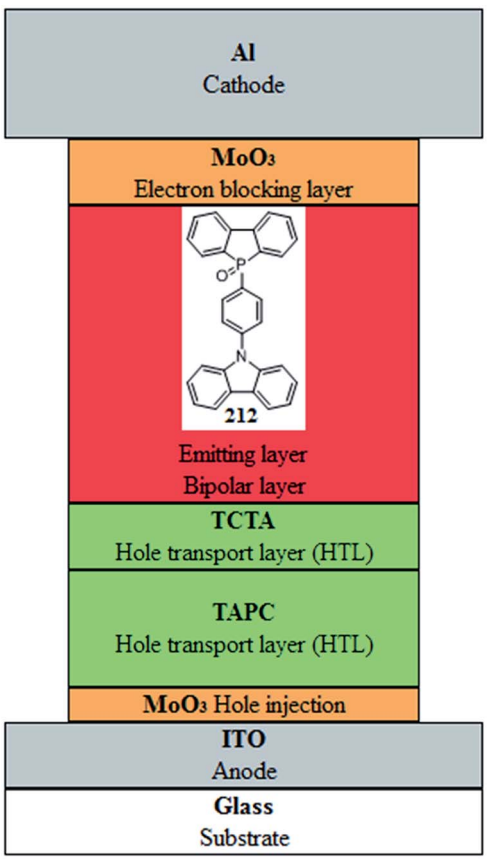


Fig. 7 The hole-only device.

lm $W^{-1}$): for CBP, efficiencies of 10.9% (21.7 cd $A^{-1}$ and 11.9 lm $W^{-1}$) and 10.1% (13.7 cd $A^{-1}$ and 10.0 lm $W^{-1}$) for the Os complexes **A** and **B** were achieved, respectively, whereas, efficiencies for the devices with BP4mPy/3DTAPBP in the second configuration of 12.9% (27.9 cd $A^{-1}$ and 21.8 lm $W^{-1}$) for the complex **A** and 10.7% (18.5 cd $A^{-1}$ and 19.3 lm $W^{-1}$) for the complex **B**, were obtained.[55]

The compound **212** was also used in the only-hole device in the following configuration: ITO/$MoO_3$ (1 nm)/TAPC-[di-[4-(*N*,*N*-ditholylamino)-phenyl]cyclohexane] (30 nm)/TCTA-[4,4′,4″-tris(carbazol-9-yl)-triphenylamine] (30 nm)/the compound **212** (100 nm)/$MoO_3$ (20 nm)/Al (110 nm), for which $MoO_3$ was applied as a hole injection/electron blocking layer, while TAPC and TCTA were used as dual hole-transport layers for providing a smooth hole-injection into the tested material as shown in Fig. 7.[55]

Analogously, an only-electron device was also prepared in the following configuration: ITO/Al(20 nm)/the dibenzophospholes **212** (100 nm)/TmPyPB-[1,3,5-tri[(3-pyridyl)-phen-3-yl]benzene] (10 nm)/TmPyPB doped with 10 wt% of n-type cesium carbonate $Cs_2CO_3$ (10 nm)/Al (110 nm), where TmPyPB was used as the electron transport layer.

Current density–voltage (*J*–*V*) characteristics of the only-hole and only-electron devices exhibited the excellent hole and electron transport capability of the dibenzophosphole **212**. Summarizing, the dibenzophosphole **212** possesses superior carrier transport properties for both positive and negative charges.

In contrast, the dibenzophosphole **66**, which was used in 2006 by Wu and Réau *et al.* as an electron transport layer, hole transport layer as well as an ambipolar material for OLEDs, turned out to be an unsuitable component for single- and two-layer OLEDs. The configuration of the single-layer OLED used was the following: ITO/PEDOT:PSS (poly(3,4-ethylenedioxythiophene):polystyrene sulfonate) (25 nm)/organic layer (100 nm)/Mg:Ag (80 nm)/Ag (150 nm) as shown in Fig. 8.[12]

Light emission was observed for a turn-on voltage of 4 V. However, the device was unstable and its electroluminescence characteristics (brightness, emission wavelength) varied rapidly with applied driving current.

The dibenzophosphole **66** was also tested in the two-layer OLEDs as an electron-transporting material (n-type) as well as hole-transporting material (p-type) in the two following

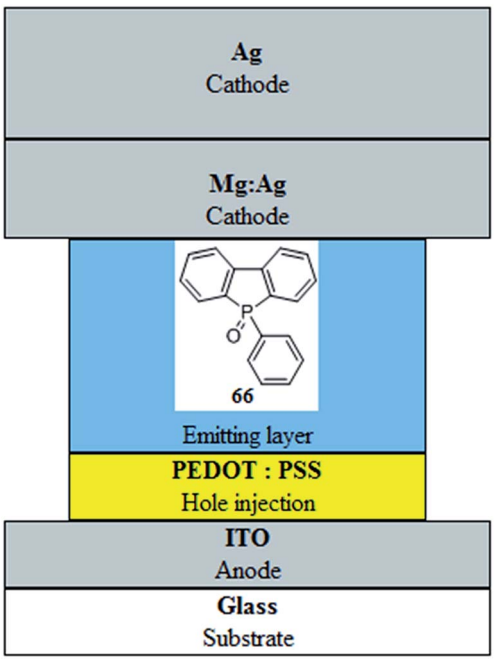


Fig. 8 Single-layer OLEDs.

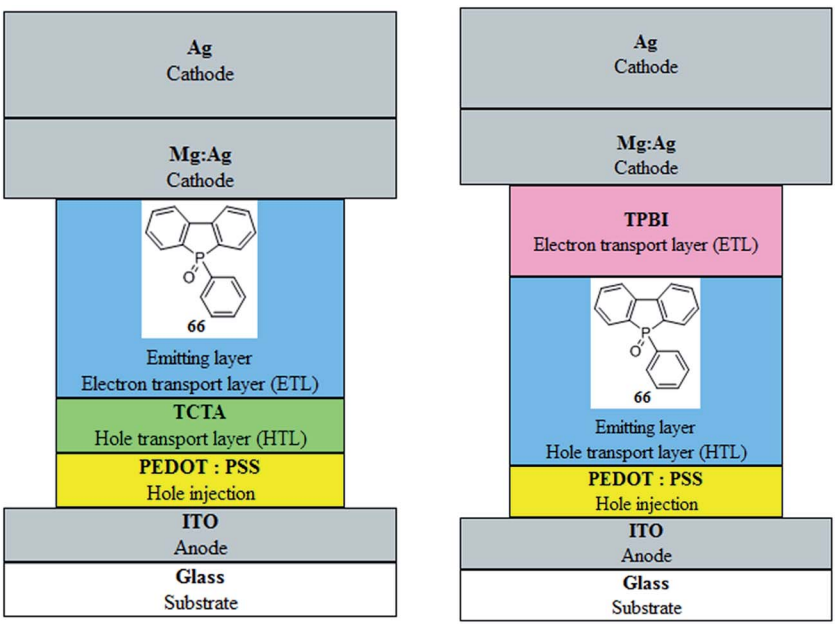


Fig. 9 Two-layer OLEDs.

configurations: ITO/PEDOT/TCT-[tris(4-carbazoyl-9-ylphenyl) amine]/the compound **66**/Mg:Ag/Ag and ITO/PEDOT/dibenzophosphole **66**/TPBI-[2,2′,2″-(1,3,5-benzinetriyl)-tris(1-phenyl-1*H*-benzimidazole)]/Mg:Ag/Ag. Thus, the compound **66** was mixed with the known p-type hole-transporting material TCTA-[tris(4-carbazoyl-9-ylphenyl)amine and with the commonly known n-type electron transporting material TPBI-[2,2′,2″-(1,3,5-benzenetriyl)-tris(1-phenyl-1*H*-benzimidazole)] to provide two unstable bulk-hetero junctions, respectively (Fig. 9).[12] A comparison of the opposite results obtained with dibenzophospholes **66** and **212** as materials for OLEDs, shows that more intensive investigations should be undertaken in this area with other representatives of dibenzophospholes, as reviewed in this article.

## 6. Conclusions

Dibenzophosphole and its derivatives are an underestimated group of heterorganic compounds which may serve as electroluminescent materials for optoelectronic devices due to easy synthesis (subsection 2) and functionalization (subsection 3), high thermal stability and the possibility of fine-tuning their electronic properties through various structural modifications both on phosphorus and the benzene rings (subsections 3.1 and 3.2). Other areas of optoelectronics are open for exploration of dibenzophospholes and their derivatives. The $^{31}$P-NMR technique may be a very useful tool for the rapid monitoring of progress in chemical synthesis and in testing chemical purity and stability of these compounds. Since, so far, only two dibenzophospholes **66** and **212** were used in construction of emitting diodes,[12,65] more intensive research with other dibenzophosphole representatives should certainly be investigated in the future.

This review shows the great potential of both simple and functionalized dibenzophospholes that should be tested more intensely as single materials, as well as in structural combinations with other π-extended conjugated aromatic and heteroaromatic systems containing phosphorus, nitrogen, silicon or sulfur atoms. The promising results obtained so far with closely related phospholes[12] may outline possible directions of further improvements in optoelectronic materials based on organophosphorus compounds.

## Acknowledgements

This work was financed by the National Science Centre (NCN), Poland on the basis of the grant number 2013/11/B/ST5/01610 and by Statutory Funds from the Ministry of Science and Higher Education in Poland.

## References

1 H. Shirakawa, E. J. Louis, A. MacDiarmid, C. Chiang and A. J. Heeger, *J. Chem. Soc., Chem. Commun.*, 1977, **16**, 578.
2 U. Mitschke and P. Bauerle, *J. Mater. Chem.*, 2000, **10**, 1471.
3 M. J. S. Dewar and N. Trinajstic, *J. Am. Chem. Soc.*, 1970, **92**, 1453.
4 B. El Hamaoui, L. Zhi, J. Wu, J. Li, N. T. Lucas, Z. Tomovic, U. Kolb and K. Mllen, *Adv. Funct. Mater.*, 2007, **17**, 1179.
5 T. Baumgartner and R. Reau, *Chem. Rev.*, 2006, **106**, 4681.
6 M. G. Hobbs and T. Baumgartner, *Eur. J. Inorg. Chem.*, 2007, **23**, 3611.
7 T. Baumgartner, *Acc. Chem. Res.*, 2014, **47**, 1613.
8 D. Joly, P.-A. Bouit and M. Hissler, *J. Mater. Chem. C*, 2016, **4**, 3686.
9 M. P. Duffy, W. Delaunay, P.-A. Bouit and M. Hissler, *Chem. Soc. Rev.*, 2016, **45**, 5296.
10 K. Fourmy, D. Nguyen, O. Cabaret and M. Gouygou, *Catal. Sci. Technol.*, 2015, **5**, 4289.
11 R. A. Aitken, *Sci. Synth.*, 2001, **10**, 817.
12 H. Su, O. Fadhel, C. Yang, T. Cho, C. Fave, M. Hissler, C. Wu and R. Réau, *J. Am. Chem. Soc.*, 2006, **128**, 983.
13 T. Baumgartner, T. Neumann and B. Wirges, *Angew. Chem., Int. Ed.*, 2004, **43**, 6197.
14 T. Baumgartner, W. Bergmans, T. Karpati, T. Neumann, M. Nieger and L. Nyulászi, *Chem.–Eur. J.*, 2005, **11**, 4687.
15 S. Durben, Y. Dienes and T. Baumgartner, *Org. Lett.*, 2006, **8**, 5893.
16 Y. Dienes, S. Durben, T. Karpati, T. Neumann, U. Englert, L. Nyulászi and T. Baumgartner, *Chem.–Eur. J.*, 2007, **13**, 7487.
17 Y. Matano and H. Imahori, *Org. Biomol. Chem.*, 2009, **7**, 1258.
18 C. Romero-Nieto and T. Baumgartner, *Synlett*, 2013, **24**, 920.
19 G. Wittig and G. Geissler, *Justus Liebigs Ann. Chem.*, 1953, **44**, 580.
20 S. Ogawa, Y. Tajiri and N. Furukawa, *Bull. Chem. Soc. Jpn.*, 1991, **64**, 3182.
21 G. Wittig and A. Maercker, *Chem. Ber.*, 1964, **97**, 747.
22 S. Affandi, R. L. Green, B. T. Hsieh, M. S. Holt, J. H. Nelson and E. C. Alyea, *Synth. React. Inorg. Met.-Org. Chem.*, 1987, **17**, 307.
23 G. Wittig and E. Kochendoerfer, *Chem. Ber.*, 1964, **97**, 741.
24 G. Wittig and E. Benz, *Chem. Ber.*, 1959, **92**, 1999.
25 D. Hellwinkel, *Chem. Ber.*, 1966, **99**, 3642.
26 O. Herd, D. Hoff, K. W. Kottsieper, C. Liek, K. Wenz, O. Stelzer and W. S. Sheldrick, *Inorg. Chem.*, 2002, **41**(20), 5034.
27 A. Bruch, A. Fukazawa, E. Yamaguchi, S. Yamaguchi and A. Studer, *Angew. Chem., Int. Ed.*, 2011, **50**, 12094.
28 Q. Ruan, L. Zhou and B. Breit, *Catal. Commun.*, 2014, **53**, 87.
29 J. A. Macor, J. L. Brown, J. N. Cross, S. R. Daly, A. J. Gaunt, G. S. Girolami, M. T. Janicke, S. A. Kozimor, M. P. Neu, A. C. Olson, S. D. Reilly and B. L. Scott, *Dalton Trans.*, 2015, **44**, 18923.
30 H. Kalkeren, S. Leenders, C. Hommersom, F. Rutjes and F. Delft, *Chem.–Eur. J.*, 2011, **17**, 11290.
31 A. Oukhrib, L. Bonnafoux, A. Panossian, S. Waifang, D. H. Nguyen, M. Urrutigoity, F. Colobert, M. Gouygou and F. R. Leroux, *Tetrahedron*, 2014, **70**, 1431.
32 T. Agou, M. D. Hossain, T. Kawashima, K. Kamada and K. Ohta, *Chem. Commun.*, 2009, **44**, 6762.
33 K. Yavari, P. Retailleau, A. Voituriez and A. Marinetti, *Chem.–Eur. J.*, 2013, **19**, 9939.

34 A. S. Ionkin and W. J. Marshall, *Heteroat. Chem.*, 2003, **14**(4), 360.
35 A. A. Diaz, J. D. Young, M. A. Khan and R. J. Wehmschulte, *Inorg. Chem.*, 2006, **45**, 5568.
36 V. Diemer, A. Berthelot, J. Bayardon, S. Juge, F. R. Leroux and F. Colobert, *J. Org. Chem.*, 2012, **77**, 6117.
37 K. Baba, M. Tobisu and N. Chatani, *Angew. Chem., Int. Ed.*, 2013, **52**, 11892.
38 Y. Unoh, T. Satoh, K. Hirano and M. Miura, *ACS Catal.*, 2015, **5**, 6634.
39 Y. Kuninobu, T. Yoshida and K. Takai, *J. Org. Chem.*, 2011, **76**, 7370.
40 S. Furukawa, S. Haga, J. Kobayashi and T. Kawashima, *Org. Lett.*, 2014, **16**, 3228.
41 Y. Cui, L. Fu, J. Cao, Y. Deng and J. Jiang, *Adv. Synth. Catal.*, 2014, **356**, 1217.
42 S. Ishikawa and K. Manabe, *Tetrahedron*, 2010, **66**, 297.
43 M. Stankevič, J. Pisklak and K. Włodarczyk, *Tetrahedron*, 2016, **72**, 810.
44 N. Fukawa, T. Osaka, K. Noguchi and K. Tanaka, *Org. Lett.*, 2010, **12**(6), 1324.
45 E. Martinez-Arripe, F. Jean-Baptiste-dit-Dominique, A. Auffrant, X. F. Le Goff, J. Thuilliez and F. Nief, *Organometallics*, 2012, **31**, 4854.
46 S. Shah, M. Cather Simpson, R. C. Smith and J. D. Protasiewicz, *J. Am. Chem. Soc.*, 2001, **123**, 6925.
47 X. Wei, Z. Lu, X. Zhao, Z. Duan and F. Mathey, *Angew. Chem., Int. Ed.*, 2015, **54**, 1583–1586.
48 O. Fadhel, D. Szieberth, V. Deborde, C. Lescop, L. Nyulászi, M. Hissler and R. Réau, *Chem.–Eur. J.*, 2009, **15**, 4914.
49 P. Bouit, A. Escande, R. Szucs, D. Szieberth, C. Lescop, L. Nyulászi, M. Hissler and R. Réau, *J. Am. Chem. Soc.*, 2012, **134**, 6524.
50 Y. Hayashi, Y. Matano, K. Suda, Y. Kimura, Y. Nakao and H. Imahori, *Chem.–Eur. J.*, 2012, **18**, 15972.
51 H. Kalkeren, S. Leenders, C. Hommersom, F. Rutjes and F. Delft, *Chem.–Eur. J.*, 2011, **17**, 11290.
52 K. Geramita, J. McBee and T. D. Tilley, *J. Org. Chem.*, 2009, **74**, 820.
53 Y. J. Ahn, R. J. Rubio, T. K. Hollis, F. S. Tham and B. Donnadeiu, *Organometallics*, 2006, **25**, 1079.
54 N. Dubrovina, H. Jiao, V. Tararov, A. Spannenberg, R. Kadyrov, A. Monsees, A. Christiansen and A. Borner, *Eur. J. Org. Chem.*, 2006, **11**, 3412.
55 C. H. Lin, C. W. H. Su, J. L. Liao, Y. M. Cheng, Y. Chi, T. Y. Lin, M. W. Chung, P. T. Chou, G. H. Lee, C. H. Chang, C. Y. Shih and C. L. Ho, *J. Mater. Chem.*, 2012, **22**, 10684.
56 H. A. van Kalkeren, C. Grotenhuis, F. S. Haasjes, C. A. Hommersom, F. P. J. T. Rutjes and F. L. van Delft, *Eur. J. Org. Chem.*, 2013, **31**, 7059.
57 H. A. Kalkeren, J. J. Bruins, F. P. J. T. Rutjes and F. L. Delft, *Adv. Synth. Catal.*, 2012, **354**, 1417.
58 E. Durán, E. Gordo, J. Granell, M. Font-Bardía, X. Solans, D. Velasco and F. López-Calahorra, *Tetrahedron: Asymmetry*, 2001, **12**, 1987.
59 J. G. L. Cortés, S. Vincendeau, J. C. Daran, E. Manoury and M. Gouygou, *Acta Crystallogr., Sect. C: Cryst. Struct. Commun.*, 2006, **62**, m188.
60 A. Decken, M. Neil, C. Dyker and F. Bottomley, *Can. J. Chem.*, 2002, **80**, 55.
61 A. Decken, M. Neil, C. Dyker and F. Bottomley, *Can. J. Chem.*, 2001, **79**, 1321.
62 D. H. Nguyen, H. Lauréano, S. Jugé, P. Kalck, J. C. Daran, Y. Coppel, M. Urrutigoity and M. Gouygou, *Organometallics*, 2009, **28**, 6288.
63 C. Thoumazet, L. Ricard, H. Gruützmacherb and P. Le Floch, *Chem. Commun.*, 2005, **12**, 1592.
64 E. Duran, D. Valasco, F. Lopez-Calahorra and H. Finkelmann, *Mol. Cryst. Liq. Cryst.*, 2010, **381**, 43.
65 J. Yin, R. F. Chen, S. L. Zhang, Q. D. Ling and W. Huang, *J. Phys. Chem. A*, 2010, **114**, 3655.
66 R. Kabe, V. M. Lynch and P. Anzenbacher, *CrystEngComm*, 2011, **13**, 5423.